A groundwater drought indicator for South Africa

LM Vermeulen

orcid.org/0000-0003-31272386

Dissertation accepted in fulfilment of the requirements for the degree *Master of Science in Environmental Sciences with Hydrology and Geohydrology* at the North-West University

Supervisor: Dr SR Dennis

Graduation July 2021

26192772

Acknowledgements

Firstly, I would like to thank my family. My mother for her love and support throughout my life and for being the one who inspired me to study what I now love. My father for his love and being the person who always motivated and encouraged me to be better every day. I am forever grateful to my parents for giving me the opportunities and experiences that have made me who I am. My brother for his unconditional support, always looking out for me, and being my best friend. To my grandfather for always being there for me, always willing to help and for being my hero.

Furthermore, I would like to thank my supervisor, Dr. SR Dennis for his consistent support and guidance during this project.

Most importantly, I would like to thank my Lord Jesus Christ for the opportunity and privilege He has given me to study and for being with me every step of the way. Without Him, nothing would be possible.

Abstract

South Africa experienced one of its most severe droughts from 2014 to 2016. The drought affected water resources in the country, and signs of recovery were first observed in 2019. Droughts circulate through the hydrological cycle and affect both surface and groundwater resources. Drought indices (DIs) are used to analyse and identify drought periods. All DIs require accurate and complete data sets, such as precipitation. Drought indices like the standardised precipitation index (SPI) and the standardised groundwater level index (SGI) are precipitation-based and groundwater-level-based. The SGI required complete groundwater level data sets in order to perform the simulation. Groundwater balance models were used to simulate groundwater levels, where insufficient groundwater level data was present in the selected study areas. Therefore, a developed index namely the groundwater drought strength index (GDSI) was used to accommodate the lack in data. The study areas were identified based on their geologies, in order to assess the developed groundwater drought indicator's ability to indicate groundwater droughts in different lithologies. Groundwater droughts were distinguishable, provided that the lag between rainfall and recharge were taken into consideration. The trend of groundwater level simulations was found to be an added benefit in understanding how groundwater levels responded to climatic conditions. The results showed groundwater drought periods and periods of groundwater level decline. By identifying these periods, sustainable management of groundwater resources can be implemented with the use of a groundwater drought indicator.

Keywords: Droughts; Drought index; Groundwater drought strength index (GDSI) Standardised precipitation index (SPI); Standardised groundwater level index (SGI); Recharge; Geology.

Table of Contents

List of Figures

List of Tables

List of Equations

Acronyms

CCDM	The Directorate: Climate Change and Disaster Management
DWAF	The Department of Water Affairs and Forestry
DWS	The Department of Water and Sanitation
FM	Geological Formation
GDSI	Groundwater Drought Strength Index
GRAII	Groundwater Resources Assessment Phase 2
GRP	Geological Group
NDVI	Normalized Difference Vegetation Index
PDSI	Palmer Drought Severity Index
RMSE	Root Mean Square Error
SBGRP	Geological Subgroup
scPDSI	Self-Calibrated Palmer Drought Severity Index
SGI	Standardised Groundwater level index
SPEI	Standardized Precipitation Evapotranspiration Index
SPI	Standardized Precipitation Index
WMA	Water Management Area
WR2012	Water Research Commission 2012

Chapter 1 Introduction

1.1 Background

Drought can be described as a condition of insufficient moisture due to the lack of precipitation over a period of time (Botai et al., 2016). Vicente-Serrano *et al.,* (2010) described a drought as a natural phenomenon, which occurs when groundwater and surface water level (dams, rivers etc.) availability is significantly below accepted levels over an extensive period and cannot meet the required demand.

Drought is a prolonged process that can affect agriculture, the hydrological cycle, economic development, as well as the environment itself, due to the sustainability of natural environments being threatened (Bhuiyan et al., 2006). Drought not only affects these factors mentioned above, but also the livelihood of people and their health.

South Africa is classified as an arid country, being one of the 30 driest countries in the world (DWAF, 2019). Droughts in South Africa are common events and can be caused by various factors, including climate change and human influences.

Droughts can be monitored and analysed for future events with the use of drought indices, such as the Palmer Drought Severity Index (PDSI), Standardized Precipitation Index (SPI), Standardized Precipitation Evapotranspiration Index (SPEI) and the Normalized Difference Vegetation Index (NDVI). These indices are commonly used around the world and have been previously applied in South Africa to analyse droughts. The PDSI and the SPI method are precipitation-based (Hayes et al., 1999). The SPI method is an improvement on the dated PDSI method due to advantages, such as the SPI's simplicity, the fact that it is based solely on precipitation and that this method is versatile in the sense that it can be calculated on numerous timescales (Hayes et al., 1999; Soulé, 1992). The SPEI method is a modification of the SPI method and it was mainly developed to address the water supply-demand issues (Botai et al., 2016). The Normalized Difference Vegetation Index (NDVI) on the other hand is a numerical indicator that uses the visible and near-infrared bands of the electromagnetic spectrum. It is used to analyse remote-sensing measurements of vegetation, as well as assess whether the vegetation being observed comprises live green vegetation or not (The Directorate: Climate Change and Disaster Management, 2014; Sruthi & Aslam, 2015).

An additional method, the Standardised Groundwater Level Index (SGI) regionally analyses and quantifies groundwater droughts. Groundwater droughts are concerned with the reductions in dam and reservoir levels, streamflow depletion, depletion of soil moisture and

the lowering of the groundwater table (Palmer, 1965). The method makes use of a cluster analysis to classify standardised groundwater level hydrographs (Bloomfield & Marchant, 2013).

1.2 Problem statement

Analyses of groundwater droughts in South Africa are problematic, largely due to the lack of groundwater level data and, to a lesser extent, the lack of rainfall data. Existing indices require adequate data sets to accurately analyse droughts. By analysing groundwater droughts, the sustainable management of these water resources can be applied.

1.3 Aims and objectives

The aim of this study is to develop a groundwater drought indicator for South Africa making use of existing data sets provided on a quaternary catchment scale.

The objectives of the study are summarised as follows:

- To identify boreholes with long-term water level monitoring data with quaternary catchments based long-term rainfall data, across South Africa.
- To model long-term groundwater levels for a borehole by making use of recharge groundwater balance models and using quaternary catchment based available rainfall data. The borehole water level data will be used for calibrating the groundwater balance model.
- To compare the modelled long-term water level record to known drought periods to formulate an appropriate drought indicator.
- Finally, to compare the newly developed groundwater drought indicator to existing drought indices, where an adequate data set (rainfall and groundwater levels) exists to verify the validity of the proposed indicator.

1.4 Thesis outline

1. **Introduction:** An introduction to the current situation in South Africa, problem statement, aims and objectives.
2. **Literature review:** A literature review that explores existing drought indices (both rainfall and groundwater) used around the world and in South Africa with a strong focus on the requirements to calculate each one. Discuss existing methodologies to model long-term borehole water levels, specifically looking at groundwater balance models. Discuss existing groundwater and rainfall databases available in South Africa.
3. **Methodology:** Formulation of the methodology based on the results of the literature review, and research that was conducted as part of this study.
4. **Case studies:** Choose boreholes with adequate data in different lithologies and present a case study per major geological classification. Shortly discuss each study area and the available data. Apply the proposed methodology to each and calculate the SPI and SGI for these study areas.
5. **Results and discussion:** Critically discuss the results from each of the case studies.
6. **Conclusions:** Present the conclusion of the study.
7. **Recommendations:** Propose how the formulated drought indicator could be improved in the future and what will be required.
8. **References:** Reference list.

   Appendices: An appendix will be created for each question to avoid cluttering the thesis with scores of graphs and data tables.

Chapter 2 Literature review

2.1 Introduction

South Africa is an arid country and one of the 30 driest countries in the world. Therefore, drought awareness is an aspect most people should understand. Drought is an extensive natural hazard affecting various aspects of a country, such as agriculture, socioeconomic activity, economic development, the hydrological cycle, and the environment (Liu et al., 2016). Drought occurs when there is extreme water scarcity in a region because of a precipitation decrease, high evaporation and mismanagement of water resources, and a combination thereof (Van Loon, 2015). These factors can also affect groundwater levels. Reduced groundwater levels may lead to a geohydrological drought, which can lead to reduced baseflow to groundwater-fed rivers, springs, and wetlands (Bloomfield et al., 2015; Mishra & Singh, 2010).

Mohammad *et al.,* (2018) stated that during a drought the quantity of the precipitation reduces, and this has a direct effect on the amount of groundwater recharge. The impact of droughts varies from region to region because of different climates. Reduced rainfall is one of the main causes of drought, but not the main parameter reflecting the impact of a drought. Soil moisture, reservoir storage, streamflow and groundwater levels are the main parameters showing the effects of a drought (Bhuiyan et al., 2006).

The hydrological factors of groundwater droughts are a complex function of meteorological aspects (Bloomfield et al., 2015; Van Loon, 2015). The impact on the groundwater resources during droughts can differ, because of how different groundwater systems react to meteorological droughts (Bloomfield et al., 2015). The way groundwater systems respond because of droughts is reflected in the groundwater levels and baseflow.

Drought indices are usually used for the monitoring of droughts. Indices, such as the Palmer Drought Severity Index and the Standard Precipitation Index (SPI), are two of the most-used methods. The SGI is a new index, developed by Bloomfield and Marchant (2013), for the characterisation of groundwater droughts based on the standardised groundwater levels and their associated time series data (Bloomfield & Marchant, 2013).

Drought is a difficult natural phenomenon to monitor and detect. Therefore, complete data records are required, as gaps in the data sets can lead to inaccurate results while using drought indices.

Although droughts are considered by many to be a natural event, Wilhite (2000) reiterated that a drought event is a combination of both natural and social components (Figure 1).

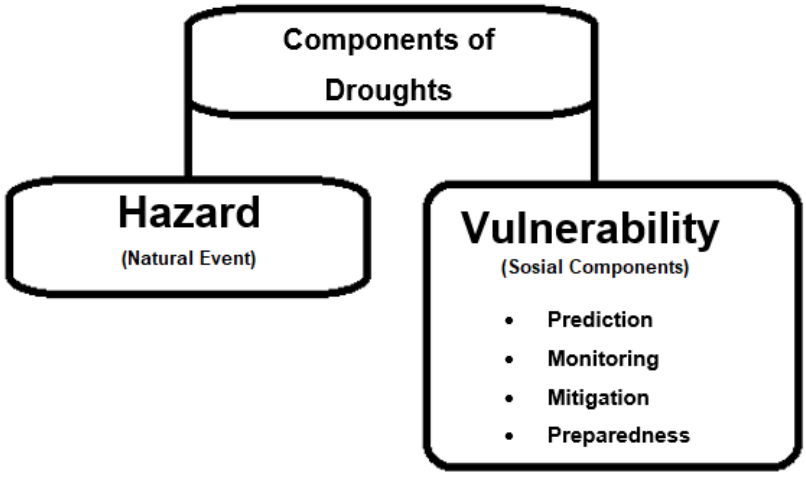

Figure 1: Components of drought (Wilhite, 2000)

Droughts are often mistaken to be rare events, but they are in fact recurring events and a normal component of climate (Wilhite, 2000). They can affect agriculture, the hydrological cycle, economic development, the livelihood of people and the environment itself (Bhuiyan et al., 2006).

2.2 Types of droughts

The effects of droughts are complex and sometimes unpredictable. Droughts affect many sectors of the economy, such as agriculture, water resources, and natural ecosystems (Botai et al., 2016).

There are different types of drought, for example meteorological, hydrologic, agricultural, and socioeconomic droughts.

2.2.1 Meteorological droughts

The lack of precipitation over a period leads to meteorological droughts (Wilhite & Glantz, 1985). Dryness and the length of the dry period determine the severity of a meteorological drought.

2.2.2 Hydrological droughts

Hydrological droughts are related to dry spells on the surface and below the surface (Panagoulia & Dimou, 1998). The severity of a hydrological drought depends on the influence

a drought has on river basins. Reductions in lake and reservoir levels, depletion of soil moisture, streamflow and a groundwater table decrease are all associated with hydrological droughts (Palmer, 1965).

2.2.3 Agricultural droughts

Agricultural drought happens when crop and pasture harvests are severely affected by the depletion of soil moisture (Panagoulia & Dimou, 1998).

Factors, such as departures from normal, precipitation shortages, or several meteorological factors like evapotranspiration (Panagoulia & Dimou, 1998; Wilhite & Glantz, 1985), play a part.

2.2.4 Socioeconomic droughts

Socioeconomic droughts arise when there are water scarcities that affect people (Monacelli et al., 2005). Shortcomings in supply and demand of water lead to socioeconomic droughts (Monacelli et al., 2005). Agricultural, meteorological, and hydrological droughts all affect socioeconomic droughts (Panagoulia & Dimou, 1998).

2.3 Droughts occurring in South Africa

South Africa comprises a variety of climates but is generally considered semi-arid (El Chami & Moujabber, 2016). Droughts in Southern Africa are caused by the interaction of several physical factors (Vogel & Drummond, 1993). These physical factors include the effects of the El Niño southern oscillation, the position and orientation of cloud bands, the actions of sea-surface temperatures and the effects of upper atmospheric waves (Vogel & Drummond, 1993).

According to Richard *et al.,* (2001), until 2001 there are two known drought periods between 1950 and 1988. The two drought periods are between 1950 and 1969, and 1970 and 1988, respectively. The drought years of 1950–1969 include 1951, 1960, 1964, 1965 and 1968 (refer to Figure 2) (Richard et al., 2001). The drought years of 1970–1988 include 1970, 1973, 1982 to 1984, 1987 and 1988 (refer to Figure 2) (Baudoin et al., 2017; Richard et al., 2001). Drought periods were also noted in 1991–1992 and 1994–1995, and the most recent noted drought period is between 2014 and 2016 (refer to Figure 2) (Baudoin et al., 2017). Historical drought periods are displayed in Figure 2. The drought of 2015–2016 severely depleted water reserves and the effects of the drought are well depicted in South Africa's water storage trends, from high levels in 2010/2011 to increasingly low levels in 2015.

Vogel and Drummond (1993) described rainfall across South Africa to be ever-changing as rainfall patterns vary with recurring dry and wet spells. The annual rainfall of South Africa varies from west to east, less than 100 mm per annum in the west to over 1 500 mm in the east (El Chami & Moujabber, 2016).

There are several areas in South Africa classified as drought areas because of the rainfall receipts being below 70% of normal (Vogel & Drummond, 1993). The most notable historical drought periods in South Africa were during the 1980s and the 1990s (Vogel & Drummond, 1993; Richard et al., 2001). During 2015 and 2016 South Africa experienced one of the driest and hottest periods in over a century (Baudoin et al., 2017).

During 2015 and 2016 drought was caused by the El Niño phenomenon and climate change. Climate change and the El Niño phenomenon increase surface water temperatures of the eastern tropical Pacific Ocean (Baudoin et al., 2017; Botai et al., 2016). The combination of increasing surface water temperatures, lack of rain and increasing temperatures that these phenomena bring, all add to the severity of a drought.

2.3.1 Historical droughts in South Africa

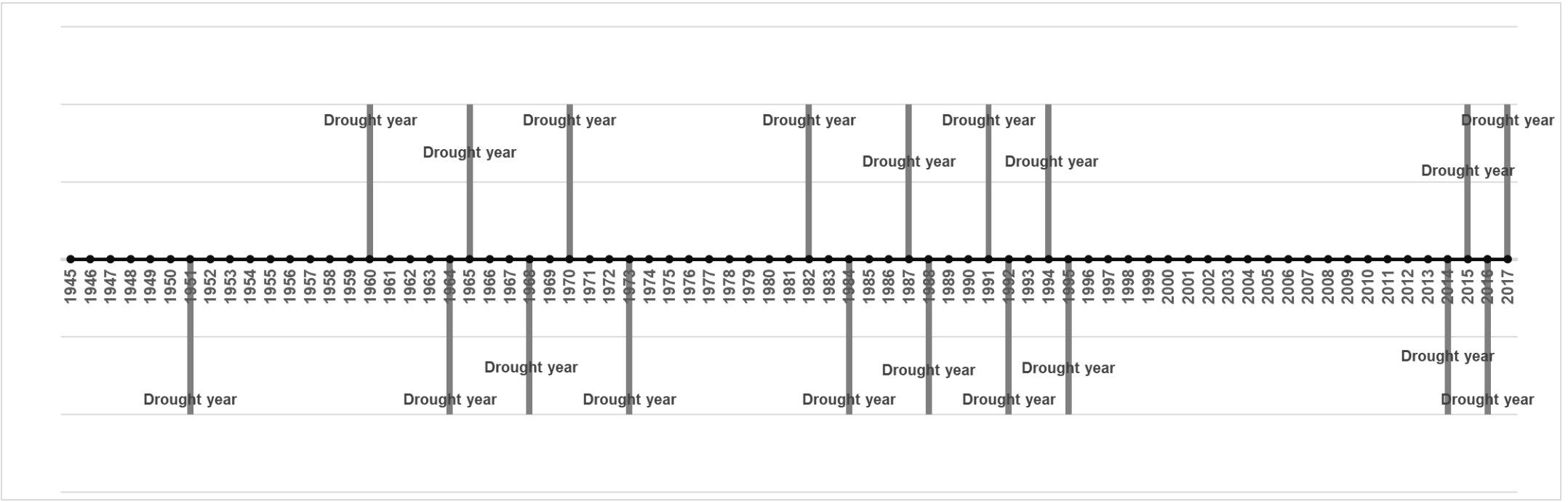

Figure 2: Historical drought periods (Baudoin et al., 2017; Richard et al., 2001)

2.4 Factors influencing and causing droughts

There are various factors that can influence droughts in terms of the severity and duration of a drought event. These factors include precipitation, hydrology, hydrogeology, geology, catchment characteristics and the climate of an area. All these factors can determine how the area may react or experience a drought event, in terms of the severity and duration of the event.

2.4.1 Climate

Climate is a difficult term to define because it consists of various meteorological variables. Meteorological variables describe the state of the atmosphere, such as surface pressure and surface temperature (Bothe, 2018; Werndl, 2014). Climate includes all meteorological variables and the variables describing the state of land surfaces and the ocean (Bothe, 2018; Werndl, 2014). The term ‘climate’, therefore, describes influencing factors, such as temperature and precipitation, as they are two of the most influential factors regarding droughts.

2.4.1.1 Precipitation

Precipitation, as Vogel and Drummond (1993) stated, is ever-changing over South Africa. Droughts are apparent after a long period without precipitation (Vicente-Serrano et al., 2010), and have a direct connection with precipitation in the sense that the lower the precipitation, the higher the risk is for droughts to occur due to the evaporation and evapotranspiration surpassing the rate of precipitation. Therefore, more water evaporates than water that infiltrates and accumulates in surface and groundwater resources. Precipitation is probably the most important aspect to study concerning droughts, as several studies have shown that precipitation is the main variable when determining the onset, duration, severity, and the end of a drought event (Chang & Cleopa, 1991; Heim, 2002). The lack of precipitation leads to less groundwater infiltration and a decrease in water accumulating in surface water resources.

2.4.1.2 Hydrogeology

Hydrogeologic components can be described in three entities, namely topography, geology and climate (Tóth, 1999). All the above components play a part in the manner in which groundwater flows beneath the surface. Groundwater behaviour depends on factors, such as the geohydrology, hydrology, vegetation, soil and rock mechanics, geomorphology and the transportation and accumulation process (Tóth, 1999; Wossenyeleh et al., 2020).

The geology of an area is important to understand in terms of the aquifers present, and the porosity of the rock and the sediment. The geologic characteristics of an area can determine

groundwater storage, the flow paths, and the interaction with the environment (Tóth, 1999; Wossenyeleh et al., 2020). It is important to consider the characteristics of different lithologies types in order to understand the movement of water and fluids below the surface. Different lithologies will manage or control water/fluid movement in different ways. Therefore, it is important to understand the fracture characteristics, infiltration rates, permeability, and porosity of geologies before conducting groundwater level and precipitation analyses for droughts (Aplin et al., 1999).

Topography is an important factor to consider as groundwater levels tend to mimic the topography. Topography together with a better understanding of the hydrogeological components of an area and the processes involved (e.g. recharge, transmissivity), the cause of hydrogeological droughts can be better understood (Wossenyeleh et al., 2020). To evaluate all the processes involved, the causes for fluctuations in groundwater level can be determined as either hydrogeological, meteorological drought or possibly anthropogenic.

2.4.1.3 Climate change

Climate change can be described as the change in global and regional weather patterns. Therefore, it is an important factor to consider when analysing droughts. Climate change occurs due to increased greenhouse gases, such as CO_2 (carbon dioxide) and CH_4 (methane). The increase in greenhouse gases affects pressure, temperature, evaporation and precipitation, ultimately affecting global and regional weather patterns.

Precipitation is the most susceptible to change in comparison to other climate variables, such as pressure and temperature, making precipitation analysis and measurements more influential (New et al., 2001). Climate change is a growing concern as it has heightened the need for accurate information about the distribution of precipitation (New et al., 2001). The importance of accurate information about the distribution of precipitation can be validated by the increase in precipitation in some regions of the world and a decrease in others (Trenberth et al., 2007). Precipitation has increased in the eastern parts of Northern Europe, North and South America, Northern and Central Asia. Precipitation decreases have been encountered in the subtropics as well as areas in Southern Africa, the Mediterranean, Southern Asia and Sahel region (Trenberth et al., 2007).

Increases in droughts have also taken place, which are consistent with the warming climate. This pattern is going to continue in the future as the effects of climate change are only going to increase (New et al., 2001; Trenberth et al., 2007).

2.4.2 Catchment characteristics

Catchment characteristics are also a factor to consider when studying or analysing droughts. It is important to note that when determining drought duration and deficit, it is reliant on scale (local, global, catchments, etc.), (Van Loon & Laaha, 2015). Catchment characteristics refer to the area, amount of precipitation, water bodies, vegetation and land cover, hydrological and hydrogeological factors of the catchment (Van Loon & Laaha, 2015). Drought deficits have a strong correlation with climate and catchment characteristics in the sense that areas of higher altitude have more precipitation than those at lower altitude (Van Loon & Laaha, 2015). Van Loon and Laaha (2015) also reiterated that catchment characteristics affect the severity and deficit of a drought by comparing hydrographs of two catchments represented in the same cluster. Two catchments can show similar drought periods but differ in deficit volumes. Van Loon and Laaha (2015) found that catchments with higher discharge are also prone to higher deficit volumes. Catchment characteristics are an important factor to consider due to each catchment and how they respond to water deficit and drought events.

2.5 Drought indices

Coverage and intensity are two of the key factors contributing to the severity of a drought. These factors may differ from drought to drought (Jönson, 2017). The development period of droughts can vary from a few months to over several seasons or years, which complicates the monitoring process because of the uncertainty of its intensity and coverage (Jönson, 2017).

There have been various methods and techniques developed to analyse and monitor droughts (Vicente-Serrano et al., 2010). Drought indices are one method used to analyse and monitor droughts (Vicente-Serrano et al., 2010; Jönson, 2017). The Palmer Drought Severity Index (PDSI) is a well-known drought index developed by Palmer (1965). The PDSI makes use of precipitation, runoff and evaporation inputs to describe the soil water content. It can monitor dry and wet periods, but the PDSI method requires a calibration site other than the site of interest, which can lead to complications (Vicente-Serrano et al., 2010).

The Standardised Precipitation Index (SPI) is an index also based on precipitation, but the SPI is the preferred index to the PDSI. Mckee *et al.,* (1993) developed the SPI and it has since been used to analyse and monitor droughts. The method is based on the probability of precipitation occurring (Svoboda et al., 2012). The SPI is a convenient calculation because only precipitation data is required (Svoboda et al., 2012).

The Standardised Groundwater Index (SGI) can analyse and indicate groundwater droughts at both local and regional scale (Bloomfield & Marchant, 2013; Kumar et al., 2016). The

variations in groundwater and precipitation can be examined by combining the SPI and SGI indices, using cross-correlation (Bloomfield & Marchant, 2013). The cross-correlation process between the SPI and SGI methods shows a degree of spatial variability because of different lags and accumulations during the accumulation process (Kumar et al., 2016). Kumar *et al.,* (2016) concluded that the use of drought indices, such as the SPI in relation to SGI, is not enough to analyse groundwater droughts. Physical factors, such as hydrogeological properties and land use characteristics, should also be considered (Van Loon & Laaha, 2015).

Li and Rodell (2015) conducted a study in the Mississippi River basin and they found that there is a similar relationship when comparing the accumulation period to the depth to water table. Kumar *et al.,* (2016) and Li and Rodell (2015) concluded in their studies that groundwater tables that are deeper or that comprise a thicker unsaturated zone, cause a decrease in high-frequency precipitation signals and also require longer precipitation accumulation periods to align with groundwater signals. For the relationship between the depth to water table and the precipitation, Kumar *et al.,* (2016) stated that there is a lag time between the rise in the groundwater level after a precipitation event and a drop in the groundwater level during a drought event or a barren rainfall period; this all depends on the aquifer and water table characteristics. The lag time, other than the use of the indices, is, therefore, also a factor to consider.

Another effect to consider during drought monitoring and with the use of drought indices is the scale element (local or regional). The size or type of scale is very important because some factors have bigger effects depending on the scale (Jönson, 2017). On a regional scale, climate is the main controlling factor, whereas on a local scale, hydrogeological factors are considered the controlling factor (Jönson, 2017). Hydrogeological factors can be slopes, land use, soil types and elevation (Van Loon & Laaha, 2015).

2.5.1 PDSI

Palmer (1965) developed the PDSI method and is one of the most popular meteorological drought indices used in the United States of America (Zargar et al., 2011). The PDSI method is not based on precipitation anomalies, but on water supply and water demand (Zargar et al., 2011). The focus of this method is on irregularities in soil deficiency instead of weather anomalies (Zargar et al., 2011). PDSI uses temperature, precipitation, and the water content data of soil. By using these inputs, the basic components of the groundwater balance equation, such as soil recharge, evapotranspiration, runoff, and surface layer moisture loss, can be calculated (Zargar et al., 2011).

The following inputs are the parameters included as potential values by the PDSI:

- Potential evapotranspiration
- Potential recharge
- Potential loss
- Potential runoff

These parameters are incorporated into the model as pre-determined values derived from climatic and hydrological sources to acquire the Z-value. Each potential value is either calculated using a parameter specific equation or included as pre-determined values. The Z value is calculated by subtracting the outflows (potential evapotranspiration, loss, and runoff) to the inflows (potential/effective recharge).

Refer to Equation 1:

$$PDSI_i = 0.897 PDSI_{i-1} + \frac{1}{3} Z_i$$

Equation 1: PDSI

PDSI calculations start at the current time step (i) month, and i – 1 is the previous time step. The simulation will end at the specified end date or month (Zoljoodi & Didevarasl, 2013). Currently the Self-Calibrated Palmer Drought Severity Index (scPDSI) is a software-based program, based on the PDSI principles. The scPDSI only requires the input parameters – the index is then self-calibrated to the user's specifications.

2.5.2 SPEI

The Standardised Precipitation Evapotranspiration Index (SPEI) method was first introduced by Vicente-Serrano *et al.,* (2010) as a drought index that focused on the effects global warming has on the severity and the nature of droughts. The SPEI method relates to the PDSI, as both methods consider the effect evapotranspiration has on drought severity, but the SPEI method can identify different droughts and drought effects on diverse systems as opposed to the PDSI (Beguería et al., 2013).

The SPEI method combines the PET (Potential Evapotranspiration) and SPI (Standardised Precipitation Index). Precipitation and evapotranspiration are the main inputs into the method. The method calculates the difference between precipitation and the reference evapotranspiration gathered during a certain time frame (Bezdan et al., 2019).

The SPEI method is comparable to the SPI method with the only difference being that the integration with the SGI is more complex than with the SPI (Zargar et al., 2011).

Refer to Equation 2:

$$SPEI = W - \frac{C_O + C_1 W + C_2 W^2}{1 + d_1 W + d_2 W^2 + d_3 W^3}$$ **Equation 2: SPEI**

W is defined by $W = \sqrt{-2In(P)}$, where P is the precipitation input monthly or weekly. C_0, C_1, C_2, d_1, d_2 and d_3 are all constant values where:

- C_0= 2.515517
- C_1= 0.802853
- C_2= 0.010328
- d_1= 1.432788
- d_2= 0.189269
- d_3= 0.001308

2.5.3 NDVI

The Normalized Difference Vegetation Index (NDVI) is a numerical indicator that uses the visible and near-infrared bands of the electromagnetic spectrum. It is used to analyse remote-sensing measurements of the vegetation and assess whether the vegetation being observed comprises live green vegetation or not (CCDM, 2014).

The Normalized Difference Vegetation Index (NDVI) is a remote-sensing-based index that makes use of advanced high-resolution radiometer (AVHRR) to measure vegetation conditions (Rouse et al., 1974). The radiometer reflects red and near-infrared channels in order to estimate if the vegetation is sparse, healthy or unhealthy (Zargar et al., 2011).

Refer to Equation 3:

$$NDVI = \frac{NIR - R}{NIR + R} x + c$$ **Equation 3: NDVI**

NIR represents the near-infrared spectral reflectance, whereas R is the visible red spectral reflectance (Zargar et al., 2011). The green substance in plants that produces carbohydrates is known as chlorophyll. The chlorophyll in healthy vegetation, therefore, will absorb light and reflect less R. On the other hand, unhealthy vegetation will reflect higher R (Zargar et al., 2011). To elaborate, higher R values result in lower NDVI and lower R values in higher NDVI. NDVI measures dryness, therefore, high NDVI values represent non-drought conditions, whereas low NDVI values represent dry conditions, that is drought conditions.

2.5.4 The Standardised Precipitation Index (SPI)

The occurrence and progression of the conditions of a meteorological drought event is a well-known and well-studied concept, because of rainfall being the primary driver of such an event (Kumar et al., 2009). The SPI is used to describe or analyse meteorological droughts at specific locations (Zin et al., 2012). Mckee *et al.,* (1993) designed the SPI to quantify and measure precipitation shortages for several timescales and consider the intensity, propagation and duration of droughts (Bloomfield & Marchant, 2013; Haas & Birk, 2016).

The SPI and PDSI methods are both precipitation-based. The SPI, according to Hayes *et al.,* (1999), is more simplistic, as precipitation is the only input. The SPI can also be implemented in winter months, unlike the PDSI method, and topography does not affect the results (Hayes et al., 1999).

The SPI can be calculated on various pre-defined timescales (e.g. three-, six-, nine-, 10-, 24- and 48-month timescales) (Zin et al., 2012). Precipitation and other meteorological factors are stationary during the calculation process with no temporal trends (Botai et al., 2016).

A precipitation record of 30 continuous years is required. The method is based on long-term precipitation data at a certain location for a specified time period (Jönson, 2017). Mckee *et al.,* (1993) suggested that the most suitable time periods to use are three-, six-, nine-, 10-, 24- and 48-month timescales because of the effects precipitation can have on the various components of the hydrological cycle.

The SPI results are given as a cumulative precipitation distribution of the precipitation records and are calculated by making use of a probability density function. In most cases the gamma distribution and the Pearson Type III distribution are used (McKee et al., 1993; Guttman, 1998). It then transforms the cumulative distribution to represent a standard normal distribution, to derive values as seen in Table 1. A value of zero represents the mean, and positive values represent wet periods, whereas negative values represent drought periods. As the magnitude of the value increases, the intensity of the wet or drought period increases. In some cases, extreme events can occur where the values exceed +2 or – 2; this indicates severe wet periods or severe droughts (Jönson, 2017). The SPI defines a drought as a time period during which the SPI value will be negative, and the drought period ends when the SPI value reaches a positive value, as is shown in Figure 3 (McKee et al., 1993). Due to the SPI being normalised, wetter and drier climates can be represented, therefore, wetter periods can also be monitored using the SPI (Svoboda et al., 2012; Jönson, 2017).

Table 1: SPI value classification

SPI values	
Values	**Description**
2.0+	Extremely wet
1.5 to 1.99	Very wet
1.0 to 1.49	Moderately wet
-.99 to .99	Near normal
-1.0 to -1.49	Moderately dry
-1.5 to -1.99	Severely dry
-2 and less	Extremely dry

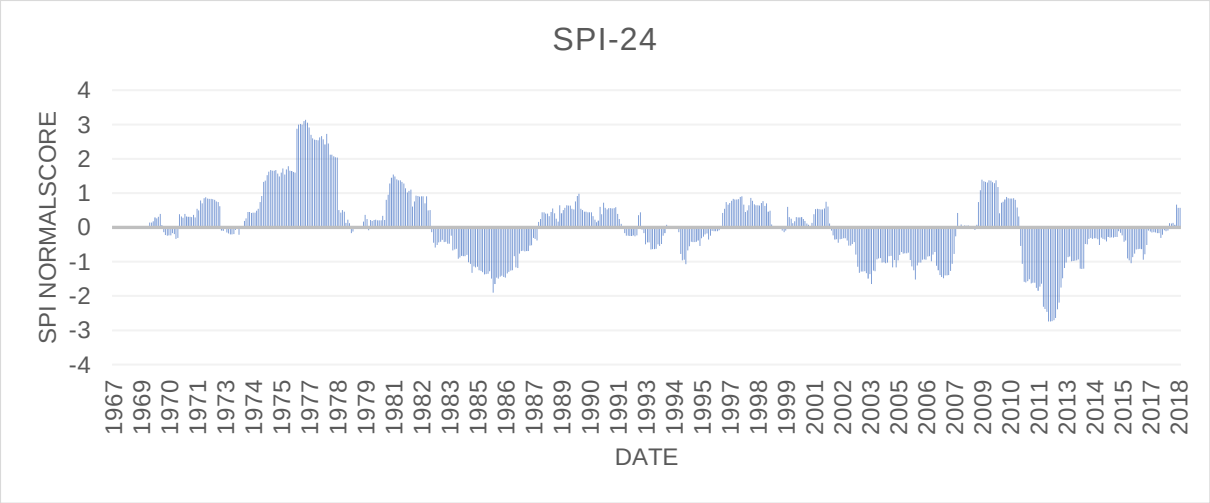

Figure 3: SPI-24 time series

2.5.4.1 SPI timescales

The SPI can characterise meteorological droughts on a range of timescales. Short timescales are related to soil moisture, whereas longer timescales are related to reservoir and groundwater storage (Keyantash, 2018). They quantify observed precipitation as a standardised departure from a certain probability distribution function that models the raw precipitation data (Keyantash, 2018).

2.5.4.1.1 SPI one-month to three-month

For drought analysis, short-term periods, such as one-month and three-month SPI values, may be misleading because of small deviations in SPI value on either side of the mean, which can lead to large positive and negative SPI values (Svoboda et al., 2012). Short-term

timescales are used to show monsoon regions and not to identify droughts (Svoboda et al., 2012).

2.5.4.1.2 SPI six-month

The length of an SPI period is of the same length as the historical data it is going to be compared to. A precipitation period of six months is being compared to the same six-month period of the historical record (Svoboda et al., 2012).

The six-month SPI shows seasonal to medium-term trends in precipitation, which are more sensitive to conditions than the PDSI at this scale. A six-month SPI can be very effective in showing the precipitation over distinct seasons (Svoboda et al., 2012). For example, a six-month SPI at the end of March would be a good indicator of the amount of precipitation that has fallen during the wet-season period from October through March for certain Mediterranean locales (Svoboda et al., 2012). Information from a six-month SPI may also be associated with anomalous streamflow and reservoir levels, depending on the region and time of year (Svoboda et al., 2012).

2.5.4.1.3 SPI nine-month

The nine-month SPI timescale shows inter-seasonal precipitation patterns over a medium timescale duration (Svoboda et al., 2012). This timescale period is the link between short-term seasonal drought and longer-term droughts that may become more intricate, such as hydrological or multi-year droughts (Svoboda et al., 2012).

2.5.4.1.4 SPI 12-month to 48-month

The SPI at longer timescales reflects long-term precipitation patterns. The 12-month SPI is a comparison of the precipitation for 12 consecutive months with that of the recorded precipitation in the same 12 consecutive months of all previous years of data (Svoboda et al., 2012). These timescales are the cumulative result of shorter periods that can be above or below normal. Longer SPIs gravitate toward zero unless a distinctive dry or wet trend is clear. Longer timescales are tied to reservoir levels, streamflows, and groundwater levels (Svoboda et al., 2012). SPI-12 to SPI-48 can be also an indicator for reduced groundwater recharge. Longer SPI timescales will have a greater correlation with groundwater levels.

2.5.4.2 Advantages and limitations of the SPI method

The greatest advantage of the SPI method is its simplicity as it is solely based on precipitation (Hayes et al., 1999). The method is also versatile and can be calculated on various timescales (Hayes et al., 1999; Bloomfield & Marchant, 2013). The versatility of the SPI method gives the SPI the capability to monitor conditions deemed to be important for both hydrological and agricultural applications (Hayes et al., 1999). The SPI was developed in Colorado, California but can be applied to any area that has 30 years of continuous precipitation data (McKee et al., 1993).

The SPI method has some limitations regarding the quality of the data in the sense that the accuracy of the SPI results is only as good as the data used to calculate the results (Hayes et al., 1999). The SPI in itself can also not identify areas or regions that are more prone to droughts (Hayes et al., 1999).

2.5.5 The Standardised Groundwater Level Index (SGI)

The SGI is a new drought index that was first introduced by Bloomfield and Marchant (2013). The SGI is to a degree based on the SPI method, but with two distinct differences. The SGI is based on groundwater levels whereas the SPI is based on precipitation (Bloomfield & Marchant, 2013; Haas & Birk, 2016; Jönson, 2017). The most distinctive difference between the methods is the manner in which the raw data is transformed and fitted to distributions. The SPI makes use of a fixed gamma distribution (or Pearson Type III) and the SGI of a non-parametric normal score transformation (Jönson, 2017).

Monthly groundwater level time series data is used for the calculation. This data is expressed as a hydrometric time series in groundwater level data (Bloomfield & Marchant, 2013). The index cannot measure groundwater levels at boreholes but can express the quantitative status of groundwater resources during a drought period (Bloomfield & Marchant, 2013). SGI results are expressed in the same value range as the SPI values after the transformation process as seen in Table 2.

Table 2: SGI value classification

SGI values	
SGI value	**Water level**
SGI +	High water table
SGI = 0	Normal water table
SGI -	Low water table

2.5.5.1 Advantages and limitations of the SGI method

The SGI is one of only a few indices that describe the state of the groundwater resources by analysing groundwater levels in boreholes. As mentioned, the SGI is to a degree based on the SPI method, therefore, these methods can be used in conjunction with one another to analyse drought periods.

The challenge regarding the SGI method is related to the availability of groundwater level data. Gaps in the data will lead to inaccurate results during the integration process (Bloomfield & Marchant, 2013). Groundwater level data in South Africa is very sparse on a public scale, only adding to a more challenging calculation process.

Figure 4 illustrates an SGI calculation where values below 0 indicate groundwater drought periods and values above 0 indicate normal to saturated groundwater levels.

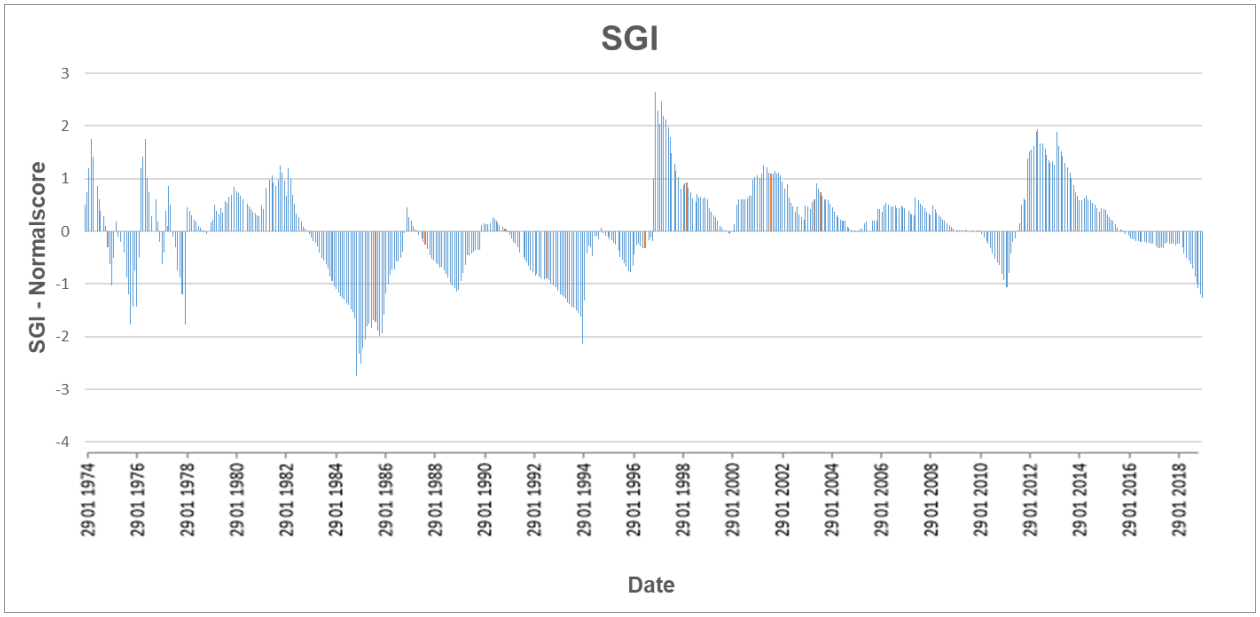

Figure 4: SGI time series illustration

2.5.6 Integration of the SPI and SGI methods

The SGI method is built on the SPI method, but the SGI uses groundwater level data as opposed to the SPI that is precipitation-based. In contrast with the SPI, the SGI is not suitable to fit the gamma distribution function (Jönson, 2017). The SGI makes use of a non-parametric normal score transformation, which leads to different distributions of the groundwater level time series. These normal scores assign a value to the groundwater level for each month respectively and is based on the rank of the groundwater level in the data set (Jönson, 2017). The normal scores are transformed by applying an inverse normal cumulative distribution

function. This results in the SGI values being in the same value range as the SPI values (between -3 and +3) (Jönson, 2017). SPI and SGI have to display the same trend in order to have an acceptable correlation, but an assumption can be made that the SGI trend may be delayed due to the infiltration of the water.

2.6 Historical droughts: drought indices applied in South Africa

There have been several drought studies conducted in South Africa, whether it be to measure the effects thereof or identifying droughts through the use of drought indices. Indices used in South Africa include the SPI, SPEI, PDSI and NDVI.

Botai *et al.,* (2017) conducted a study by evaluating dam levels and applying a SPI simulation to 23 rainfall stations across the Western Cape. Refer to Figure 5:

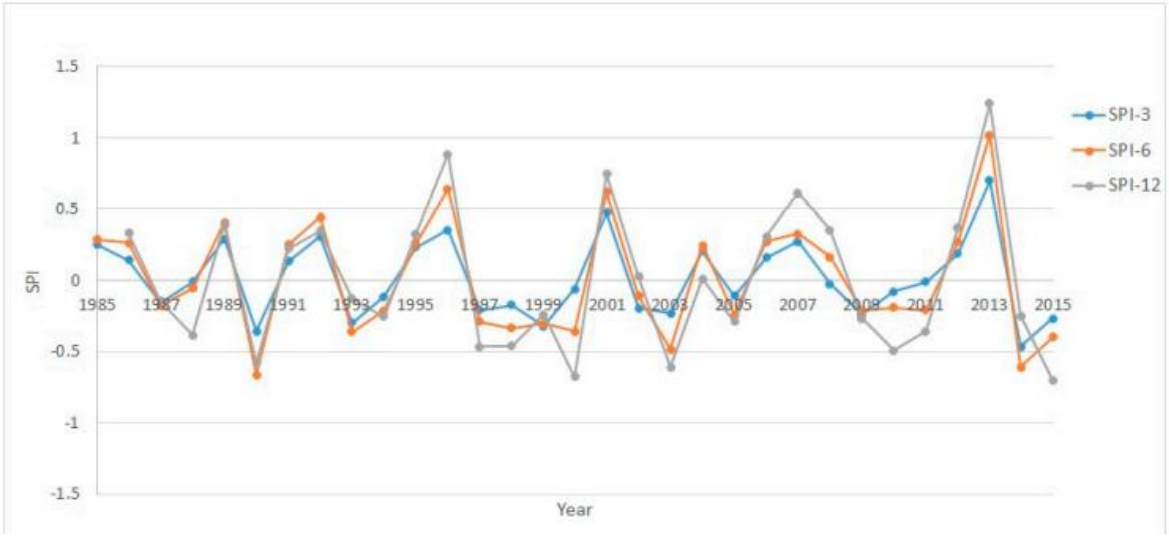

Figure 5: Annual average SPI time series data (Botai et al., 2017)

He concluded that between 1985 and 2016, the Western Cape experienced recurring minor meteorological, agricultural, and hydrological drought conditions (Botai et al., 2017). The most notable drought periods indicated in Figure 5 were between 1987–1988, 1991–1992, 1994–1995 and from 2015 across all timescales.

The interannual rainfall variability over central and eastern parts of South Africa is related to sea-surface temperature anomalies and the El Niño southern oscillation (Richard et al., 2001; Vogel & Drummond, 1993). Rouault *et al.,* (2019) conducted a study on the intensity and spatial extension of drought in South Africa. They conducted the study by dividing South Africa into sections. Gauteng (central South Africa) is referred to as area 6. Their study involved using the PDSI and SPI methods.

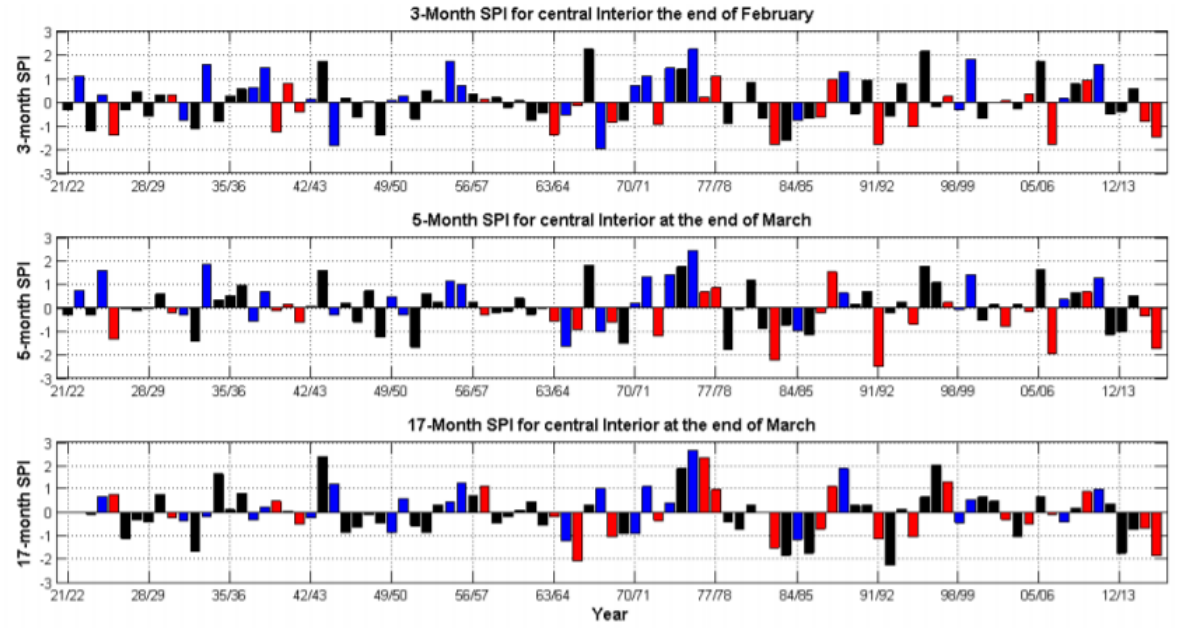

Figure 6: SPI-three, five- and 17-month timescales for central regions (Rouault et al., 2019)

Results of the study are indicated in Figure 6; the years affected by the El Niño southern oscillation were 1966, 1970, 1973, 1979, 1983, 1987, 1992 and 1995 (Rouault et al., 2019). Dry periods in area 6 or the Gauteng region were 1982, 1983 and 1984.

In the Free State and North West region, Botai *et al.,* (2016) conducted a study on the characteristics of drought. SPI and SPEI methods were used to characterise and analyse droughts in these provinces. Meteorological data from 14 weather stations within the Free State and North West were used to simulate the methods. Variations in drought intensity, frequency, duration, and severity were found in both provinces between 1985 and 2015. Botai *et al.,* (2016) divided this period into three decades, 1985–1994 (first decade), 1995–2004 (second decade) and 2005–2015 (third decade).

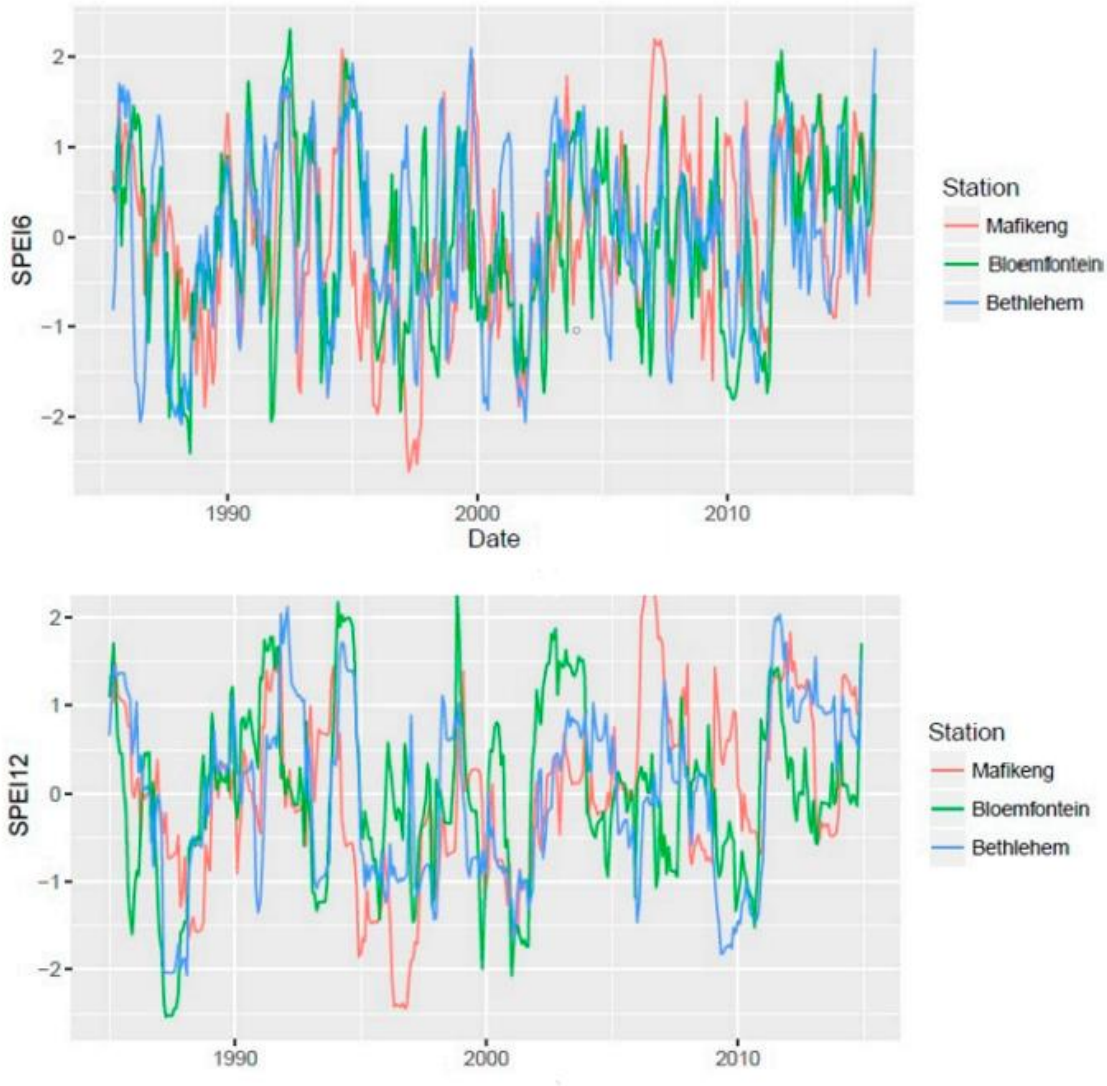

Figure 7: SPEI-6 and SPEI-12 time series (Botai et al., 2016)

The SPEI results are shown in Figure 7, Botai *et al.,* (2016) discovered that the SPI-6 drought index noted instances of moderate droughts, whereas the SPEI-6 presented a rise in moderate droughts for the first decade. However, in the second and third decades the simulations remained rather stable in both the Free State and North West (Botai et al., 2016).

The SPI-6 and SPEI-6 both illustrated intense droughts in Free State during the first and second decades (Botai et al., 2016). SPI-6 presented a rise in intense droughts through the first decade, becoming negligible during the second decade with a notable increase in the third decade (Botai et al., 2016). The SPEI-6 showed a rise in intense droughts during the first and second decades, but a decline in the third decade (Botai et al., 2016).

Based on the SPI-12, Botai *et al.,* (2016) found that moderate droughts increased from 1985 to 2015 in the Free State. The SPEI-12 also showed the same results as the SPI-12, except

for a slight decline in droughts during the third decade. Moderate drought occurrences remained high during the first and third decades, while decreasing during the second decade in North West (Botai et al., 2016). Both provinces showed similar trends for moderate droughts, moderate drought occurrences developed during the first and second decades with a decline in the third decade (Botai et al., 2016).

The SPI-12 results for the Free State displayed notable severe droughts during the third decade, whereas, the SPEI-12 detected severe droughts occurrences for both Free State and North West. According to the SPEI-12, Botai *et al.,* (2016) concluded that severe droughts occurred in the Free State and North West between 2005-2015 and 1995-2004. The SPI also detected severe to extreme drought periods for the same periods in both provinces.

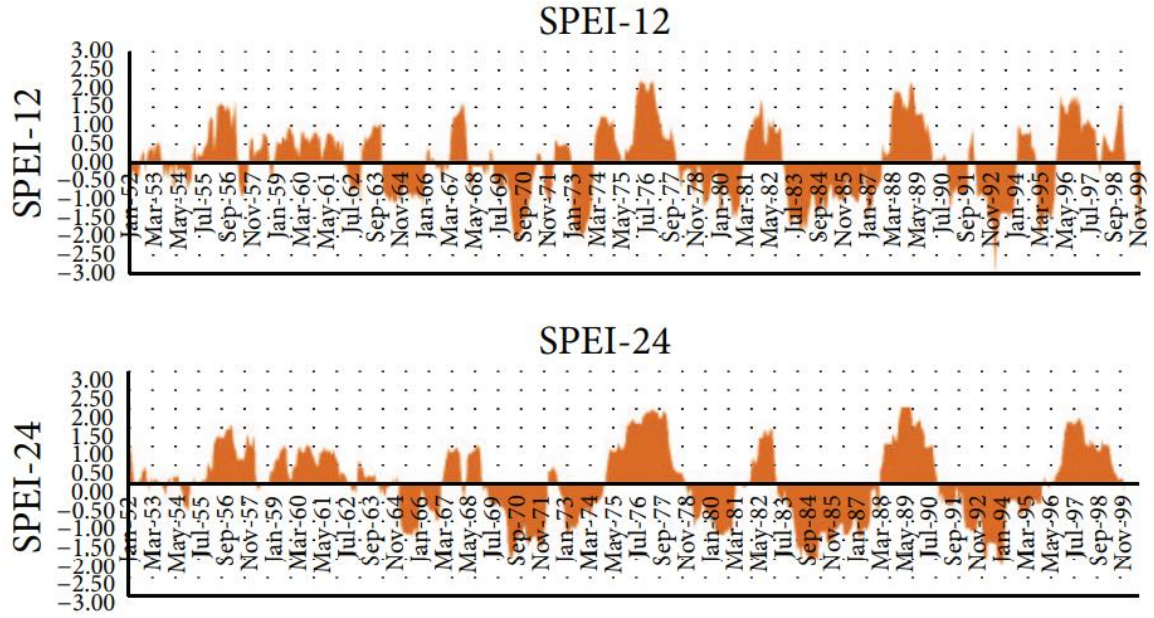

Figure 8: SPEI-12 and SPEI-24 simulation results (Edossa et al., 2014)

In addition to the findings of Botai *et al.,* (2016), Edossa *et al.,* (2014) conducted SPEI-12 and SPEI-24 in South Africa. Edossa *et al.,* (2014) conducted the SPEI analysis for a period spanning from 1952 to 1999 – results are shown in Figure 8. They found that the years 1953, 1964, 1969, 1973, 1977, 1983, and 1995 were the most affected by drought.

2.7 Groundwater balance methods

Groundwater balance models or recharge balance models are used to simulate groundwater level data, calculate recharge and other aquifer parameters. Groundwater balance models can be used to simulate recharge when fitting simulated groundwater levels to observed groundwater levels. Groundwater levels, therefore, can be simulated when the recharge and precipitation are known, given unreliable observed values.

Groundwater balance methods are not influenced by the various mechanisms controlling the individual components in the groundwater balance (Wang et al., 2010). The methods can be applied over a variety of timescales, extending from seconds to a global climate model over centuries (Wang et al., 2010). There are a few disadvantages associated with groundwater balance models, such as groundwater recharge, as recharge values lead to minor differences between large values, which can result in cumulative errors from component fluxes. This is common in arid and semi-arid areas, such as South Africa (Wang et al., 2010). Apart from recharge being the residual, another disadvantage is that groundwater balance methods cannot calculate some fluxes like evapotranspiration as some of the required mechanisms to do so are not available. Therefore, it is more beneficial to incorporate recharge as effective recharge where evapotranspiration and all other variables are already accounted for (Lerner et al., 1990; Scanlon et al., 2002).

The accuracy of groundwater balance methods in arid and semi-arid environments are inconsistent, because of limitations in soil moisture budgeting models in these environments. These models are susceptible to large errors in calculating recharge, attributed to potential evapotranspiration being greater than rainfall (Wang et al., 2010; Hendrickx and Walker, 1997).

2.7.1 The Water Table Fluctuation (WTF) method

Healy and Cook (2002) developed the WTF method and the method applies to unconfined aquifers. The method is based on the rise in groundwater levels because of recharge (Delin et al., 2007). Groundwater level variations are the basis of the WTF, because of recharge into the groundwater system (Varni et al., 2013). Specific yield is a crucial variable in the WTF method and in the calculation process (Varni et al., 2013).

This method is mostly used in areas with shallow water tables that can display sudden increases and decreases in water levels following rainfall events. The WTF method can only estimate recharge when water is received at the water table at a superior rate than it is leaving (Healy & Cook, 2002). There are also challenges when applying the WTF method to fractured

aquifers, as fractures serve as the primary conduits for water movement (Healy & Cook, 2002; Risser et al., 2005). Fractures are a small percentage of the storage in an aquifer, therefore, care must be taken when selecting the specific yield.

The WTF is a commonly used method, but the method must be applied to a scenario where data availability is sparse, as the WTF is based on changes in water level (change in groundwater storage).

Refer to Equation 4 (Healy & Cook, 2002):

$$R = \Delta S_{GW} = S_y \frac{dh}{dt}$$

Equation 4: Water table fluctuation

The WTF method requires S_y (specific yield), ΔS_{GW} (change in groundwater storage, which is the equivalent of recharge in this method) and the water level to calculate recharge.

R is groundwater recharge, ΔS_{GW} is the change in groundwater storage, *h* the water level and t is the time. As mentioned above, specific yield (S_y) at the fluctuating water table depth is required to calculate WTF.

Refer to Equation 5 (Healy, 2010):

$$S_y = \varphi - S_r$$

Equation 5: Specific yield

φ is porosity whereas, S_r is specific retention. Laboratory, water budget, water table response to recharge and aquifer tests are commonly used methods to determine specific yield (Varni et al., 2013). Laboratory methods determine S_y by measuring porosity and specific retention, and the application of Equation 5. Laboratory methods usually have large variability when determining S_y (Varni et al., 2013).

The calculation of S_y by making use of aquifer tests relies on the distance between the pumping and observation wells, as this method provides S_y measurements over large areas (Varni et al., 2013).

2.7.2 Saturated Volume Fluctuation method

The Saturated Volume Fluctuation (SVF) method includes inputs in relation to specific outputs for a limited time and describes the transformation in the system because of imbalances

between the various components (Adams et al., 2004). Imbalances in the system relate to the time it takes for recharge to occur. Catchment characteristics are thus required for the method to account for lag, arising from aspects such as different soil, geologies and drainage types (Adams et al., 2004).

The SVF method models the water level response of an aquifer, by using specific yield and effective recharge as parameters (Adams et al., 2004). The method is one of the most-applied groundwater balance methods, as it determines annual fluctuation in recharge and average annual precipitation (Adams et al., 2004).

The SVF method is suitable for most aquifer management applications and hydrological analysis. It is based on the saturated groundwater balance (Bredenkamp et al., 1995). Refer to Equation 6:

$$h[i] = h[i-1] + \frac{\%Recharge \times P[i]}{S_y} + \frac{Inflow[i] - Outflow[i]}{S_y \times Area}$$

Equation 6: Saturated volume fluctuation

S_y represents specific yield, $h[i]$ represents the head, which is the groundwater level for month i, $h[i-1]$ represents the previous calculated groundwater level value, $Inflow$ is the water inflow into the system, $Outflow$ represents the outflow or abstraction out of the system and $\%Recharge$ is the percentage of the rainfall allocated for recharge.

The SVF method simulates an aquifer based on recharge that in turn results in groundwater level fluctuations and the variation with time by simulating from an initial groundwater level record (Adams et al., 2004).

Certain assumptions are made when applying the SVF method regarding the characteristic of the catchment or area. The following assumptions are made:

- The aquifer is underlain by an aquiclude.
- ET losses are added to the abstraction or incorporated in the effective recharge.
- The calculated recharge will represent the effective percolation to groundwater resources (Adams et al., 2004).

The inflow and outflow of a system affect the total volume of the water stored over a specified time interval (Adams et al., 2004). Outflow in an aquifer represents the flow of springs, lateral flow (flow between aquifers), groundwater contribution to baseflow and abstraction (Adams et al., 2004). Inflow represents lateral flow and recharge (Adams et al., 2004).

Hydrological processes respond to rainfall events, but their combined response, affecting groundwater levels, are delayed (Adams et al., 2004). The combined response to a rainfall event is delayed, as groundwater levels may rise, but the effects thereof may remain for several months even if no rainfall events occurred after the initial event (Adams et al., 2004).

2.7.3 Cumulative Rainfall Departure method

The Cumulative Rainfall Departure (CRD) method is similar to the SVF method except for the fitting parameters. The CRD method, unlike the SVF method, struggles to determine aquifer statistics and cannot narrate water level trends (Adams et al., 2004).

The CRD calculates recharge as $Fraction(\ P[i]\ -\ Cutoff)$, where the fraction represents the recharge percentage, P represents your precipitation and $Cutoff$ represents the value below which no recharge occurs (Xu & Van Tonder, 2001).

Refer to Equation 7:

$$h[i] = h[i\ -1]\ + \frac{Fraction(\ P[i]\ -\ Cutoff)}{S_y} + \frac{Inflow[i]\ -\ Outflow[i]}{S_y\ \times\ Area}$$

Equation 7: The CRD method

2.7.4 Extended model for Aquifer Recharge and Soil Moisture Transport through the Unsaturated Hardrock

The Extended model for Aquifer Recharge and Soil Moisture Transport through the Unsaturated Hardrock (EARTH) method is a lumped parametric hydrological model (Van der Lee & Gehrels, 1990). The EARTH model is used to simulate soil water content, percolation/recharge, groundwater level fluctuations, precipitation and evapotranspiration (Wang et al., 2014).

Refer to Equation 8:

$$[i] = h[i-1]\ + \frac{h[i-1]}{Resistance} + \frac{Fraction\ \times\ P[i]}{S_y}$$

Equation 8: EARTH

The EARTH method includes the input parameter $Resistance$, which represents the specific drainage area's resistance.

2.7.5 Summary of groundwater balance models

All the aforementioned methods (SVF, CRD and EARTH) are very similar in terms of their general method of calculation. The results of each method are expected to be similar, except for minor differences in the simulated groundwater levels, as not all the input parameters are the same throughout the different methods (Refer to Table 3).

Table 3: Summary of groundwater balance models

Description	WTF	SVF	CRD	EARTH
Method description	The method is mainly based on the rise in groundwater levels because of recharge and is heavily reliant on the specific yield of an aquifer.	Simulates an aquifer based on recharge that results in groundwater level fluctuations and the variation with time by simulating from an initial groundwater level record. Assumption made while using the SVF method are: The aquifer is underlain by an aquiclude; ET losses are added to the abstraction or incorporated in the effective recharge; The calculated recharge will represent the effective percolation to groundwater resources (Adams et al., 2004).	The Cumulative Rainfall Departure (CRD) method is similar to the SVF method except for the fitting parameters. The CRD calculates recharge as $Fraction(\ P[i]\ -\ Cutoff)$, whereas the SVF makes use of $\%Recharge,$ as the percentage of the rainfall allocated for recharge.	Lumped parametric hydrological model. The EARTH method makes use of the input parameter $Resistance$ to calculate groundwater table fluctuations.
Use in South Africa	This method is mostly used in areas with shallow water tables that can display sudden increases and decreases in water levels following rainfall events. South Africa has diverse aquifer depths. Therefore, the method can be used if shallow aquifers are studied	The SVF method is suitable for most aquifer management applications and hydrological analysis within South Africa give the needed input parameters.	The CRD method struggles to determine aquifer statistics and cannot narrate water level trends as accurately as the SVF method. The main reason is due to differences in the input parameters and the accuracy and availability on public scale in South Africa..	EARTH model is a fairly simple method to used given the correct data. The main difficulty for all models is the availability of accurate data on public scale, and the same goes for the EARTH method.

Chapter 3 METHODOLOGY

3.1 Preamble

The development of a groundwater drought indicator for South Africa was based on existing data sets provided on a regional scale. Different lithologies relate to different aquifer parameters and boreholes in different lithologies were used to validate the capability of the groundwater drought indicator. Therefore, study areas were primarily based on their geologies. Figure 9 illustrates the methodological framework.

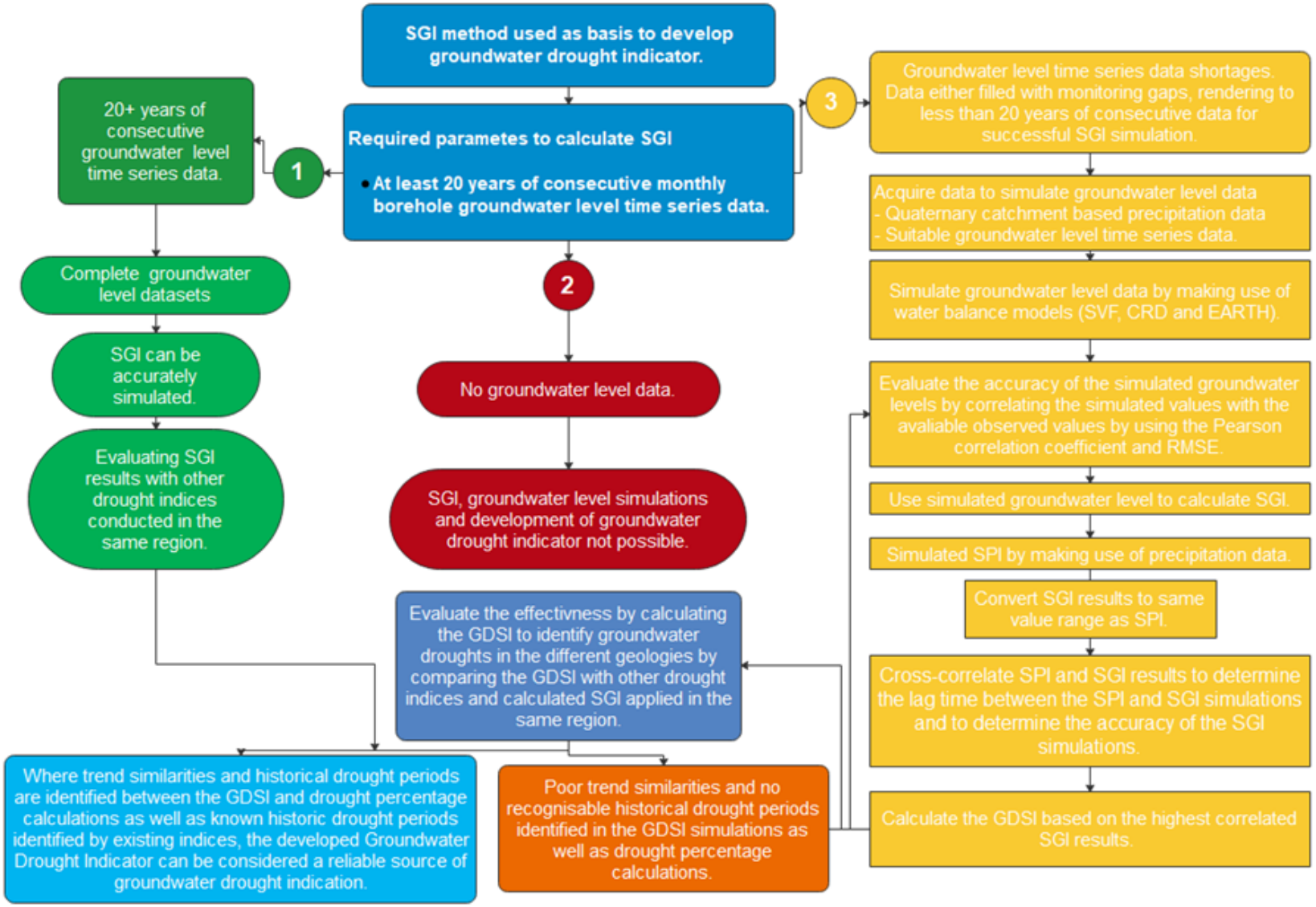

Figure 9: Methodological framework

3.2 Study area determination

Continuous groundwater level data is required as input to calculate the SGI over 20 years on a monthly time step. However, no sites that met these criteria were found in South Africa.

Rain gauges from the Department of Water and Sanitation (DWS) were identified but the associated monitoring data was also found to be periodic. These rain gauges were also too far away from study areas in order to simulate accurate results. The water resources of South Africa, Lesotho, and Swaziland (WR2012) provided complete, quaternary-catchment-based precipitation data files. These data files are generated by way of patching, combining various rainfall stations on quaternary scales, to populate continuous long-term precipitation data records. These precipitation files were used to simulate groundwater levels, given that there was at least periodic groundwater level monitoring data.

Groundwater level data was acquired from the DWS-CHART hydrogeological analysis program (CHART, 2021). CHART is a software program developed by DWS and is used to capture borehole groundwater level monitoring data, which is categorised according to the water management areas (WMA).

In order to simulate groundwater levels, additional parameters, other than precipitation data, are required. Effective recharge percentage values for the simulation were acquired from Groundwater Resources Assessment Phase Two project (GRAII) (DWAF, 2005), which was developed by the Department of Water Affairs and Forestry (DWAF). The GRAII database consists of recharge percentage values on quaternary catchments scale (see Figure 40 in Appendix A for GRAII recharge map of South Africa).

As illustrated in Figure 9 there were three possible paths to identifying likely study areas. Firstly, one can have an ideal scenario where all the required years of consecutive groundwater level time series data are available, but this was not the case for the whole of South Africa. The possibility of obtaining 20 to 30 years of consecutive groundwater level time series data is very scarce, as periodic monitoring were found at all of the borehole sites across South Africa.

Secondly, no groundwater level and precipitation data or no borehole data but precipitation data was found. Various sites either had no precipitation data or groundwater level data on which groundwater levels could be simulated.

The third methodological path was the only option that could be applied. Groundwater level time series data was available, but the data had gaps. The data either had monitoring gaps, or less than 20 years of consecutive data for successful SGI simulation.

With corresponding precipitation data and partial groundwater level data, groundwater balance models can be used to simulate groundwater level data. With the simulated groundwater level data, the SGI can be calculated.

Chapter 2.6 of *Historical droughts: drought indices applied in South Africa* was used to evaluate the accuracy of the SGI results in determining historical drought periods. Drought indices, such as the SPEI and SPI, were used to determine these historical droughts; all the drought indices previously used in South Africa are meteorologically based. Therefore, a lag time between the drought periods displayed on the SGI and the SPEI and SPI can be expected, due to factors, such as recharge rate, percolation, surface cover, and infiltration rate, which need to be considered.

The lag time between precipitation and the groundwater recharge was determined using cross-correlation between the SGI and SPI to determine the time as to when the groundwater droughts will occur in relation to meteorological drought periods.

3.3 Groundwater balance models

The SVF, CRD, and EARTH models were used to simulate groundwater levels. A model was designed to simulate groundwater level data on the basis of the WR2012 and GRAII data sets. The initial groundwater level simulation was conducted by applying the SVF, CRD and EARTH equations and making use of the WR2012 precipitation data and the available GRAII parameters, which included the recharge percentage and specific yield. Inflow, outflow, recharge, resistance, fraction, cut-off and specific yield are used as the initial fitting parameters dependent on the model required inputs.

After the initial simulation had been conducted, the simulated values were correlated with the known observed values. The Pearson correlation coefficient and the Root Mean Square Error (RMSE) were used to evaluate the accuracy of the simulation. The evaluation process could only be done by correlating the simulated values with the months that have been monitored. Therefore, the correlation had to be done in sections between the simulated values and known observed values.

In order to acquire the optimal Pearson correlation and the RMSE, the Excel Solver data analysis tool was used. The solver tool is an optimisation tool that runs a genetic algorithm.

The Genetic Algorithm (GA) is a stochastic search algorithm based on principles of competition between data, such as groundwater level monthly readings (Nijhout, 1997). The GA can also be defined as an optimisation technique based on the principles of selection (Nijhout, 1997). The solver tool, therefore, alters assumptions or parameters to determine the best possible result. Finally, after applying the solver tool the simulated groundwater level time series data was calculated and used to calculate the SGI.

3.4 SGI calculation

The SGI method makes use of monthly groundwater level readings to acquire a normal score value in order to represent the SGI results in the same value range as the SPI results.

The SGI was determined using an Excel model that converts the simulated groundwater levels to a value range similar to that of the SPI. Excel model formulas are described in Appendix B.

3.5 SPI calculation

The SPI was calculated making use of the SPI program to simulate meteorological droughts (Svoboda et al., 2012). The SPI is a drought index that has been widely used across the world for drought indication and is considered to be one of the most reliable indices. The SPI was used to simulate three-month, six-month, nine-month, 12-month, 24-month, 36-month, and 48-month meteorological drought timescales.

The respective rainfall records are fitted to a probability distribution, which is then transformed into a normal distribution in order for the mean SPI value to be zero for the location and desired period (Svoboda et al., 2012). Precipitation values are normalised using a probability distribution function, in order to see standard deviations from the median.

3.6 SGI and SPI results

The results of the SGI simulations are compared to the results of the SPI for the same period. The SGI may have a lag time compared to the SPI results as percolation needs to be considered when comparing the two indices.

By having the SGI results in the same value range as the SPI, the two data ranges can be compared to one another. Similarities and patterns between the data sets can be compared and ultimately be validated by known drought periods identified by other drought indices.

3.7 Groundwater Drought Strength Index (GDSI)

The SGI results are evaluated by comparing the results with other drought indices previously conducted in the same regions as well as the calculated SPI. In addition to comparing the results with other drought indices the SGI results were used to calculate the GDSI.

The GDSI is based on the RSI (relative strength index). RSI in the technical analysis of stocks, mainly used to determine strength of financial stock markets. The RSI methodology was transformed to calculate the GDSI, a stress indicator.

The GDSI is calculated as follows:

For each period an upward change U or downward change D is calculated. Upward periods are characterised by the close of the following month's SGI value (specified as now) being higher than the previous month's SGI value close (specified as previous), Refer to Equation 9:

$$U = Close_{now} - Close_{previous}$$

Equation 9: GDSI upward close period

Contrariwise, a down period is characterised by the close (specified as now) being lower than the previous close. Refer to Equation 10:

$$D = Close_{previous} - Close_{now}$$

Equation 10: GDSI downward close period

The average U and D values are calculated using an n-period defined as a smoothed or modified moving average (SMMA or MMA). The ratio of these averages is defined as groundwater drought strength (GDS). Refer to Equation 11:

$$GDS = \frac{SMMA(U,n)}{SMMA(D,n)}$$

Equation 11: Groundwater drought strength

The GDS factor is converted to the GDSI between 0 and 100%. Refer to Equation 12:

$$GDSI = 100 - \frac{100}{1 + GDS}$$

Equation 12: Groundwater Drought

Strength Index

The GDSI evaluates the SGI results in terms of the drought periods indicated. The values range between 0% and 100%, which are then used to identify increases and decreases in groundwater drought conditions. Groundwater drought periods were identified by working between 30% and 70%. Near 70% indicating no groundwater table stress and near 30% indicating increased stress on the groundwater table. The RSI is a reversion strategy that provides financial analysis on stock growth potential and serves as an indication tool as to when to buy and sell stocks. The GDSI is also a reversion strategy that provides groundwater table stress analysis on groundwater table fluctuations to indicate groundwater resource stress periods. The strategy gives a probable start, when GDSI indicates a drought cycle as the values moves from 70% or higher to a value equal to, or lower than 30%. As the GDSI moves above 70% the drought cycle concludes. The GDSI is calculated on a 12-month or one-year running window. The running window refers to the 12-month timeframe, measured on a scale from 0 to 100, with high and low levels marked at 70% and 30%.

Consequently, as the curve move from 70% (or above) to 30% (or below), the model indicated a drought period. The model is reversed where the curve moves from 30% (or below) to 70% (or above) indicating the end of the drought period. The cycle from above 70% to below 30% back to 70% is defined as a confirmation of a groundwater drought event.

Where the model moves from 70% or higher to lower percentage values but does not reach 30% or lower, the groundwater drought period is not confirmed. Hence, a period like this is described as a drought warning given as a percentage drought. A percentage drought is determined by evaluating the relation of the trend between 70% and 30% and can be defined as a moderate to serious drought, dependent on the percentage value. The percentage value is determined by taking the average of the curve (av) value between two points on the curve, taking the average and calculating the difference between the average and the recovery percentage (Rp) of 70%, divided by 40 (the points total between 70% and 30%). Refer to Equation 13:

$$Groundwater\ drought\ percentage\ = \frac{(Rp - av)}{40}$$

Equation 13: Groundwater drought percentage

The result of using the groundwater drought percentage will give an estimate of the average percentage point the period is from groundwater table recovery. Table 4 illustrates the drought percentage classification criteria.

Table 4: Groundwater drought percentage classification

Drought percentage range	Classification
0% – 39.9%	Slight groundwater table stress
40% – 59.9%	Moderate groundwater table stress
60% – 79.9%	Severe groundwater table stress
80% – 99.9%	Extreme to depleted groundwater table stress

Historical drought periods are evaluated in comparison to the GDSI results. The results of the GDSI are compared with existing drought indices, such as the SPI, SPEI and NDVI, simulated with adequate data sets (rainfall and/or groundwater levels). By comparing these indices, the validity of the proposed indicator can be verified. Where trend similarities and similar drought periods are found between the developed groundwater drought indicator and existing indices, the indicator can be considered a reliable source of groundwater drought indication.

3.8 Cross-correlation between SPI and SGI

The lag time between the SPI and SGI can be measured by means of cross-correlation, once the two indices are in the same value range (Quiero et al., 2015). Therefore, the cross-correlation process will determine the appropriate lag time for the SGI.

Groundwater level fluctuations may be delayed due to the infiltration of surface water to groundwater. Therefore, a lag time between groundwater level fluctuations may be present after a drought or wet period. Lag time will differ from region as geology, landcover, infiltration rates and the amount of recharge will differ. Determining the lag time will help in determining the end of a groundwater drought.

Cross-correlation was calculated to compare the SGI with calculated lag time to the GDSI. The model, SGI with calculated lag time or GDSI, which best defines groundwater droughts can be determined.

Chapter 4 CASE STUDIES

CASE STUDIES

4.1 Preamble

Study areas were selected according to their lithostratigraphy (geology). Areas of different lithostratigraphy were chosen in order to assess the credibility of the developed groundwater drought indicators to identify groundwater drought periods in different lithologies.

Areas with different lithostratigraphy were selected to determine groundwater droughts, but because of the lack of groundwater level data and sparseness of the data, the number of study areas suitable for use were limited. Most of the sites identified are in the water management areas (WMA), where the bulk of South Africa's mining and agricultural activities are situated.

4.2 Case studies areas

The identified study areas were primarily chosen based on available precipitation and groundwater level data. The sites with the most reliable data were chosen to correlate the monitored observed periods with the simulated groundwater levels.

Thirteen sites were identified across South Africa. Figure 10 displays the locations of the study areas. Figure 11 illustrates the decline in rainfall monitoring stations, which only emphasises the limitations on data availability. Table 5 to Table 17 presents an overview of all the study areas in terms of the locality, lithology/geology, borehole and rainfall data.

Sparse precipitation, borehole groundwater levels and flow gauging data records are evident across the whole of South Africa. Most of the study areas are in water management areas (WMA) where heavy industrial, mining and agricultural activities occur. Therefore, monitoring of rainfall and boreholes in these regions area is a requirement of the government environmental authorities, but is still lacking in terms of the completeness and continuity of data records.

The locality, geology, rainfall, and recharge values of each study area are important factors to take into account when simulating groundwater levels. As each parameter can have a deciding effect on the determination of groundwater drought periods, a detailed overview of each study can be seen Annexure A.

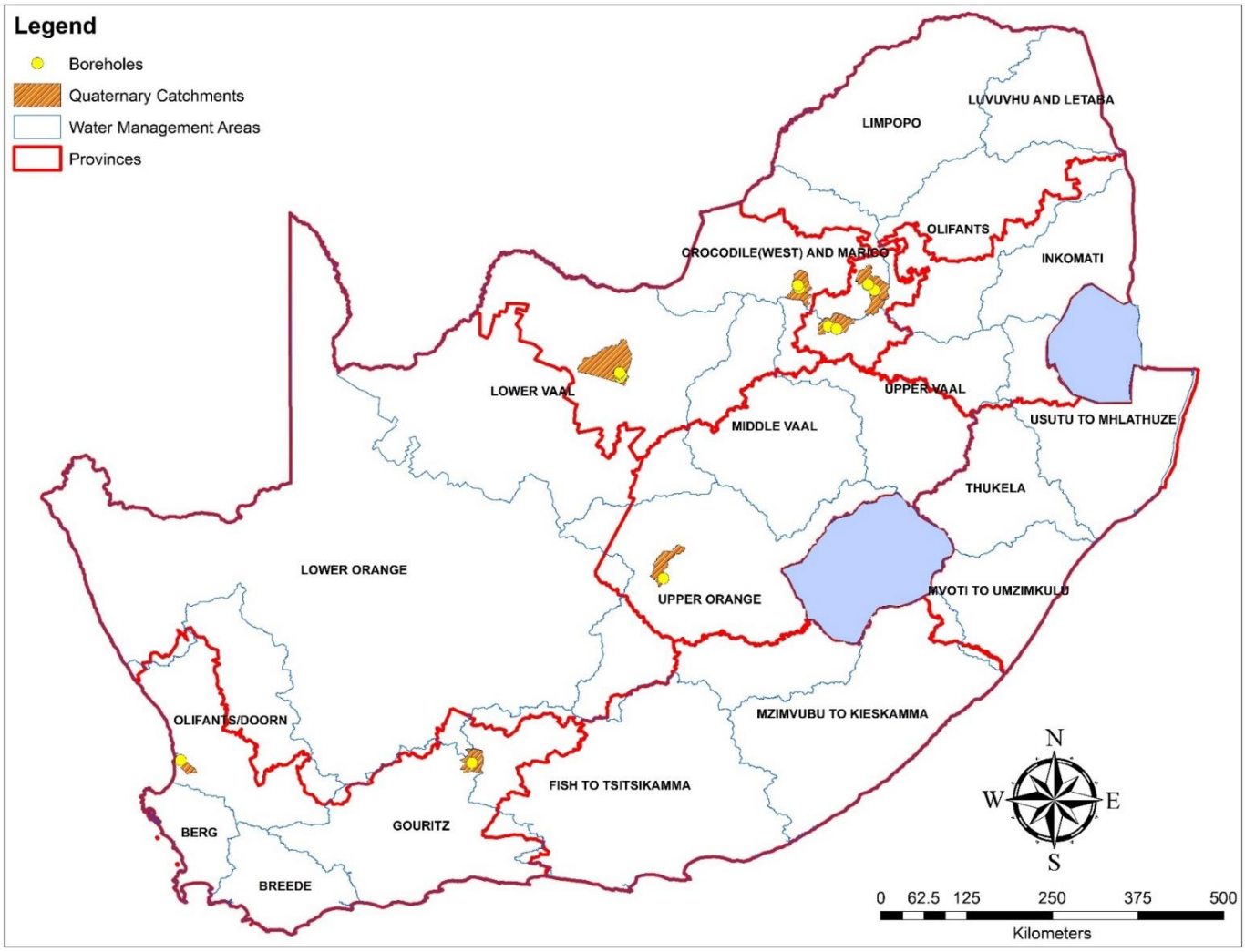

Figure 10: Identified study areas

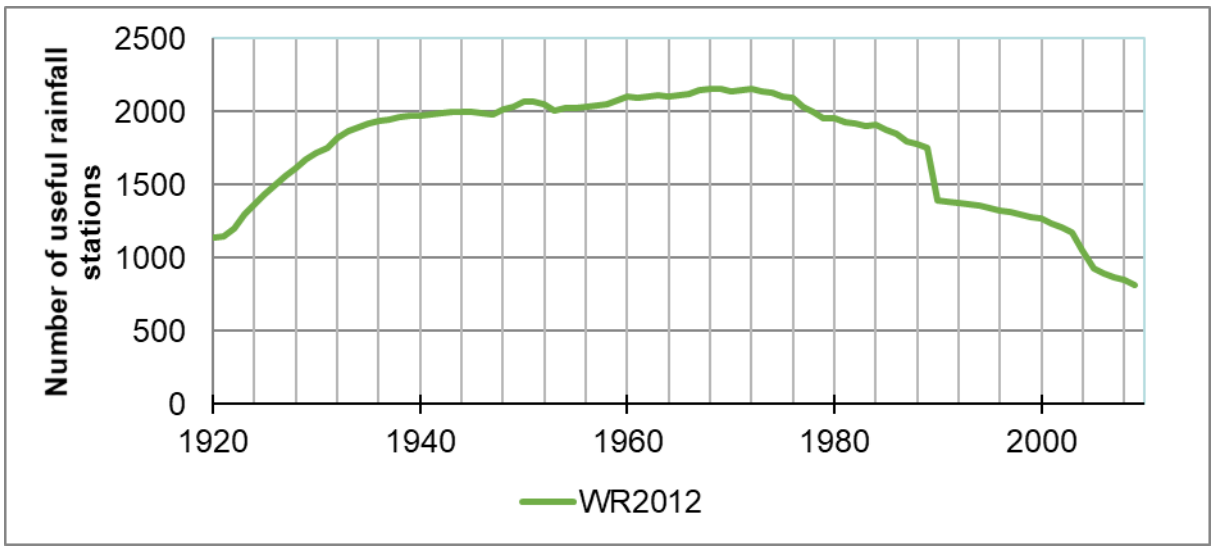

Figure 11: Decline of WR2012 rainfall stations (WR2012)

4.2.1 Teekloof Formation

Table 5: Summary of the Teekloof Formation

Locality	Lithostratigraphy	Geology description	Borehole ID	Borehole coordinates	Borehole data range	Rainfall zone	Rainfall data range	Average recharge (mm/a)
- Western Cape - Gouritz WMA - Quaternary catchment J21A	Teekloof Formation	Brownish-red and greenish-grey mudstone, subordinate siltstone, and sandstone	3222BC00151	-32.351; 22.583	1974-01-29 to 2018-11-07	J2A (WR2012)	1965-07-31to 2018-11-01	N/A

4.2.2 Loam and sandy loam

Table 6: Summary of the loam and sandy loam geology

Locality	Lithostratigraphy	Geology description	Borehole ID	Borehole coordinates	Borehole data range	Rainfall zone	Rainfall data range	Average recharge (mm/a)
- Western Cape Province - Olifants/Doorn WMA - Quaternary catchment G30E	N/A	Loam and sandy loam soil/pedology	33568	-32.306; 18.421	1987-11-07 to 2019-12-05	G3B (WR2012)	1900-01 to 2009-12	N/A

4.2.3 Malmani Subgroup

Table 7: Summary of the Malmani Subgroup

Locality	Lithostratigraphy	Geology description	Borehole ID	Borehole coordinates	Borehole data range	Rainfall zone	Rainfall data range	Average recharge (mm/a)
- Gauteng - Upper Vaal WMA - Quaternary catchment C23D	Malmani Subgroup	Dolomite, subordinate chert, minor carbonaceous shale, limestone, and quartzite	2627BC00051	-26.294; 27.666	1963-08-06 to 2018-05-15	C2E (WR2012)	1900-01 to 2009-12	3

4.2.4 ECCA Group

Table 8: Summary of the ECCA Group

Locality	Lithostratigraphy	Geology description	Borehole ID	Borehole coordinates	Borehole data range	Rainfall zone	Rainfall data range	Average recharge (mm/a)
- Gauteng - Upper Vaal WMA - Quaternary catchment C22A	ECCA Group	Shale, with sandstone-rich units present towards the basin margins in the south, west and north-east and coal seams in the north-east	2627BD00056	-26.327; 27.784	1986-02-09 to 2018-05-18	C2B (WR2012)	1900-01 to 2009-12	4 - 5

4.2.5 Hekpoort Formation

Table 9: Summary of the Hekpoort Formation

Locality	Lithostratigraphy	Geology description	Borehole ID	Borehole coordinates	Borehole data range	Rainfall zone	Rainfall data range	Average recharge (mm/a)
- Gauteng - Crocodile (West) and Marico WMA - Quaternary catchment A23A	Hekpoort Formation	Andesitic lava, subordinate pyroclastic rocks, minor quartzite, shale and conglomerate	036017	-25.805; 28.324	1986-02-28 to 2018-05-30	A2H (WR2012)	1900-01 to 2009-12	50

4.2.6 Strubenkop Formation

Table 10: Summary of the Strubenkop Formation

Locality	Lithostratigraphy	Geology description	Borehole ID	Borehole coordinates	Borehole data range	Rainfall zone	Rainfall data range	Average recharge (mm/a)
- Gauteng - Crocodile (West) and Marico WMA - Quaternary catchment A23E	Strubenkop Formation	Andesitic lava, subordinate pyroclastic rocks, minor quartzite, shale and conglomerate	Shale, subordinate siltstone, minor quartzite	2528CA00015	-25.729; 28.23	1967-01-01 to 2019-02-27	A2H (WR2012)	37

4.2.7 Diabase

Table 11: Summary of the diabase geology

Locality	Lithostratigraphy	Geology description	Borehole ID	Borehole coordinates	Borehole data range	Rainfall zone	Rainfall data range	Average recharge
- Gauteng - Crocodile (West) and Marico WMA - Quaternary catchment A23E	N/A	Diabase	11452	-25.726; 28.233	1956-06-14 to 2019-02-27	A2H (WR2012)	1900-01 to 2009-12	36

4.2.8 Kolobeng Norite

Table 12: Summary of the Kolobeng Norite

Locality	Lithostratigraphy	Geology description	Borehole ID	Borehole coordinates	Borehole data range	Rainfall zone	Rainfall data range	Average recharge (mm/a)
- North West - Crocodile (West) and Marico WMA - Quaternary catchment A22H	Kolobeng Norite	Norite, quartz norite	023502	-25.741; 27.232	1971-09-21 to 2013-09-04	A2F (WR2012)	1900-01 to 2009-12	32

4.2.9 Silverton Formation

Table 13: Summary of the Silverton Formation

Locality	Lithostratigraphy	Geology description	Borehole ID	Borehole coordinates	Borehole data range	Rainfall zone	Rainfall data range	Average decharge (mm/a)
- North West - Crocodile (West) and Marico WMA - Quaternary catchment A22G	Silverton Formation	Shale, minor limestone/dolomite, basalt, and tuff	2528CD00065	-25.783; 27.252	1976-05-21 to 2019-09-04	A2F (WR2012)	1900-01 to 2009-12	35

4.2.10 Vryburg Formation (quartzitic sandstone)

Table 14: Vryburg Formation (quartzitic sandstone)

Locality	Lithostratigraphy	Geology description	Borehole ID	Borehole coordinates	Borehole data range	Rainfall zone	Rainfall data range	Average recharge (mm/a)
- North West - Lower Vaal WMA - Quaternary catchment C32B	Vryburg Formation	Quartzitic sandstone, mudrock, andesitic/basaltic lava, siltstone, clastic dolomite/limestone, minor conglomerate, tuff and chert.	032611	-26.921; 24.691	1982-08-01 to 2018-11-29	C3C (WR2012)	1917-01 to 2009-12	14

4.2.11 Vryburg Formation (andesitic lava)

Table 15: Summary of the Vryburg Formation (andesitic lava)

Locality	Lithostratigraphy	Geology description	Borehole ID	Borehole coordinates	Borehole data range	Rainfall zone	Rainfall data range	Average recharge (mm/a)
- North West - Lower Vaal WMA - Quaternary catchment C32B	Vryburg Formation	Andesitic lava	2528DC00019	-26.937; 24.692	1981-09-11 to 2018-11-29	C3C (WR2012)	1917-01 to 2009-12	14 - 15

4.2.12 Dwyka Group

Table 16: Summary of the Dwyka Group

Locality	Lithostratigraphy	Geology description	Borehole ID	Borehole coordinates	Borehole data range	Rainfall zone	Rainfall data range	Average recharge (mm/a)
- North West - Lower Vaal WMA - Quaternary catchment C32B	Dwyka group	Diamictite (polymictic clasts, set in a poorly sorted, fine-grained matrix) with varved shale, mudstone with dropstones and fluvioglacial gravel common in the north	2624DC00026	-26.957; 24.718	1982-01-25 to 2020-08-20	C3C (WR2012)	1917-01 to 2009-12	14 - 15

4.2.13 Tierberg Formation

Table 17: Summary of the Tierberg Formation

Locality	Lithostratigraphy	Geology description	Borehole ID	Borehole coordinates	Borehole data range	Rainfall zone	Rainfall data range	Average recharge (mm/a)
- Free State - Upper Orange WMA - Quaternary catchment C51J	Tierberg Formation	Grey shale with interbedded siltstones in the upper part	2925CD00009	-29.750; 25.316	1967-02-17 to 1995-05-26	C5B (WR2012)	1900-01 to 2009-12	9

Chapter 5 RESULTS AND DISCUSSION

5.1 Introduction

The accuracy of the groundwater level simulations through groundwater balance models can only be correlated with the available observed data, as the observed data has incomplete data sets.

The observed and simulated groundwater levels, as well as the precipitation of each study area, are presented in Appendix A – Description of study areas.

Cross-correlation (r) between the SPI and SGI over different periods, three-month, six-month, nine-month, 12-month, 24-month, 36-month and 48-month periods, is calculated. Correlation values near +1 imply a positive relationship, near -1 a negative relationship and values at or close to 0 imply a weak or no linear relationship. Strong positive correlations refer to high precipitation and high groundwater level values, whereas a strong negative relationship refers to a high precipitation value and a low groundwater level value.

The three-, six- and nine-month correlations are more suited for seasonal to medium-term trends, whereas simulations of the 12-, 24-, 36- and 48-month periods are more suited to longer-term simulations, such as hydrogeological droughts (refer to 2.5). The 24-month and 48-month timescales are most commonly used to evaluate meteorological droughts in relation to hydrological droughts.

The simulations, trends and correlations are compared to known drought periods, identified by similar or other drought indices. Comparisons are conducted in order to evaluate the effectiveness of the developed groundwater drought indicator (refer to 4.2).

The groundwater level simulations for each study area were calculated using recharge groundwater balance models. Each model required parameters in order to simulate the groundwater levels, using either the SVF, CRD or EARTH recharge groundwater balance models. All the models gave similar results, with only slight differences in the correlations at each study area. The SVF and EARTH models were found to be the most consistent when simulating the groundwater levels of the study areas. Table 33 in Appendix B, indicates the model used and the respective parameters of the models used to simulate the groundwater levels at each study area. The specific yield, inflows, outflows, and resistance were fitting parameters and the solver analysis tool determined

the values of these parameters, whereas, the recharge percentage were only altered in accordance with the GRAII data.

Some study areas may indicate weak correlations, which only highlight the need for further analyses that take into account factors that are independent from precipitation. Particular attention should be paid to the physical properties of the land in the vicinity of the observation site, the hydraulic properties, and anthropogenic influences.

5.2 Groundwater simulations

The groundwater level simulation results, together with the rainfall and observed groundwater levels (see *Appendix A – Description of study areas* under the heading of *Rainfall and groundwater levels*), are displayed in Annexure A. The graphs in Annexure A also display the gaps in the observed groundwater level data, portraying the sparseness in groundwater level data and the absence of monitoring.

By using groundwater balance models, complete groundwater level data sets could be simulated (see *Appendix A – Description of study areas* under the heading of *Rainfall and groundwater levels*).

The simulated groundwater levels were evaluated by comparing the simulated values with the available observed values using the RMSE and the Pearson correlation coefficient. The results are given in Table 31.

Groundwater balance models SVF and EARTH gave similar results, differing only by decimal points, whereas the CRD method also gave similar results to the SVF and EARTH. However, on separate occasions the results were fairly inaccurate compared to the SVF and EARTH models, in terms of the RMSE and Pearson correlation coefficient.

5.3 SPI and SGI simulations

The 24-month and 48-month SPI simulations are the two preferred timescales to represent hydrogeological droughts (Svoboda et al., 2012). The 24-month and 48-month SPI and the subsequent SGI results are displayed in Figure 12 to Figure 24.

5.3.1 SPI and SGI Results

5.3.1.1 Teekloof Formation

The SPI and SGI results of the Teekloof Formation are displayed in Figure 12. The SPI 24-month and 48-month timescales are plotted with the SGI results.

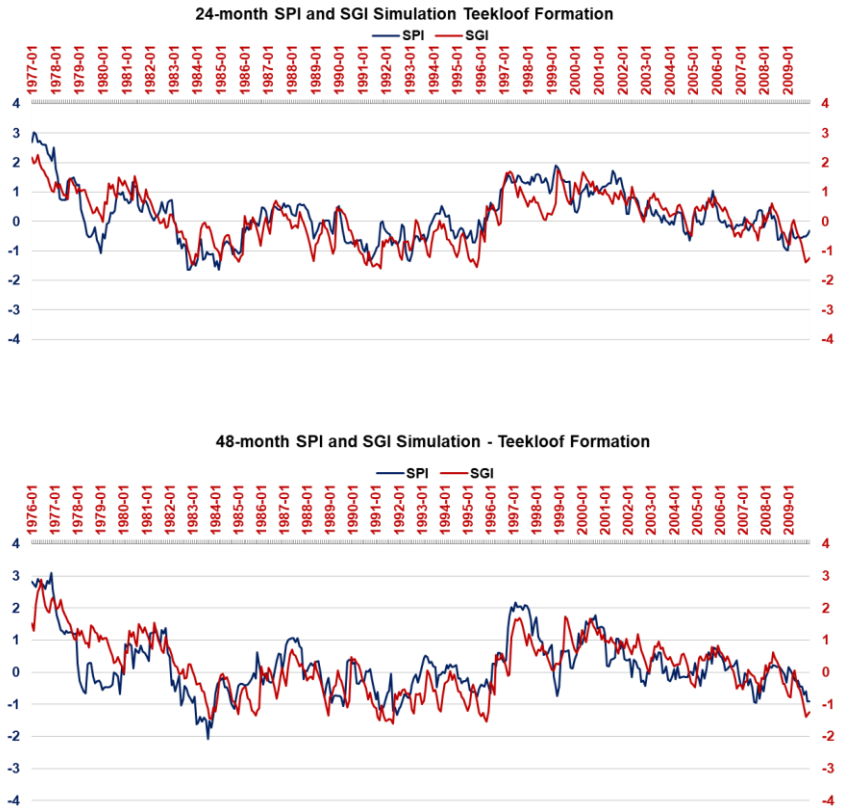

Figure 12: Teekloof formation SPI and SGI results

The SPI and SGI results have a very similar trend in terms of value as seen in Figure 12. It is evident that the SGI tends to have erratic readings as the SPI increases and decreases at some intervals. It should be noted that an increase in precipitation often leads to a slightly delayed increase in groundwater levels. Therefore, it can be assumed that the groundwater recharge rate is relatively high in this geology.

5.3.1.2 Loam and sandy loam geology

The SPI and SGI results of the loam and sandy loam geology/pedology are displayed in Figure 13. The SPI 24-month and 48-month timescales are plotted together with the SGI results.

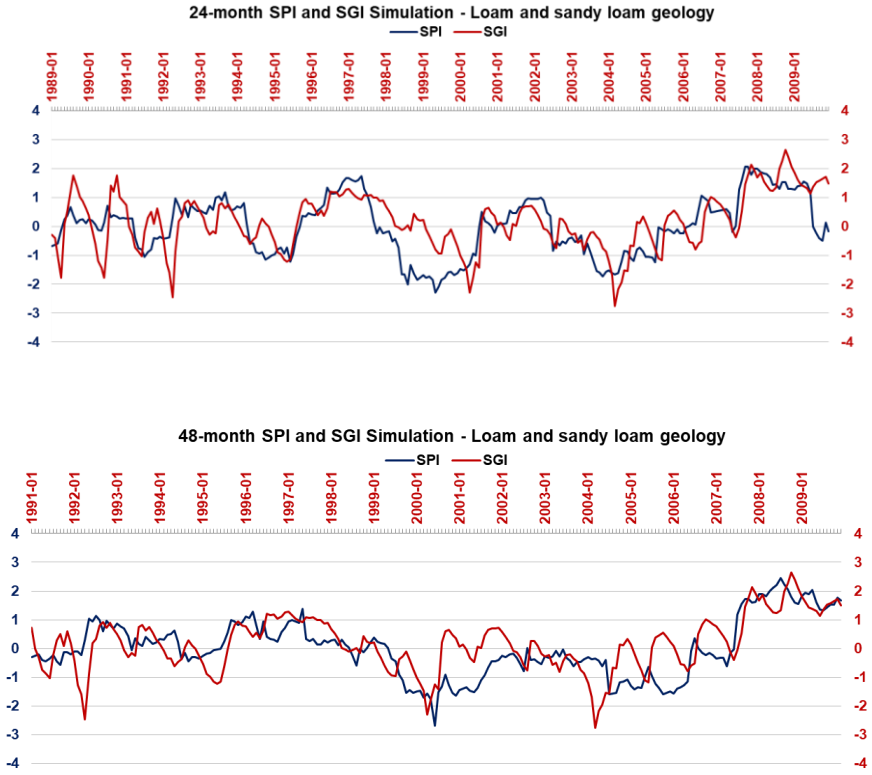

Figure 13: Loam and sandy loam geology SPI and SGI results

Correlation between the SPI and SGI values is evident in Figure 13 for both the 24-month and 48-month timescales. However, where there are slight changes in the SPI values, the SGI indicated extreme changes in values. As the SPI (overall precipitation) values increase and decreases, a delayed and very erratic response in SGI is noted.

5.3.1.3 Malmani Subgroup

The SPI and SGI results for the Malmani Subgroup are displayed in Figure 14. Similar to the loam and sandy loam geology, the SGI responds erratically to increases and decreases in precipitation.

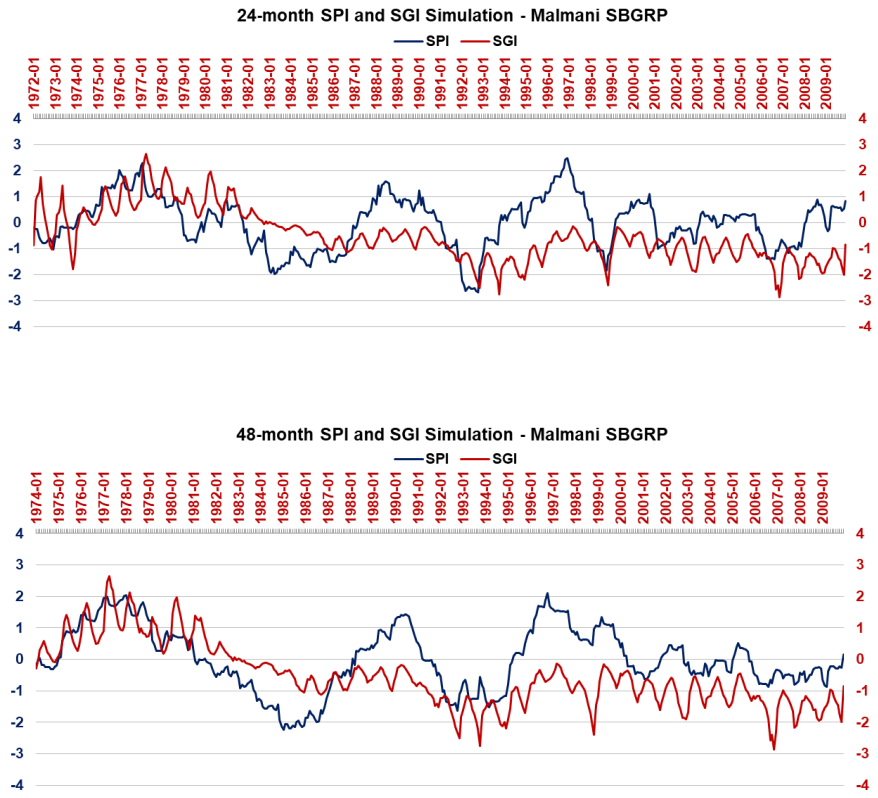

Figure 14: Malmani Subgroup SPI and SGI results

The drought periods are identifiable in Figure 14, however similar to the loam and sandy loam geology, the duration of groundwater drought periods is unclear, as the SGI in some periods is irregular. It is irregular in the sense of erratic readings in comparison to the SPI, where the drought durations are more recognisable.

5.3.1.4 ECCA Group

The ECCA Group SPI and SGI results are displayed in Figure 15. Both SPI simulations (24-month and 48-month) records start at 1986-05 due to the groundwater level data has a lengthier timeseries than rainfall data. being longer

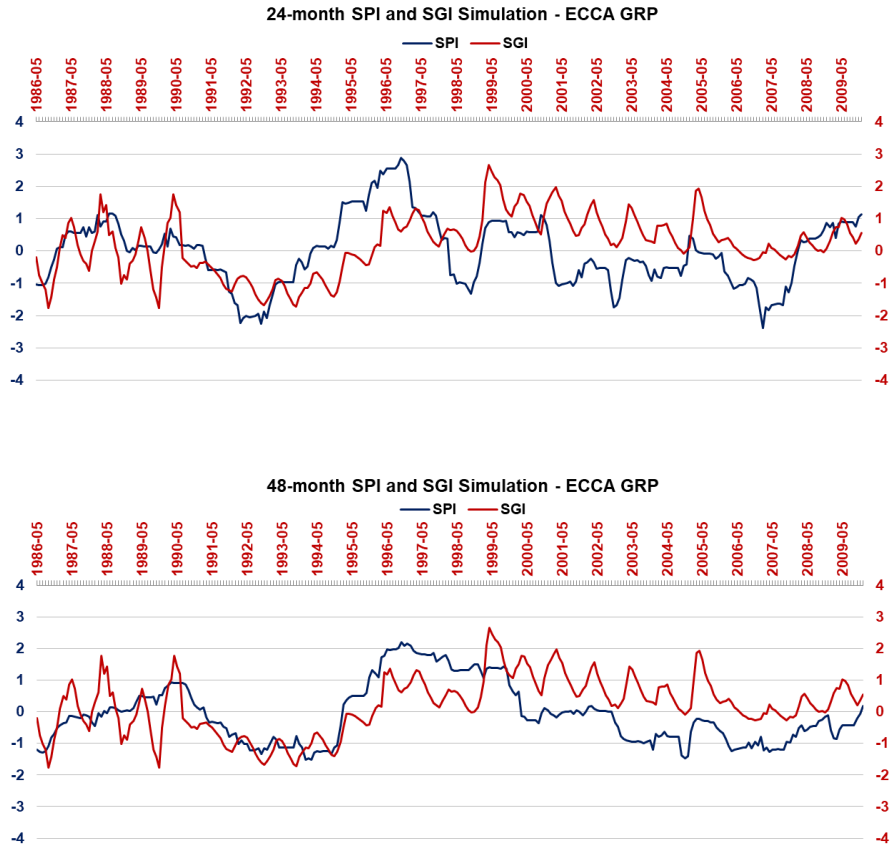

Figure 15: ECCA Group SPI and SGI results

A decline in the SPI ultimately displays a decline in the amount of precipitation leading to a decline in the SGI values as well.

5.3.1.5 Hekpoort Formation

The Hekpoort SPI and SGI results are shown in Figure 16. Both the SPI and SGI results indicate clear drought periods for this region.

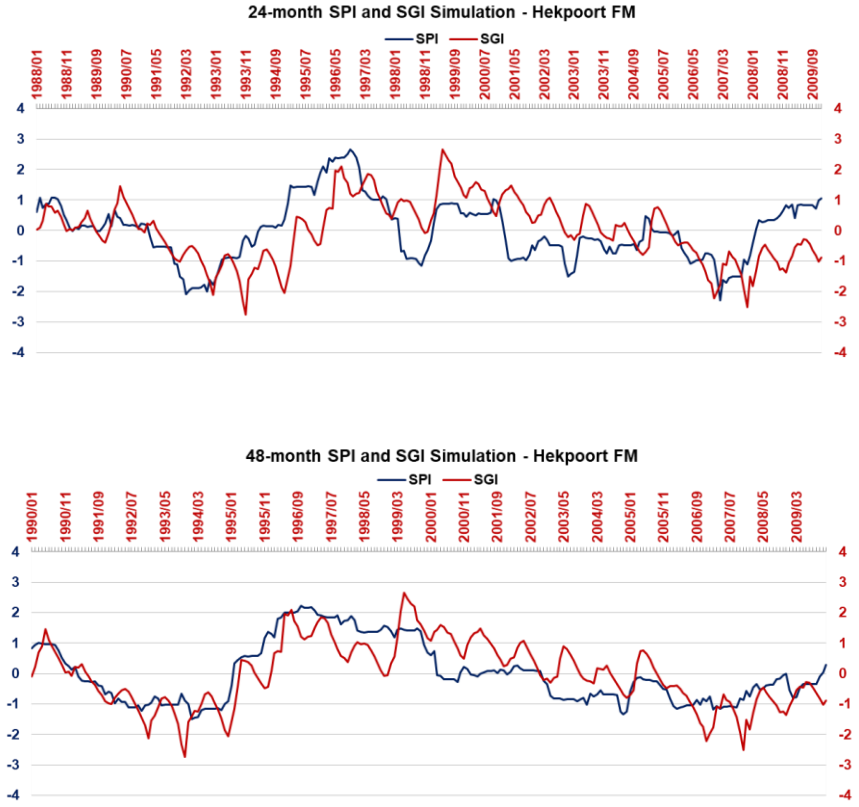

Figure 16: Hekpoort SPI and SGI results

In Figure 16 the SPI and SGI display a similar trend, except for the slightly delayed SGI. It should be noted that the SGI tends to increase and decrease as the SPI increases or decreases.

5.3.1.6 Strubenkop Formation

SPI and SGI results for the Strubenkop Formation are displayed in Figure 17. In both diagrams in Figure 17 it is evident that there is an ample delay between the SPI and SGI results.

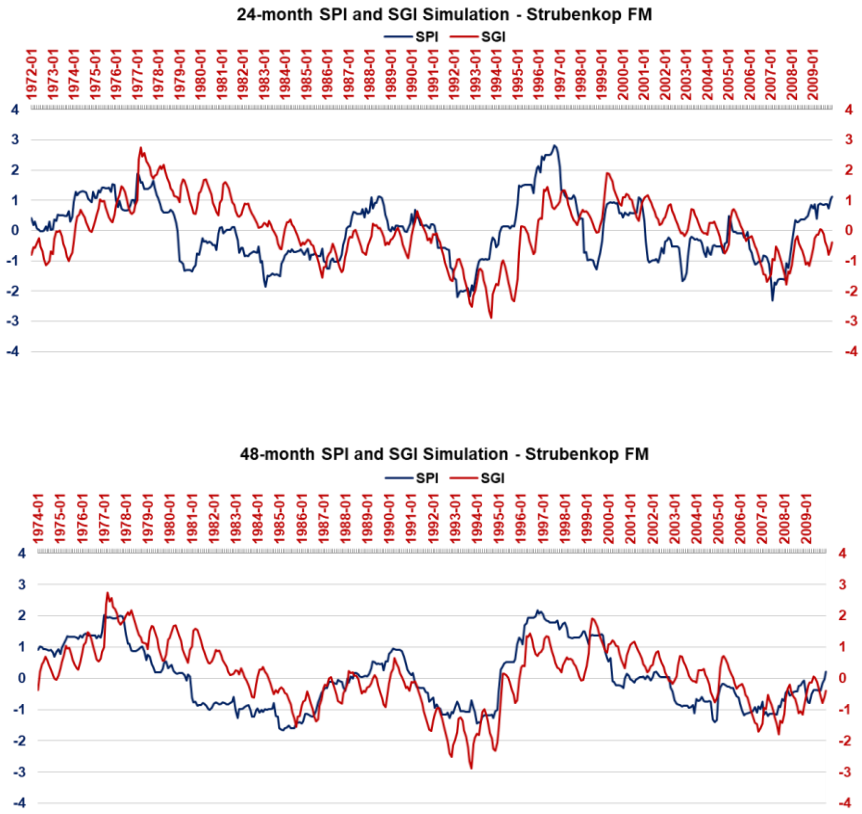

Figure 17: Strubenkop Formation SPI and SGI results

As seen in the previous geologies, the increase in SPI leads to an increase in the SGI. The 24-month diagram follows a similar trend to the SPI although it gives erratic readings.

5.3.1.7 Diabase geology

Figure 18 displays the SPI and SGI results for the diabase geology. The SGI displays the same trend as the SPI in terms of the value, with a notable delay in time between the SPI and SGI.

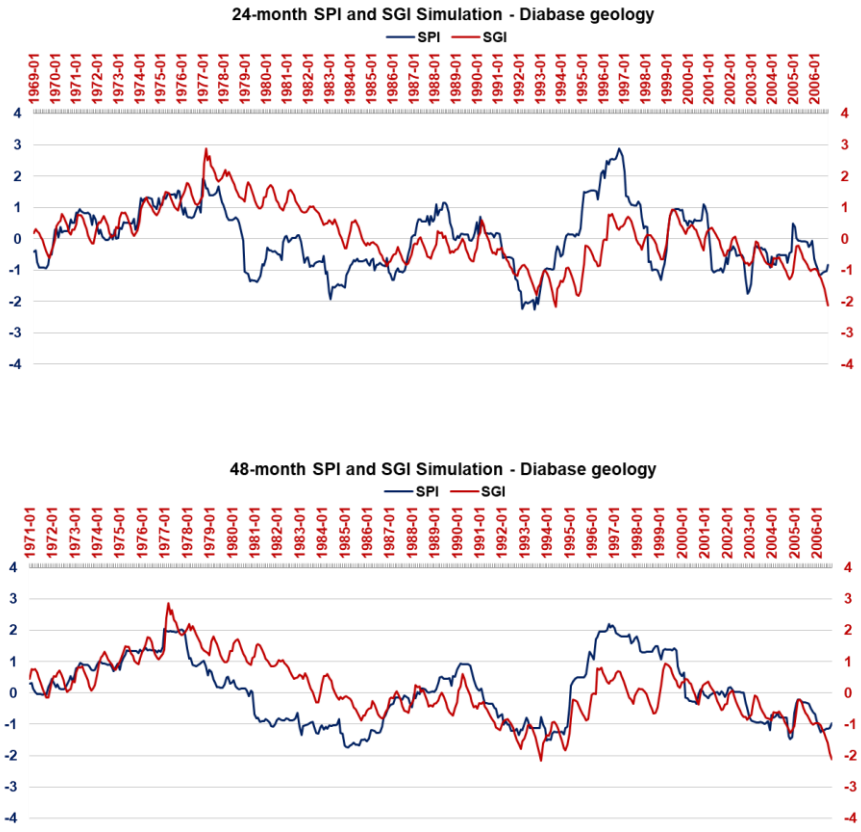

Figure 18: Diabase geology SPI and SGI results

Declines in SPI and SGI are noted during similar periods. The SGI values increase and decrease as the SPI does with a very slight delay. Therefore, a rise in groundwater level is related to the increase in precipitation for this region as well.

5.3.1.8 Kolobeng Norite

The SPI and SGI results of the Kolobeng Norite indicate a fairly similar trend, with a delay between the SPI and SGI. Irregularities between the SGI and SPI are found between 2001 to 2009-12, as the SGI increases rapidly in comparison to the SPI.

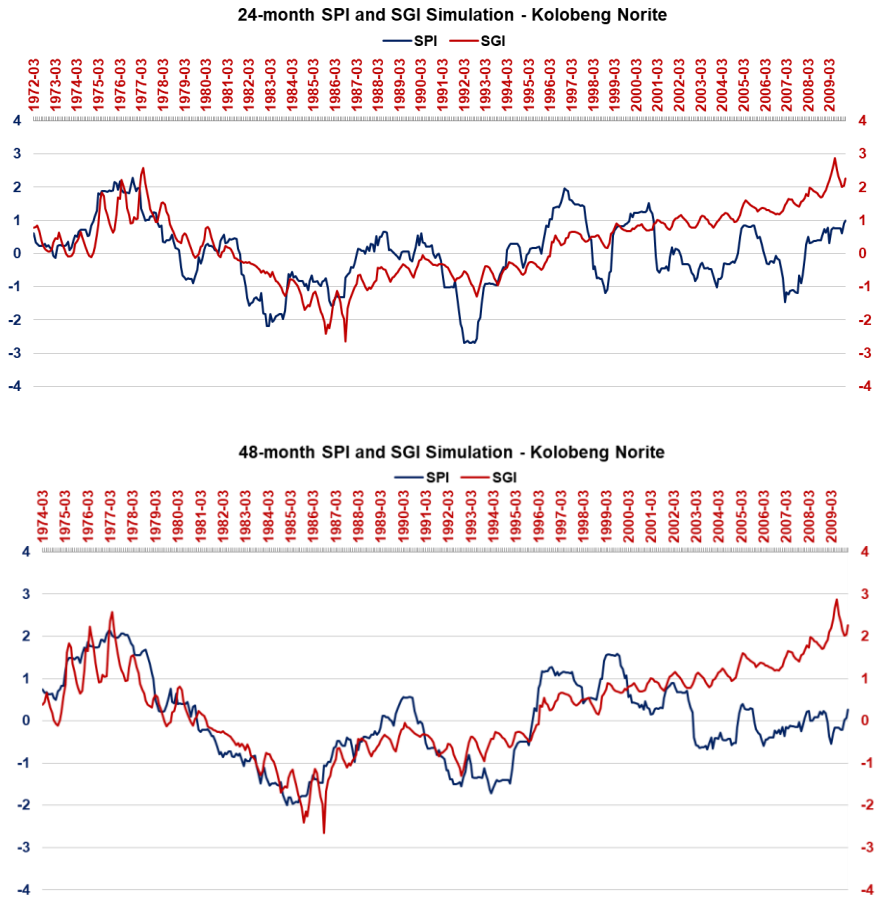

Figure 19: Kolobeng Norite SPI and SGI results

Figure 19 indicates a similar trend in SPI and SGI for both the 24- and 48-month simulations. However, an increase in SGI from 2000 to 2009 is noted, which can be due to extreme rainfall events that occurred between 1997 and 2001, which, in turn, led to high groundwater tables.

5.3.1.9 Silverton Formation

The SPI and SGI results are displayed on Figure 20. The SGI for the first decade increases as the precipitation increases, but from there on a steady decline in SGI is observed.

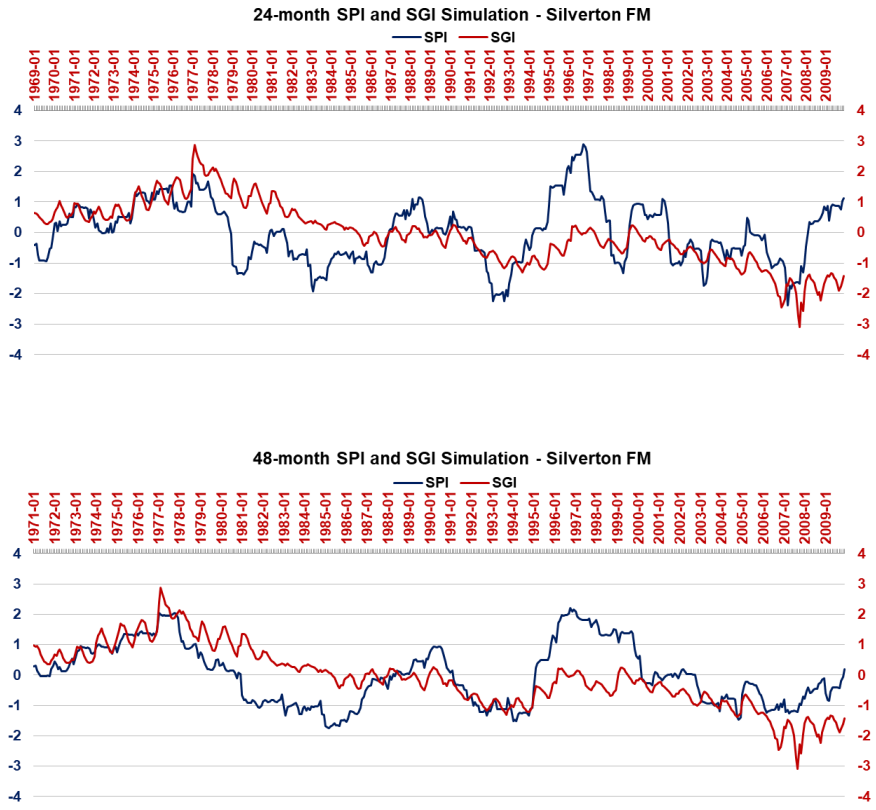

Figure 20: Silverton Formation SPI and SGI results

The 48-month simulation indicates a smoother representation of the SGI results in comparison to the SPI results. Increases in precipitation led to an increase in SGI but not as much in comparison to the SPI.

5.3.1.10 Vryburg Formation (andesitic lava)

The SPI and SGI results of the Vryburg Formation (andesitic lava) are shown in Figure 21. The SGI values of the 24-month simulation tend to rise as the SPI/precipitation does, there is however a substantial delay when the SGI values rise in comparison to the SPI. The 48-month simulation has the same trend as the 24-month, but the response of the SGI in comparison to the SPI is more rapid.

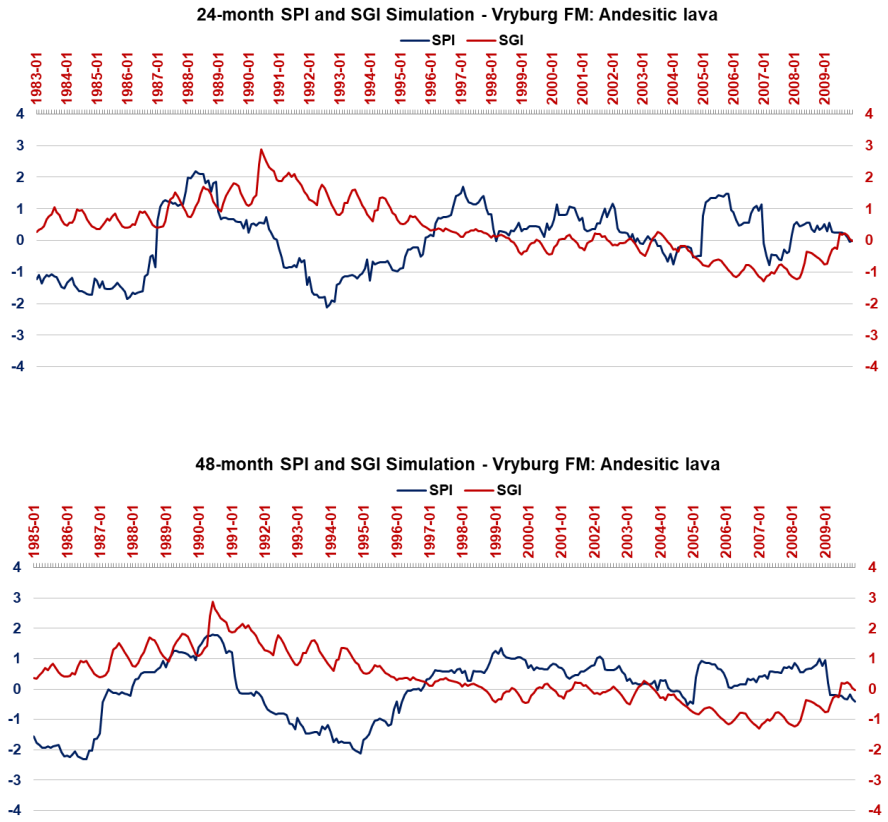

Figure 21: Vryburg Formation (andesitic lava) SPI and SGI results

The SGI does not indicate any significant decline in value, and does not decrease to the extent that the SPI decreases.

5.3.1.11 Dwyka Group

Figure 22 indicates the SPI and SGI results for the Dwyka Group. The SGI increases and the SPI increases with a notable delay between the SPI and SGI.

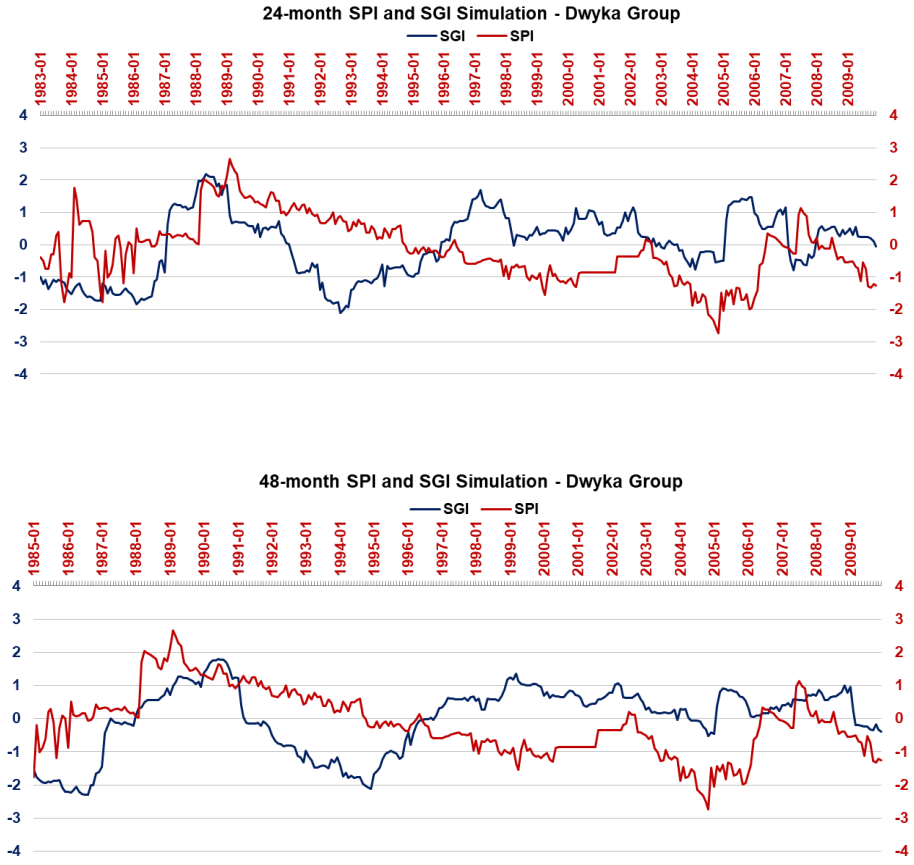

Figure 22: Dwyka Group SPI and SGI results

The trend between the SPI and SGI is similar and contradictory in different periods. Both indices increase and decrease at the same time during the first decade, but during the second decade the SGI decreases as the SPI increases. The 2005–2015 period also displays a decrease in SPI and SGI values from 2005 to 2006 and then from 2008 to 2009.

5.3.1.12 Vryburg Formation (quartzitic sandstone)

SGI increases and decreases in relation to the SPI, as seen in Figure 23. The response time of the SGI in comparison to the SPI decreases from the 24-month to 48-month simulations. A decline in precipitation often leads to a decline in the SGI.

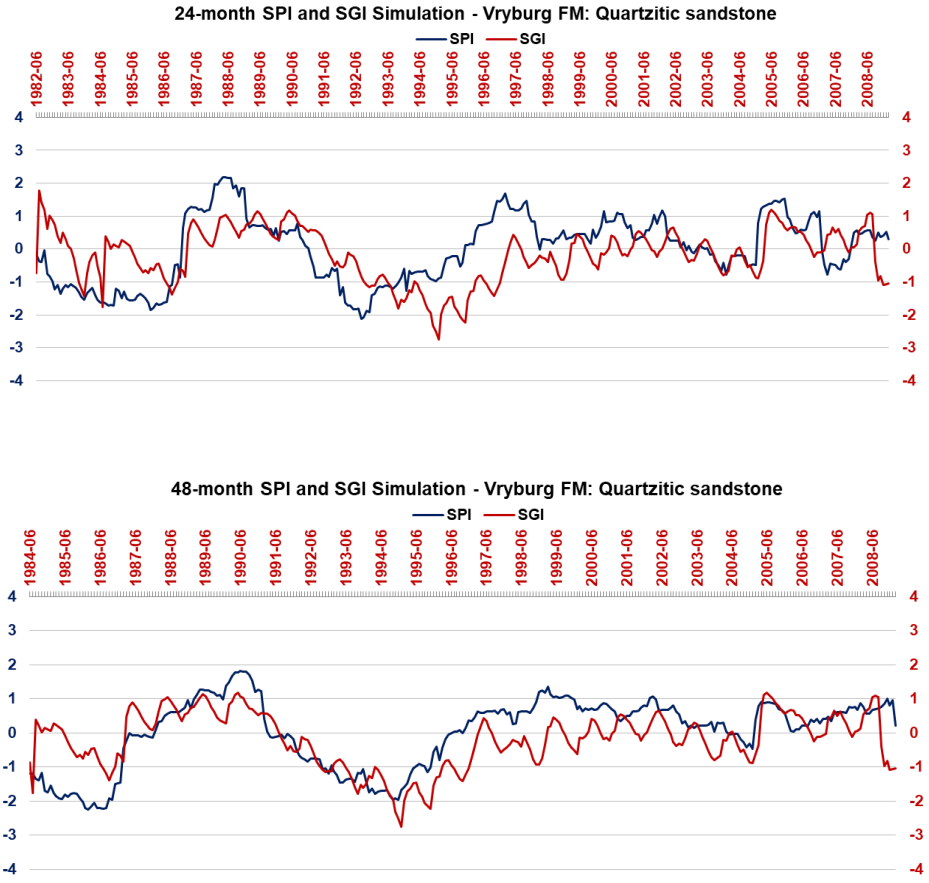

Figure 23: Vryburg Formation (quartzitic sandstone) SPI and SGI results

The 48-month diagram indicates similarities with the SPI results. As the SPI increases and decreases, the SGI follows the same path, however the SGI increases and decreases erratically with various fluctuations in value whereas the SPI is smooth.

5.3.1.13 Tierberg Formation

The Tierberg Formation groundwater level data only ranges from 1967 to 1995. The results of the SPI and SGI simulation are indicated in Figure 24.

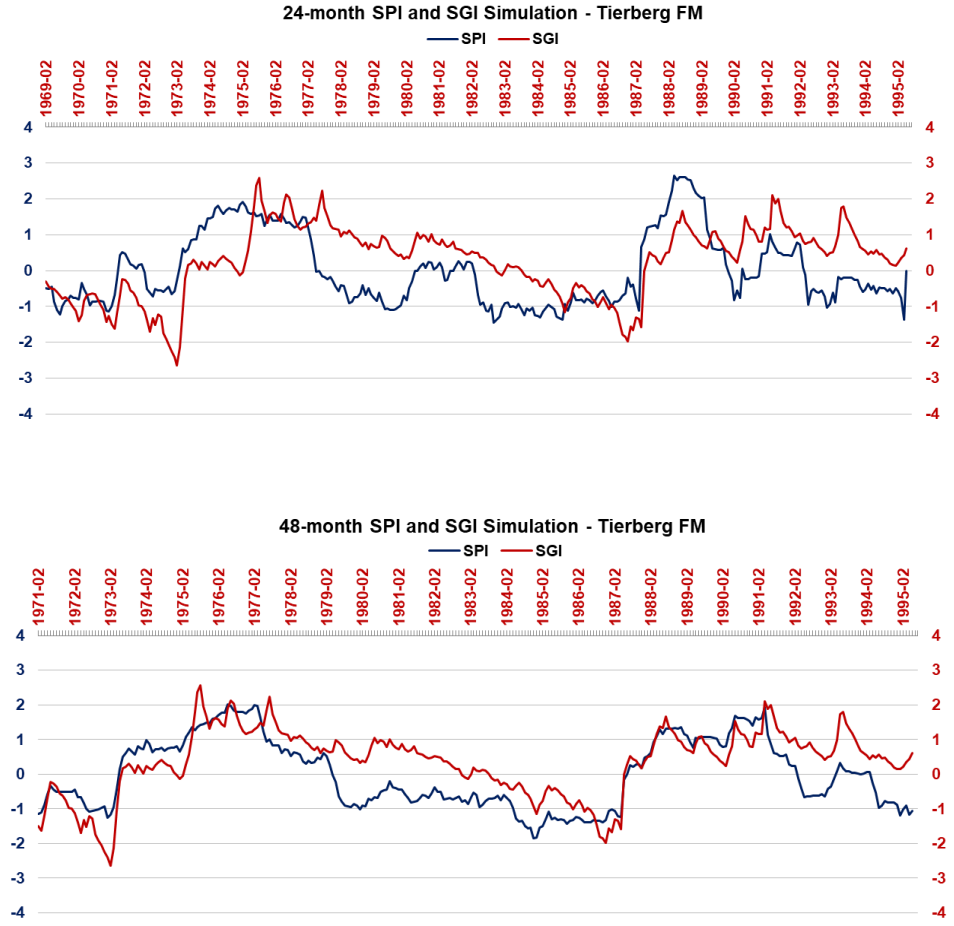

Figure 24: Tierberg Formation SPI and SGI results

An increase in SPI leads to an increase in SGI and a decrease in SPI leads to a decrease in SGI. The 24-month simulation represents these increases and decreases well, but the 48-month simulation indicates the changes in SGI with an improved comparison toward the SPI.

5.3.2 SPI and SGI lag time results

5.3.2.1 Teekloof Formation: Borehole 3222BC00151 (J21A)

The study area is J21A where borehole 3222BC00151 is situated. Precipitation data used in the simulations is the WR2012 rainfall data sets.

Table 18: Borehole 3222BC00151 cross-correlation

SPI and SGI cross-correlation – borehole 3222BC00151 (J21A)		
Calculated time period	Correlation value	Lag time
Three-month	0.38	1 month
Six-month	0.54	1 month
Nine-month	0.65	1 month
12-month	0.72	1 months
24-month	0.87	2 months
36-month	0.88	1 months
48-month	0.77	1 months

A low correlation was simulated for the three-month and six-month period. The 12-month and nine-month periods illustrate higher correlation values than the previous time periods, whereas, the 24-month period shows the best correlation between the SPI and SGI values. The 24-month and the 36-month timescale periods show longer-term droughts, such as hydrological or hydrogeological droughts. Longer-term simulations, such as the 24-month and 36-month periods, are more suited to simulation groundwater droughts.

Lag time across all simulations is very consistent, which gives rise to an accurate representation of the geology. The 24 and 36-month periods, with a lag time of two months and one month respectively, correspond well to the Teekloof mudstone and sandstone geologies. The mudstones (Teekloof Formation comprises 75 to 80% mudstone) promote fluid flow between surface environments, which leads to the area only having a lag time of one to two months.

5.3.2.2 Loam and sandy loam: Borehole 33568 (G30E)

The groundwater level data for G30E (033568) ranges from 1987-12 to 2009-12. No groundwater level data was recorded between 1988-01 and 2002-10. This gives rise to the low correlation, as there were more frequent data gaps and barely 20 years of data.

Table 19: Borehole 033568 cross-correlation

SPI and SGI cross-correlation – borehole 033568 (G30E)		
Calculated time period	Correlation value	Lag time
Three-month	0.23	4 months
Six-month	0.39	4 months
Nine-month	0.44	2 months
12-month	0.44	1 months
24-month	0.55	1 months
36-month	0.52	1 months
48-month	0.55	1 months

The 48-month timescale displays a correlation value of 0.55, which is inadequate. There is, however, a trend between the two indices and drought periods are recognisable.

Although drought periods are not accurately represented in the diagram, notable decreases in SGI values are noted at known drought periods. The geology of the area comprises sandstone with conglomerates and mudrock. The geology is similar to that of A21J, therefore, groundwater droughts in this study area can be accurately represented if the desired range of data is available.

5.3.2.3 Malmani Subgroup: Borehole 2627BC00051 (C23D)

A weak correlation between SPI and SGI is observed for borehole 2627BC00051 in quaternary catchment C23D. The 48-month correlation of 0.51 is the highest simulated correlation.

Table 20: Borehole 2627BC00051 cross-correlation

SPI and SGI cross-correlation – borehole 2627BC00051 (C23D)		
Calculated time period	Correlation value	Lag time of SGI
Three-month	0.17	2 months
Six-month	0.20	1 months
Nine-month	0.25	4 months
12-month	0.28	3 months
24-month	0.38	3 months
36-month	0.46	3 months
48-month	0.51	1 month

The geology of the area forms part of the Malmani Subgroup. The geology is associated with a karst environment, which consists mainly of carbonate rocks (dolomite, limestone). Geologies consisting mainly of carbonate rocks have high groundwater yield and recharge values. Karst environments are also known to have higher-than-normal infiltration rates and water retention.

The cross-correlation lag time values are also inconsistent. This suggests that lag time in a karst system will vary regularly. The highest correlation value recorded was the 48-month simulation of 0.51.

5.3.2.4 ECCA Group: Borehole 2627BD00056 (C22A)

The groundwater level simulation data for C22A (2627BD00056) ranges from 1986-05 to 2009-12. This gives rise to the low correlation between the SPI and SGI, as less than 30 years of data was available for use.

Table 21: Borehole 2627BD00056 cross-correlation

SPI and SGI cross-correlation – Borehole 2627BD00056 (C22A)		
Calculated time period	Correlation value	Lag time of SGI
Three-month	0.19	2 months
Six-month	0.21	1 months
Nine-month	0.25	2 months
12-month	0.30	1 months
24-month	0.40	1 months
36-month	0.42	1 months
48-month	0.49	1 months

The 24-month correlation value was 0.4 and the 48-month was 0.49. The geology of the area is predominantly shale. The permeability of shale is an intricate subject to determine because in time the permeability will increase, as a result of water-shale interactions causing fractures to increase in amount and size. The amount of groundwater flow within the fractures beneath the surface and the amount of infiltration from precipitation and surface water sources are dependent on the state of the shale.

This may also have an effect on the overall accuracy and correlation of the simulations. To accurately simulate groundwater droughts in a shale-rich environment, it is important to have adequate data sets, know the state of the shale in terms of permeability and alter or add the required simulation parameters.

5.3.2.5 Hekpoort Formation: Borehole 036017 (A23A)

The groundwater level simulation data for C23A (036017) ranges from 1986-02 to 2009-12.

Table 22: Borehole 036017 cross-correlation

SPI and SGI cross-correlation – Borehole 036017 (A23A)		
Calculated time period	Correlation value	Lag time
Three-month	0.14	5 months
Six-month	0.20	4 months
Nine-month	0.27	4 months
12-month	0.32	5 months
24-month	0.49	5 months
36-month	0.69	4 months
48-month	0.76	2 months

A weak correlation was found for the three-month, six-month and nine-month simulations. The 24-month correlation is considerably higher than the 12-month, where each simulation has a five-month lag time. The 36-month and 48-month correlations are high, 0.69 and 0.76 respectively, in comparison to the other simulated timescales, given the time series comprises less than 30 years of data. A lag time of two months associated with the 48-month timescale is also more accurate considering a permeable geology, as the andesitic geologies, such as the Hekpoort Formation, comprise fractured material.

The smaller timescales (three-months) show small deviations in SPI and SGI values on either side of the mean. This resulted in large positive and negative values, which led to a weak correlation value.

As the Hekpoort Formation is heavily influenced by aquifer and surface resource interactions, the correlation values will be better at longer-term timescales as they are usually related to reservoir levels, streamflows, and groundwater levels.

5.3.2.6 Strubenkop Formation: Borehole 2528CA00015 (A23E)

The groundwater level simulation data for C23E (2528CA00015) ranges from 1970-01 to 2009-12. The long-term simulations show stronger correlations than the short- and medium-term timescales.

Table 23: Borehole 2528CA00015 cross-correlation

SPI and SGI cross-correlation – Borehole 2528CA00015 (A23E)		
Calculated time period	Correlation value	Lag time of SGI
Three-month	0.14	5 months
Six-month	0.22	5 months
Nine-month	0.28	5 months
12-month	0.33	5 months
24-month	0.48	5 months
36-month	0.60	5 months
48-month	0.68	5 months

This only adds to the noticeable trend that longer SPI and SGI timescales have a greater correlation to groundwater levels.

The borehole is situated in the Strubenkop Formation. The area is characterised by a relatively high annual recharge, with a low groundwater yield. The 48-month timescale indicates the strongest correlation value of 0.68.

.

5.3.2.7 Diabase: Borehole 11452 (A23E)

The groundwater level simulation data for C23E (11452) ranges from 1967-01 to 2009-12. The correlation values for all the timescales are considered weak throughout.

Table 24: Borehole 11452 cross-correlation

SPI and SGI cross-correlation – borehole 11452 (A23E)		
Calculated time period	Correlation value	Lag time of SGI
Three-month	0.24	4 months
Six-month	0.29	3 months
Nine-month	0.32	3 months
12-month	0.34	1 months
24-month	0.45	2 months
36-month	0.53	3 months
48-month	0.59	2 months

The borehole is situated in diabase, which is similar to dolerite. Diabase occurs mostly as shallow intrusions, such as dykes and sills. These intrusions are characterised by high permeability and serves as conduits for groundwater flow.

The correlation values are relatively weak with 0.59 for the 48-month simulation being the highest. Weak correlation values can be due to the geology of the area. The various inflows and outflows of the aquifer system may contribute to the weak correlations as it is difficult to incorporate all the various influences on the system. Although the groundwater level simulations are based on precipitation, it should be noted that highly permeable environments may be difficult to simulate.

5.3.2.8 Kolobeng Norite: Borehole 023502 (A22H)

The groundwater level simulation data for A22H (023502) ranges from 1970-03 to 2009-12. The borehole is situated in the Kolobeng Norite, which consists of norite and quartz norite with possible gabbro, chromitite and magnetite. Kolobeng Norite forms part of the Bushveld igneous complex.

Table 25: Borehole 023502 cross-correlation

SPI and SGI Cross-Correlation – borehole 023502 (A22H)		
Calculated time period	Correlation value	Lag time of SGI
Three-month	0.30	4 months
Six-month	0.43	5 months
Nine-month	0.54	5 months
12-month	0.60	5 months
24-month	0.75	5 months
36-month	0.85	3 months
48-month	0.90	1 months

Strong correlation values were simulated for the 24, 36 and 48-months timescales. Lag times between the last three timescales are inconsistent. Irregularities between the SGI and SPI are found between 2001 to 2009-12. This may be due to an increase in evaporation as the SPEI simulation indicated an increase in droughts for the third decade (2005–2015). Evaporation increase may have led to the SPI value decrease during this decade.

5.3.2.9 Silverton Formation: Borehole 2528CD00065 (A22G)

The correlation values calculated for the observation period demonstrate a low correlation value for the three-month and six-month timescales. The 12-month and nine-month time periods illustrate higher correlation values than the previous time periods, but are not considered satisfactory.

Table 26: Borehole 2528CD00065 cross-correlation

SPI and SGI cross-correlation – borehole 2528CD00065 (A22G)		
Calculated time period	Correlation value	Lag time of SGI
Three-month	0.23	5 months
Six-month	0.34	4 months
Nine-month	0.41	3 months
12-month	0.45	4 months
24-month	0.59	1 months
36-month	0.64	1 months
48-month	0.70	1 months

The 24-month, 36-month and 48-month periods indicate improved correlations between the SPI and SGI values all at a one-month lag time.

5.3.2.10 Vryburg Formation (andesitic lava): Borehole 2624DC00019 (C32B)

The groundwater level simulation data for the Vryburg Formation (andesitic lava) ranges from 1982-01 to 2009-12. Borehole 2624DC00019 is found in the andesitic lava geology of the Vryburg Formation.

Table 27: Borehole 2624DC00019 cross-correlation

SPI and SGI cross-correlation – borehole 2624DC00019 (C32B)		
Calculated time period	Correlation value	Lag time of SGI
Three-month	0.04	4 months
Six-month	0.09	4 months
Nine-month	0.22	5 months
12-month	0.30	5 months
24-month	0.48	5 months
36-month	0.66	5 months
48-month	0.79	4 months

Andesitic lava in this region has a high groundwater yield, which substantiates the occurrence of only moderate groundwater drought. The short-term timescales demonstrate a low level of correlation, whereas, the longer-term timescales from the 24-month period illustrate an increase in correlation, with the 48-month timescale value of 0.79 the highest.

The correlation of 0.79 (48-month) is a good correlation value. Lag time across all the simulations is consistent as it varies between four and five months.

5.3.2.11 Dwyka Group: Borehole 2624DC00026 (C32B)

The groundwater level simulation data for C32B (2624DC00026) ranges from 1982-01 to 2009-12. The short-term timescales indicate low correlation values. The borehole is situated in the Dwyka Group, and the area has similar recharge values to the Vryburg Formation.

Table 28: Borehole 2624DC00026 cross-correlation

SPI and SGI cross-correlation – borehole 2624DC00026 (C32B)		
Calculated time period	Correlation value	Lag time of SGI
Three-month	0.12	0 months
Six-month	0.15	0 months
Nine-month	0.27	0 months
12-month	0.34	0 months
24-month	0.52	1 months
36-month	0.71	1 months
48-month	0.76	1 months

Groundwater yield values of 0.5 and 2 L/s differ from the Vryburg Formation and the andesitic lava geology. The groundwater yield is lower than 2624DC00019, which is evident in the fluctuation of SGI values, making this geology more susceptible to groundwater droughts.

The 48-month timescale had the highest correlation value at 0.76. The lag times are also consistent as they vary between zero and one month.

5.3.2.12 Vryburg Formation (quartzitic sandstone): Borehole 032611 (C32B)

The groundwater level simulation data for C32B (032611) ranges from 1982-01 to 2009-12. Borehole 032617 is situated in a diamondiferous type geology. The geology originated from the weathering of the Ventersdorp bedrock, lithostratigraphic groups in the surrounding area and other groups/formations, such as the Dwyka Group, Venterdorp Supergroup, and the Vryburg Formation.

Table 29: Borehole 032611 cross-correlation

SPI and SGI cross-correlation – borehole 032611 (C32B)		
Calculated time period	Correlation value	Lag time of SGI
Three-month	0.21	1 months
Six-month	0.36	5 months
Nine-month	0.47	5 months
12 -month	0.55	5 months
24-month	0.73	5 months
36-month	0.79	1 months
48-month	0.79	1 months

Taking into account all the characteristics of the weathered geologies, such as the groundwater yield, annual recharge, storativity and so forth, the SGI will be erratic at some point in the simulation but the trend and correlations acquired will still give an accurate representation of the groundwater level fluctuations and groundwater drought periods.

Both the nine- and 12-month timescale correlations indicate moderate correlation values with a lag time of five months. The 24- to 48-month correlations all indicate strong correlations of above 0.7. The 24-month timescale has a lag time of five months whereas the 36 and 48-month timescales have a one-month lag time.

5.3.2.13 Tierberg Formation: Borehole 2925CD00009 (C51J)

The groundwater level simulation data for C51J (2925CD00009) ranges from 1967-02 to 1995-12. The lag times for the different timescales are inconsistent, ranging from one to five months.

Table 30: Borehole 2925CD00009 cross-correlation

SPI and SGI cross-correlation – borehole 2925CD00009 (C32B)		
Calculated time period	Correlation value	Lag time of SGI
Three-month	0.29	1 months
Six-month	0.37	5 months
Nine-month	0.41	5 months
12-month	0.45	2 months
24-month	0.64	5 months
36-month	0.81	3 months
48-month	0.90	1 months

The correlation values calculated demonstrate a low value of correlation for the three-month to nine-month timescales, whereas the 24-month timescale shows a considerable increase in correlation value. The 36 and 48-month correlations both have values higher than 0.8.

The 48-month timescale simulated the best correlation with a lag time of one month. With a low annual recharge, the SGI stays relatively constant, except for severe meteorological drought periods where the SGI values also decrease.

5.4 Groundwater Drought Strength Index (GDSI)

The GDSI results are evaluated in terms of groundwater table levels, where a high-water table level will have a high percentage and a low water table level a low percentage. A decline in percentage from high to low indicates the start of a drought event, whereas an increase in a low percentage value to a high percentage value indicates the end period of a drought event. The GDSI is calculated on a 12-point (12-month) period in order to assess the GDSI fluctuations on a yearly and monthly basis.

Each groundwater table stress or drought period is indicated with arrows on Figure 25 to Figure 37 for the respective study areas. Green arrows indicate a complete groundwater drought cycle. Therefore, decreases and increases in these periods are a strong possibility but are defined as a singular groundwater stress period, as recovery only occurs when the GDSI value is above 70%. Orange arrows are defined as percentage drought periods, as the GDSI does not fully recover to 70%.

5.4.1 Teekloof Formation

GDSI results for the Teekloof Formation situated in the Western Cape are illustrated in Figure 25. Historical drought periods are identified in red.

Drought periods in this region are 1982–1984, 1987–1988, 1991–1992 and 1994–1995 (see 2.6 for previously studied and identified drought periods).

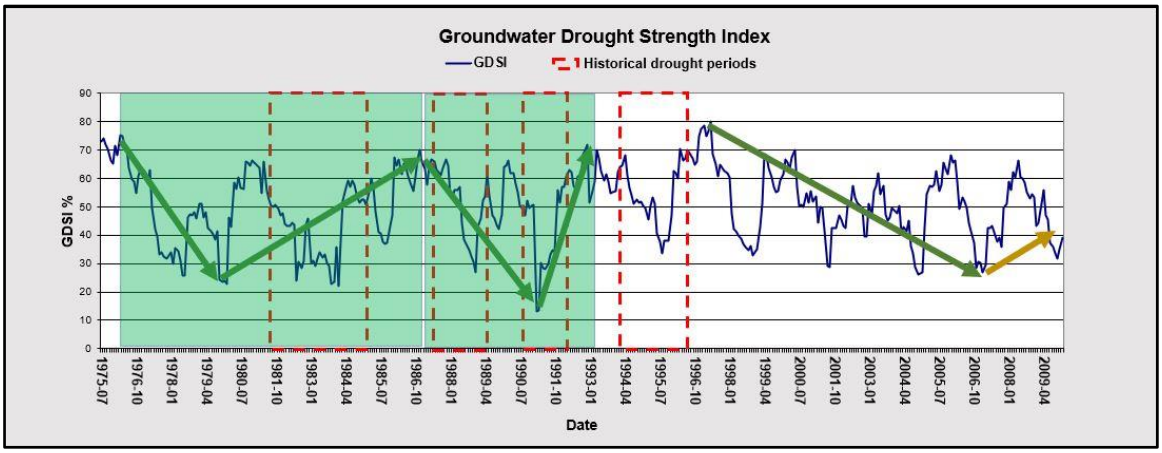

Figure 25: Teekloof Formation GDSI results

Each of the historical drought events starts at a relatively high GDSI of 70% or above, with a decline in value down to between 30% and 10%. The period between 1976 and 1987 can be defined as a groundwater stress period as the GDSI decreases from 75% to a minimum of 23% and recovers to 70% in 1987. The average GDSI is 47.7%. The drought percentage for the entire 1976 to 1987 period is 55.75%, but, as illustrated in Figure 25 between 1977 and 1984 the average GDSI is 41.4%. This results in a 71.5% drought percentage, which is considered to be a severe drought.

The 1991–1992 drought indicates the lowest GDSI percentage but for the shortest period in comparison to the other identified drought periods. A decline in GDSI values from 70% in 1987 to 13% in 1991 is visible. The recovery of the groundwater table between 1991 and 1993 where the GDSI reaches 71% is also observed. The average GDSI is 50.6%. The drought percentage for the period is 48.5%. As illustrated in Figure 25, between 1991 and 1992 the average GDSI is 41.51%. This results in a 71.23% drought percentage, which is considered to be a severe drought.

The GDSI fluctuates considerably during this period. The GDSI decreases below 30% but never recovers fully to 70%. This period has an average of 45% GDSI and a groundwater drought percentage of 63%, indicating a severe groundwater drought period.

In comparison to the values obtained in the SGI (Figure 12) based on the simulated groundwater levels, the drought periods are fairly similar. The 1982–1984, 1991–1992 and 1994–1995 are indicated on both the SGI and GDSI. However, the 1987–1988 drought is clearly defined on the GDSI. SGI values for this period ranges between 1 and -1, which are considered normal to slightly low groundwater tables. Therefore, the GDSI depicts a briefly stressed groundwater table for this period. The effects on both the GDSI and SGI are evident during the 1990–1992 drought periods, as the GDSI values range between 10% and 70%, and the SGI between -1 and -2. The GDSI, however, defines more precisely the start and end period of the groundwater drought periods, as well as the fluctuations that occur during these drought periods.

5.4.2 Loam and sandy loam geology

The GDSI results for the loam and sandy loam geology situated in the Western Cape are illustrated in the Figure 26. Historical drought periods are identified in red.

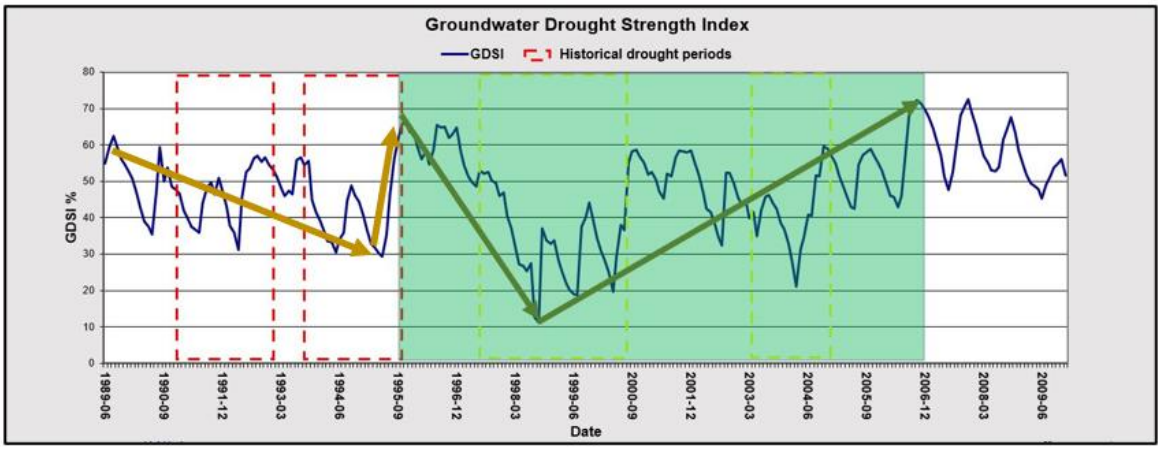

Figure 26: Loam and sandy loam GDSI results

Historical drought periods for this region are 1991, 1992 and 1994–1995. A decline in GDSI is shown during 1991, 1992 and 1994–1995, but not as severely. The periods indicated in yellow are not identified historical drought periods but do show significant decreases in GDSI.

Historical drought periods indicated in red are defined as percentage groundwater droughts as the GDSI values range between 65% and 30%. The average GDSI for this period is 43%, which indicates a groundwater drought percentage of 68%. This also indicates a severe groundwater drought period between 1989 and 1995, as the groundwater table is very vulnerable due to the lack in recovery to 70%.

Between 1996 and 2007 the GDSI model displays a groundwater stress period. The average GDSI for this period is 44.94%, resulting in a drought percentage of 62.65%: therefore, a severe groundwater drought period.

The historical drought periods are indicated in the SGI results (Figure 13) as well. Indicated drought periods between 1997–2000 and 2003–2005 are also indicated on the SGI but, as mentioned, are not noted as a historical drought period.

5.4.3 Malmani Subgroup

GDSI results for the Malmani Subgroup are illustrated in Figure 27. Historical drought periods are identified in red.

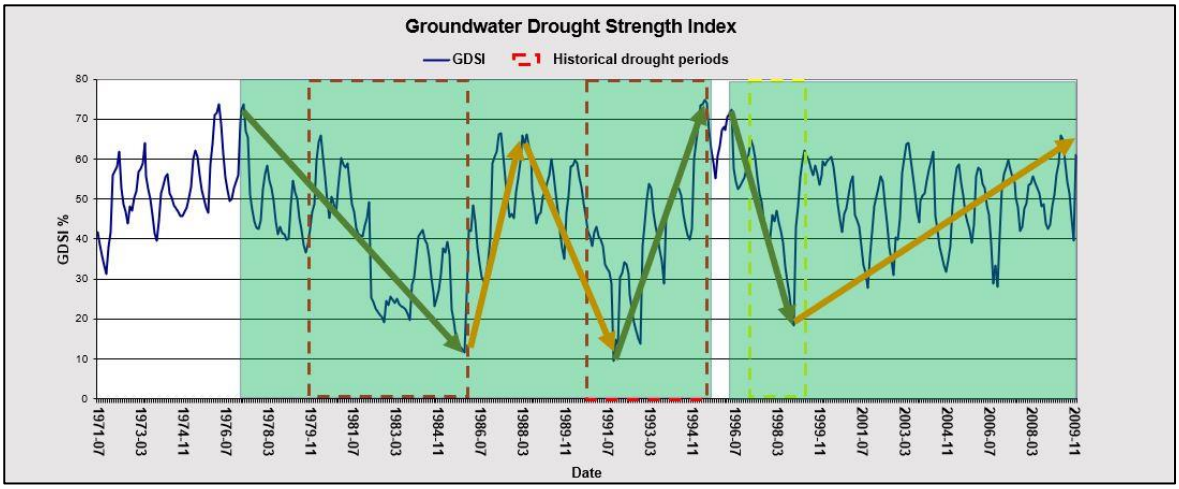

Figure 27: Malmani Subgroup GDSI results

Drought periods in this region for the simulated time period are 1979, 1983–1984, 1987, 1992 and 1995. The historical drought periods are indicated in red. A decline in GDSI values for the above-mentioned periods are illustrated in Figure 27.

The period between 1979 and 1987 indicates a groundwater level stress period as the GDSI displays a decline in value between 1979 and 1984. The GDSI increases to 66% in 1988. The period between 1985 and 1992 (orange arrows) indicates an average GDSI of 47% resulting in a 57.5% drought percentage. Therefore, the groundwater table is under moderate stress and vulnerable.

Furthermore, the period from 1996 to 2009 also indicates a groundwater table stress period, as the GDSI decreases by 72% in 1996 to a low of 20% in 1998. The GDSI does not recover to 70%. The average GDSI for this period is 49.2. This gives a drought percentage of 52.5%. Therefore, the groundwater table is under slight stress and can be considered vulnerable.

The 1987 drought period is indicated on the SGI results (Figure 14), as the values range between 0 and -1, which are considered a near normal groundwater table level. The GDSI indicates a decline in percentage but is not indicative of a severe stress period on the groundwater table, as the GDSI indicates a minimum percentage of 45% for this period. Other historical drought periods, namely 1983–1984 and 1992–1995, are indicated by the SGI. SGI values decrease during the 1983–1984 period as the GDSI indicates that the effects on the groundwater table are visible from 1981 to 1985 until recovery in 1987. The GDSI also illustrates the 1992 and 1995 drought, by indicating a decline from 60% in 1989 to a low of 10% in 1992 and an overall recovery of the groundwater drought period in 1995 at 75%. The SGI results display a drought occurring in 1992 to 1995 with values fluctuating between 0 and -2 for this period. The SGI, however, does not recover above 0 until past 2009 (Figure 14).

5.4.4 ECCA Group

GDSI results for the ECCA Group are illustrated in Figure 28. Historical drought periods are identified in red. Periods indicated in yellow are groundwater drought periods identified by the GDSI and are not known historical drought periods.

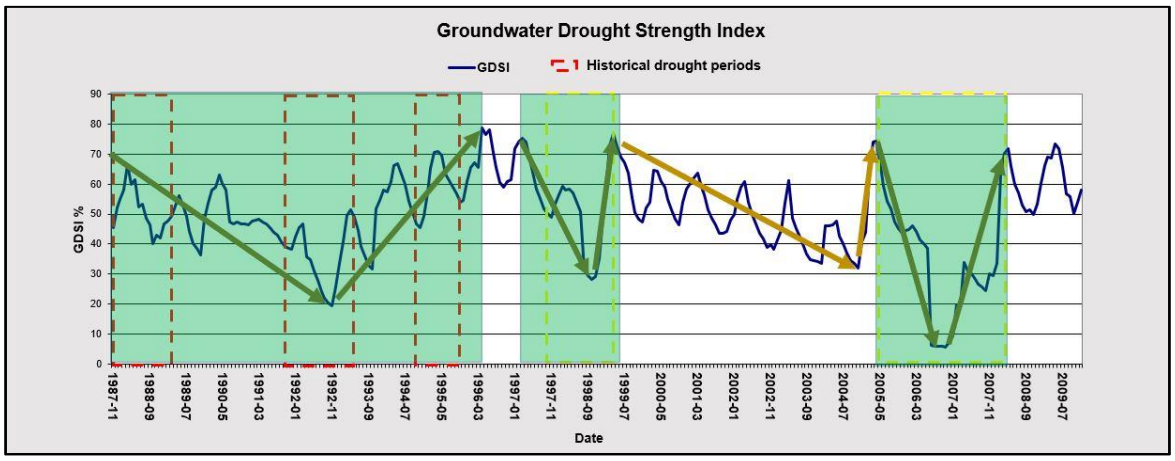

Figure 28: ECCA Group GDSI results

Historical drought periods for the simulated time period are 1987, 1992 and 1995. The 1992 drought is well illustrated by the GDSI values for this period, whereas the GDSI for the 1987 drought has no clear indication of a groundwater drought. The 1995 drought indicates a decline in GDSI value but only from 65% to roughly 45%. Other notable groundwater droughts occur during 1997 and 1999, as well as between 2005 and 2008. The GDSI decreases from 75% to 28% for the 1997 to 1999 period and from 75% to 5% for the 2005 to 2008 period.

The average GDSI for the 1987 to 1997 period is 48.58%, resulting in a drought percentage of 53.55%. Therefore, the period indicates a moderate groundwater table stress period.

A short-term groundwater drought is observed between 1997 and 1999. The average GDSI for this period is 47.7%, resulting in a drought percentage of 55.75%, therefore, indicating a moderate groundwater table stress period.

In addition to the above-mentioned drought periods another drought period is identified between 2005 and 2008. The average GDSI for this period is 32.73%, resulting in a drought percentage of 93.2%. This is considered an extreme groundwater table stress period.

Between 1999 and 2005 a decrease in GDSI is observed as the GDSI decreased from 75% in 1999 to 32% in 2004. This is not indicative of a groundwater table stress period, it is merely a description of the groundwater drought percentage. The average GDSI is 50.1%, which gives a drought percentage of 49.9%. This is a moderate drought where the groundwater table is under stress and the groundwater table is considered to be slightly vulnerable.

The 1992 and 1995 historical drought is well illustrated by die SGI results (Figure 15), as the values range from -0.5 to -1.7. Other groundwater droughts during 1997 and 1999 and between 2005 and 2008 are not indicated on the SGI, as shown on the GDSI. This may be an anomaly in the simulation, but the SGI is declining during this period, however, does not proceed below zero.

5.4.5 Hekpoort Formation

The ECCA Group GDSI simulation is illustrated in Figure 29. Historical drought periods are identified in red. Periods indicated in yellow are groundwater drought periods identified by the GDSI and are not known historical drought periods.

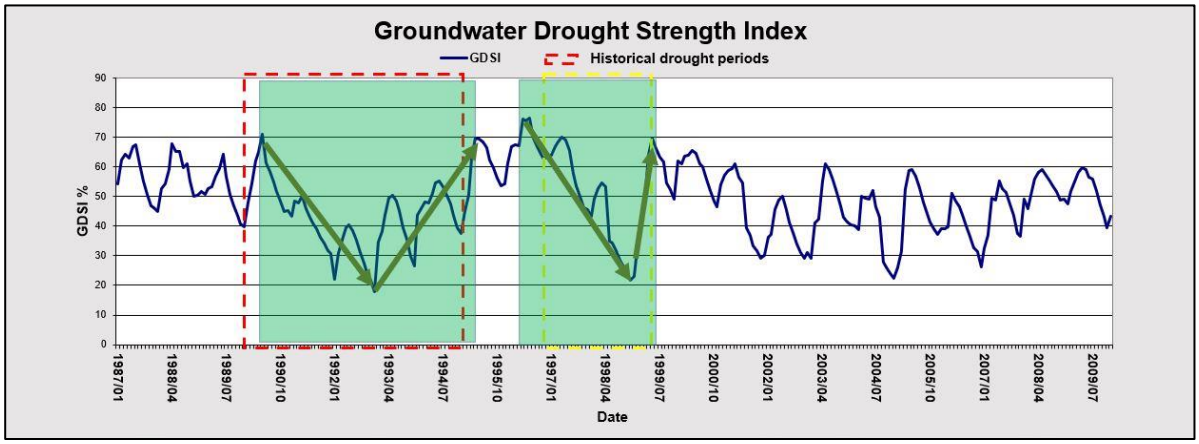

Figure 29: Hekpoort Formation GDSI results

As mentioned in 2.6, the identified historical drought periods in the area are between 1992 and 1995. The GDSI decreases from 70% to below 20% until the drought period ended in 1995 where the GDSI was at 70%. A groundwater drought can also be observed during the 1997 and 2000 period, as the GDSI in 1996 is at a value of 77%, decreases to 21% in 1998 and then recovers to 70% in 1999.

The groundwater drought period identified between 1989 and 1995 has an average GDSI of 45.37%. This leads to a drought percentage of 61.57%, indicating a moderate groundwater table stress period.

The average GDSI for the identified drought period between 1996 and 1999 is 48.39%. This results in a drought percentage of 54.03% indicating a moderate groundwater table stress for this period.

Furthermore, the GDSI remains between 20% and 65% from 2000 to 2009. The GDSI values for this period fluctuate as the GDSI decreases from 70% and do not recover to 70% throughout the specified period. The average GDSI for this period is 46.4% resulting in a 59% drought percentage. Therefore, the groundwater table is under moderate stress and vulnerable.

The SGI results (Figure 16) also simulate the 1992 to 1995 historical drought period, however, only decreases in SGI values are observed in the 24-month and 48-month simulation (Figure 16) during the 1997 to 2000 period.

5.4.6 Strubenkop Formation

The GDSI results for the Strubenkop Formation are illustrated in Figure 30. Two distinct historical drought periods are identified in red. Periods indicated in yellow are not known historical drought periods but were identified by the GDSI.

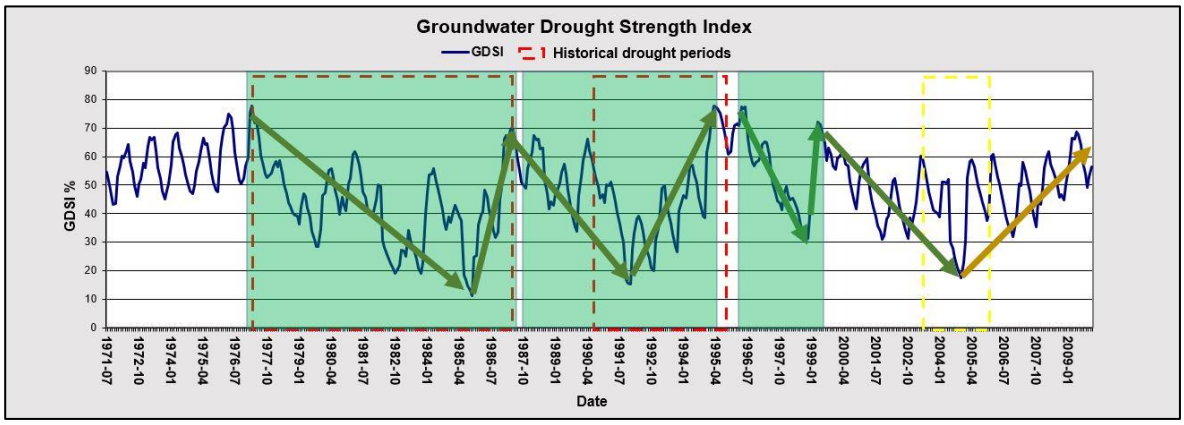

Figure 30: Strubenkop Formation GDSI results

Drought index studies identify 1973, 1979, 1982, 1983, 1984, 1987, 1992 to 1995 as drought periods in this region.

The GDSI indicates a groundwater drought spanning from 1977 until 1987. In this period moderate drought periods, as well as severe groundwater drought periods, are identified. Initially a decrease in GDSI is found between 1977 and 1979. Between 1979 and 1982 recovery in GDSI can be seen, whereas from 1984 to 1987 a groundwater drought is indicated by the GDSI values.

One of the most notable severe groundwater drought periods is observed between 1991 and 1995, as the GDSI decreases from almost 70% to almost 10%.

The groundwater drought period identified between 1977 and 1987 has an average GDSI of 41.59%, resulting in a drought percentage of 71.03. This indicates a severe groundwater table stress period.

Between late 1987 and 1995 the GDSI indicates a groundwater drought period with an average GDSI value of 45.44%, resulting in a drought percentage of 61.4%. This indicates a severe groundwater table stress period.

A short-term drought is observed between 1996 and 2000 with an average GDSI of 50.1%. The drought percentage for this period is 49.75% indicating a moderate groundwater table stress period.

Additionally, a groundwater table stress period is observed between 2004 and 2006. The GDSI starts to decrease in 2000 at 70% to a low of 18% in 2004/2005. The recovery of the groundwater table occurs rapidly, as a spike in GDSI is already seen in 2005. However, the GDSI does not reach 70% during the data series with only a high of 69% in mid-2009 being the closest to 70%. The average GDSI is 48.33% resulting in a 54.2% drought percentage. Therefore, the groundwater table is under moderate stress and vulnerable.

The SGI results (Figure 17) also simulate drought periods during 1977 and 1987 as a decline in 1977 can be seen until the SGI value in 1987 reaches 0. Similar to the 1990 to 1995 drought indicated by the GDSI and historical drought studies, the SGI values similarly decrease from 1990 to 1993 where the values rise from 1993 to 1995. Between 2004 and 2006 a decline in SGI values is also evident.

5.4.7 Diabase geology

GDSI results for the diabase geology are illustrated in the Figure 31. Three distinct historical drought periods are identified in red. Periods indicated in yellow are not known historical droughts but are identified by the GDSI.

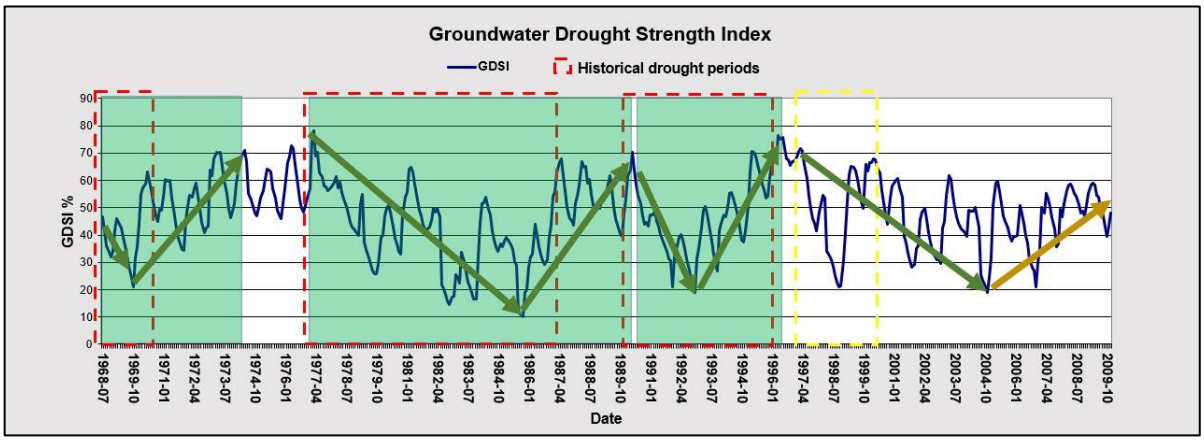

Figure 31: Diabase Geology GDSI results

Drought indices studies identified 1970, 1973, 1979, 1982, 1983, 1984, 1987, 1992 and 1995 as drought periods in this region. Additionally, a groundwater drought period between 1997 and 2000 is indicated. Drought periods identified are similar to the Strubenkop Formation, as the two-study area falls in the same quaternary catchment area.

The drought of 1970 is identified in the GDSI but stress on the groundwater table can be seen in 1969 as the GDSI value is near 20%. Between 1977 and 1990 a stressed and ever-fluctuating GDSI is observed, similar to the Strubenkop Formation. The GDSI values range from near 80% to a low of 10% during this period. As for the 1992 and 1995 droughts the GDSI simulated a stress period that spans from 1992 to 1995.

The groundwater drought period between 1968 and 1975 illustrates an average GDSI value of 48.79%, resulting in a drought percentage of 53.01%. This indicates a moderate groundwater table stress period. The groundwater table is under stress but not as severely, as a rapid recovery period of the groundwater table is illustrated between 1970 and 1975.

The drought period noted between 1977 and 1989 has an average GDSI of 43.47%, resulting in a drought percentage of 66.33%. This indicates a severe groundwater table stress period and a vulnerable groundwater table.

Furthermore, an additional historical drought identified between 1990 and 1996 has an average GDSI of 42.40%, resulting in a drought percentage of 69%. This indicates a

severe groundwater table stress period and a vulnerable groundwater table. The increase in drought percentage can be related to the previous groundwater table stress period observed between 1977 and 1989.

Additionally, a groundwater table stress period is observed between 1997 and 1999 as well as between 2004 and 2006. The GDSI starts to decrease in 1997 from 71% to a low of 20% in 1998. A recovery of the groundwater table occurs to a value of 66%. The GDSI decreases further to a low of 18% from 68% in 2004/2005. However, the GDSI does not reach 70% during the period between 1997 and 2009 with only a high of 68% in 1999. The average GDSI is 46.52% resulting in a 58.7% drought percentage. Therefore, the groundwater table is under moderate stress and vulnerable.

The SGI results (Figure 18) for the diabase geology indicates drought periods for 1984, 1987, 1992 and 1995. The 1970, 1973,1979 are not clearly indicated in the SGI results. However, a decline in SGI values is illustrated during these periods.

5.4.8 Kolobeng Norite

GDSI results for the Kolobeng Norite are illustrated in Figure 32. Two distinct historical drought periods are identified. Periods indicated in yellow are not known historical drought but are identified by the GDSI.

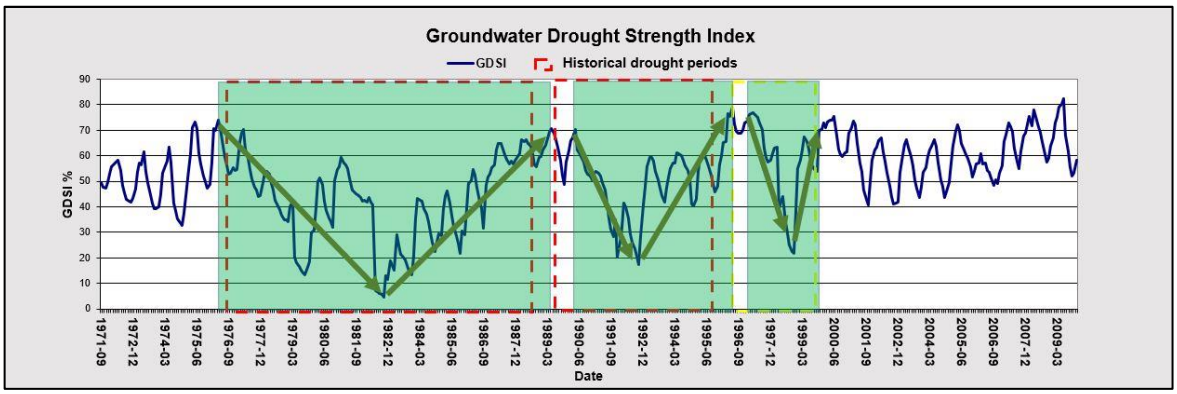

Figure 32: Kolobeng Norite GDSI results

Historical droughts identified by other drought indices (SPEI-12 and SPEI-24) indicate drought occurrences between 1982–1989 and 1992–1995. Drought occurrences however decrease during 1995–2004 (refer to 2.6), whereas severe droughts occur in 1983 and 1995.

Between 1982 and 1983 a low GDSI of below 10% is recorded, and between 1991 and 1994 a GDSI of below 20% is found. An additional groundwater drought period is identified between 1996 and 2001. The GDSI, however, increases and has a stable value, which does not fall below 40% from 2001 onwards through to 2009.

The GDSI model indicates a groundwater stress period between 1976 and 1990, with an average GDSI of 42.76% and a drought percentage of 68.1%, indicating a severe groundwater table stress period.

Between 1990 and 1996 an additional groundwater stress period is identified with an average GDSI of 48.76% and a drought percentage of 53.1%, therefore, indicating a moderate groundwater table stress period.

The concluding historical groundwater stress period identified is between 1997 and 2000, with an average GDSI of 51.95%, resulting in a drought percentage of 45.13%, therefore, indicating a moderate groundwater table stress period.

The recovery of the groundwater table is evident because the drought percentage decreases as the drought events are observed. A steady increase in SGI (Figure 19)

and GDSI can be seen from 2001 through to 2009. Historical drought periods between 1982–1989 and 1992–1995 are also simulated by the SGI results (Figure 19).

5.4.9 Silverton Formation

The Silverton Formation GDSI results are illustrated in Figure 33. Drought periods identified by drought indices are indicated in red. Periods indicated in yellow are not known historical droughts but were identified by the GDSI.

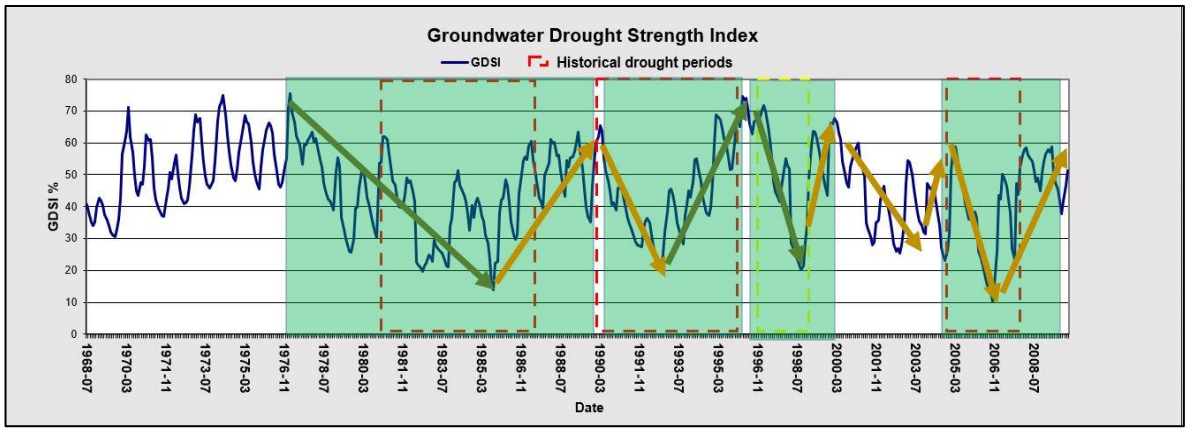

Figure 33: Silverton Formation GDSI results

Historical drought periods identified by drought indices for this region are 1982–1984, 1991–1992 and 1994. The SGI value (Figure 20) indicates a drought period for 2006–2008; this period is also indicated in the GDSI values.

The effects on the groundwater table during the drought between 1982 and 1984 can be seen from 1981, as the GDSI decreased from above 60% to 20% from 1981 to 1982. The drought ended in 1984 but the effects on the groundwater table can be seen until 1985 (GDSI of 15%); recovery is noted in 1987 where the GDSI rises above 60%.

Two groundwater table stress periods are noted for the Silverton Formation area – the first between 1977 and 1996 and the second between 1997 and 2009. The first period has an average GDSI of 43.96% and a drought percentage of 65.1%. The second period has a similar drought percentage of 43.55% and a drought percentage of 66.7%. Both periods indicate a severe groundwater table stress period. The GDSI values fluctuate throughout the drought periods, there are, however, periods of higher GDSI values of between 50% and 65% indicating partial recovery in groundwater tables.

A decrease in SGI results (Figure 20) is observed during the drought periods, however the SGI values do not decrease below 0. There is a contrast in results between the GDSI and SGI. The SGI results do not indicate any severe groundwater droughts except between 2007 and 2009 where an SGI value of -3 is observed.

5.4.10 Vryburg Formation (andesitic lava)

The Vryburg Formation (andesitic lava) GDSI results are illustrated in Figure 34. The historical droughts often had a longer effect on the groundwater level, as the GDSI indicates.

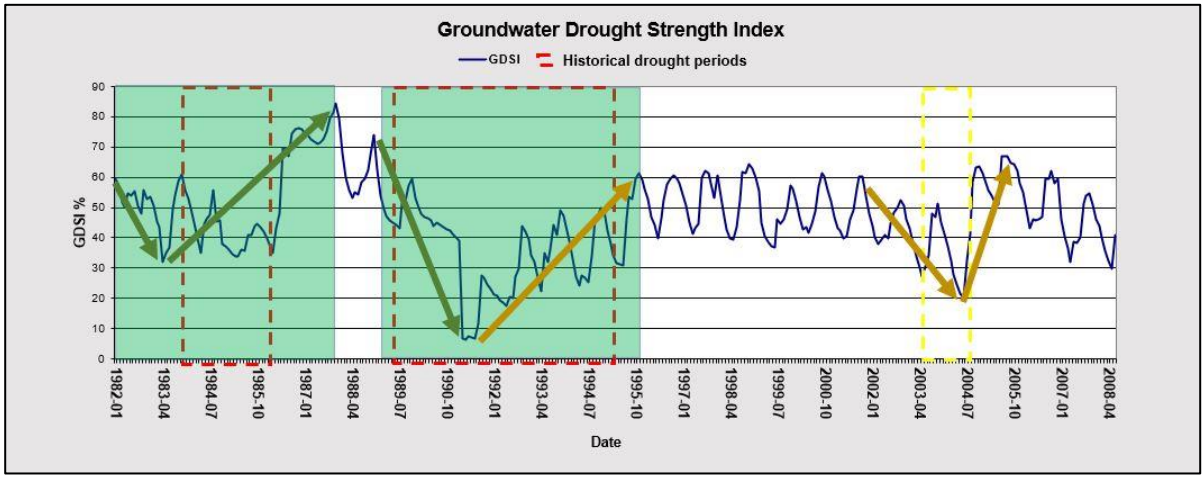

Figure 34: Vryburg Formation (andesitic lava) GDSI results

The drought indices as noted in 2.6 indicated drought periods between 1985–1987 and 1991–1995. Groundwater droughts are evident between these dates but the effects on the groundwater table according to the GDSI can be seen before the start date as well as after the drought end dates. The recovery period started at the beginning of 1992 until 1995 at a GDSI value of 60%. The 1985–1987 drought did not have such a dramatic effect on the GDSI as the 1991–1995 period, because the GDSI fluctuated between 55% and 35%.

Two groundwater table stress periods are noted for the Vryburg andesitic lava Formation. The first is between 1982 and 1989 and the second period between 1990 and 2009. The first period has an average GDSI of 46.42% and a drought percentage of 58.9%, therefore, indicating a moderate groundwater table stress period. The second period has an average GDSI of 45.14%. The second period has an average GDSI of 43.55% and a drought percentage of 62.2%. The second period indicates a severe groundwater table stress period.

The GDSI and SGI results are similar in trend; the GDSI, however, illustrates the effects on the groundwater table during historical drought periods better.

5.4.11 Dwyka Group

The Dwyka Group GDSI results are displayed in Figure 35. The GDSI is relatively high with only two periods falling below 20%.

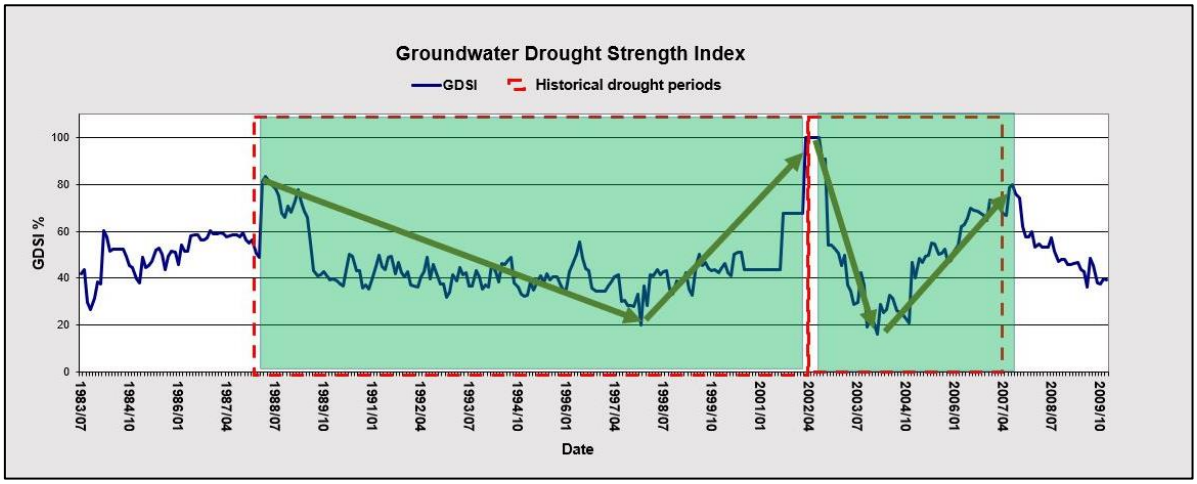

Figure 35: Dwyka Group GDSI results

Droughts were observed between 1995 and 2004 and from 2005 to 2009. These identified drought periods were identified by SPEI-12 simulation conducted in the North West. The groundwater drought however influenced the groundwater table from 1988 to 2001, as the GDSI decreased from above 80% in 1988 to 20% in 1998. The period from 1989 to 2001 saw a fluctuating GDSI ranging between 50% and 20%. The recovery period started after 2001 as the peak rose to nearly 100%.

The 1995–2004 drought identified by SPEI is identified in the GDSI results, but the groundwater table is affected during 1995 to 2001 and between 2003 to 2007. The two identified drought periods identified by SPEI affect the groundwater table throughout, which ranged from moderate to severe groundwater droughts as well as an increase in GDSI, which was observed during 2002. The 2005 to 2015 period also displays a decrease in SPI and SGI values from 2005 to 2006 and then from 2008 to 2009. A decline in GDSI is observed from 2007 to 2009, which ranges from 80% to below 40%.

Two drought periods were observed in the GDSI results for the Dwyka Group between 1988 and 2001, and 2002 and 2007. The period between 1988 and 2001 has an average GDSI of 43.51% with a drought percentage of 66.25%. Being a prolonged period of nearly 13 years, the GDSI value throughout the period low leads to a severe groundwater table stress period. The second drought period has an average GDSI of 47.94% with a drought percentage of 55.15%, indicating a moderate groundwater table stress period.

The SGI for the Dwyka Group identifies the historical drought periods and shows a similar trend to the GDSI model results. The start and recovery periods of each drought event is better defined in the GDSI results, as the SGI displays very erratic reading throughout the time series.

5.4.12 Vryburg Formation (quartzitic sandstone)

The drought periods identified by the drought indices (refer to Section 2.6 are indicated in red. It should be noted that the timeline of the identified historical drought periods differs in terms of the period during which the groundwater table is affected.

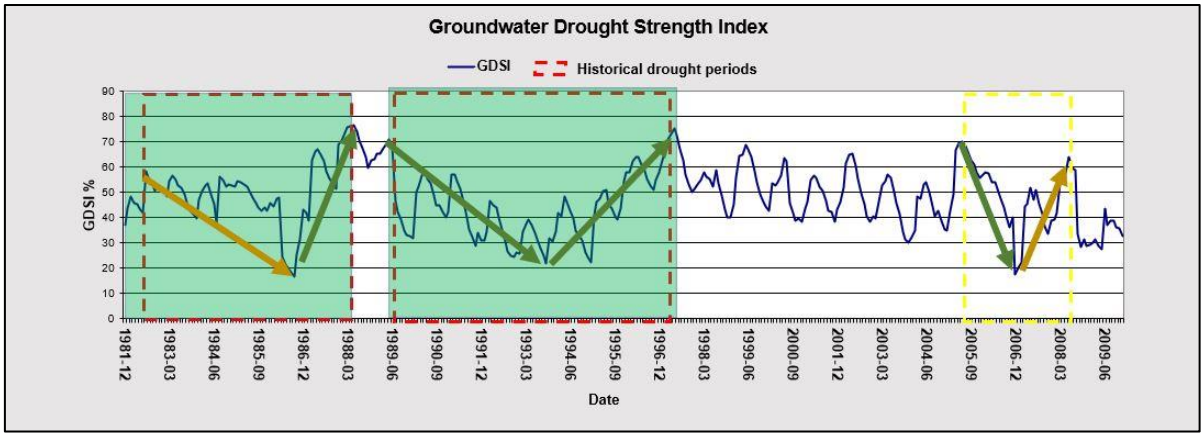

Figure 36: Vryburg Formation (quartzitic sandstone) GDSI results

The GDSI results indicate groundwater table droughts between 1982 and 1988 as well as between 1989 and 1997. SPEI-12 identifies droughts between 1983 and 1987 as well as between 1992 and 1995. The SGI also identifies these drought areas as the results are below -1 during historical drought periods.

The duration of the affected groundwater table exceeds these timeline or periods. A decline in GDSI is noted from 1982 to 1987 and recovery of the groundwater table begins between 1987 and 1988. The GDSI records an initial value of 58% at the start of 1982, which decreases to below 20% in 1986. The groundwater drought ends in 1988 when the GDSI reaches almost 80%.

The second identified drought period identified by SPEI is between 1992 and 1995. A decrease in GDSI initially starts in 1989 and increases in 1996, finally reaching the end of the groundwater drought at a GDSI of above 70% in 1997.

Two historical drought periods are observed in the GDSI results – between 1982 and 1988 and between 1989 and 1997. The period between 1982 and 1988 has an average GDSI of 48.44% with a drought percentage of 53.9%, indicating a moderate groundwater

table stress period. The period between 1989 and 1997 has an average GDSI of 45.36% with a drought percentage of 61.6%, indicating a severe groundwater table stress period.

An additional groundwater stress period is identified between 2005 and 2009. The average GDSI for this period is 46.68% with a drought percentage of 58.3%, therefore, indicating a moderate groundwater table stress period.

5.4.13 Tierberg Formation

There are five drought periods identified in the Tierberg Formation area. The droughts were identified by SPEI and SPI drought indices (refer to 2.6 and are indicated in red in Figure 37.

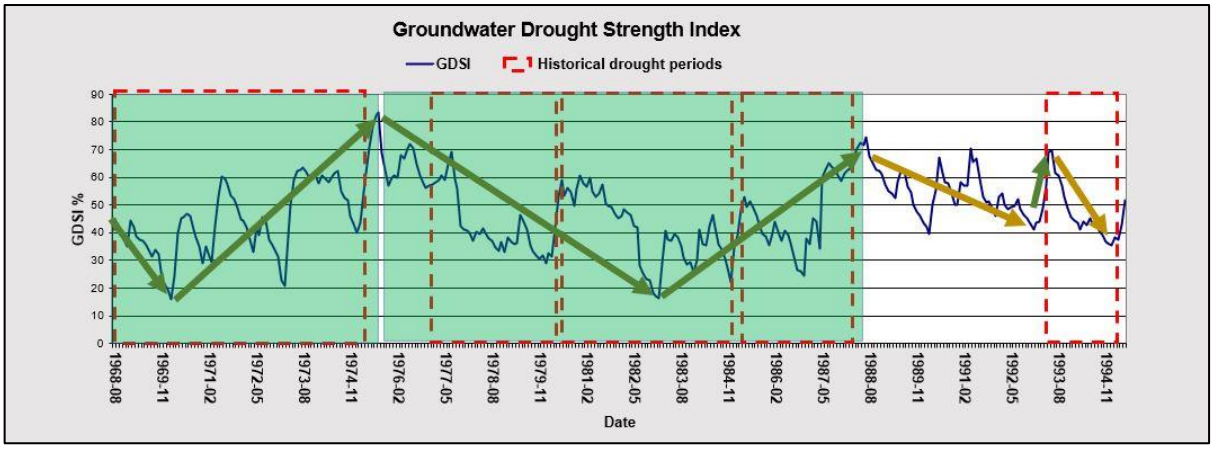

Figure 37: Tierberg Formation GDSI results

Historical drought periods identified by SPEI-12 and SPI in the Free State ranged from 1995–2004 and 2005–2015. SPEI simulations indicate drought periods in 1973, 1977, 1983, 1987 and 1995. The GDSI indicates a groundwater stress period ranging from 1968 to 1975. The GDSI indicates low values between 1972 and 1974, ranging from above 60% and decreasing to 20%. The period of 1977 to 1980 also indicates a groundwater table stress period starting at a value of 70% in 1977 decreasing to just below 30% in late 1979. This is not a notable severe groundwater drought, but the effects of the drought identified by SPE and SPI can be seen on the GDSI.

Groundwater table strain is evident from 1981 to 1989 during the identified 1983 and 1987 droughts. The GDSI is 60% in 1981 and steadily declines to below 20% in 1982/1983. A steady increase is then noted from 1983 to 1989 at which the GDSI is at a value of above 70%.

Two historical drought periods are observed in the GDSI results – the first between 1968 and 1975 and the second between 1975 and 1988. The first period does not indicate a

full cycle as the initial decrease from 70% is not illustrated on the GDSI model results. Therefore, the drought percentage will indicate a lower value and will not portray an accurate result. This only emphasises the lack of data.

The second period between 1975 and 1988 has an average GDSI of 45.44% with a drought percentage of 61.14%, indicating a severe groundwater table stress period.

The SGI and GDSI both indicate the historical drought periods as defined by the SPEI studies. The start and recovery periods of each drought event are better defined in the GDSI results. Therefore, the periods defined as groundwater table stress periods are also better defined by the GDSI.

5.5 Results summary

Table 31 indicates the average Pearson correlation coefficient and the RMSE between the simulated groundwater levels and the monitored periods of the observed values. The RMSE for all the study areas were acceptable. There were only a few study areas that had adequate Pearson correlation values of above 0.7.

The SVF method is the groundwater balance model mostly used. The groundwater simulation parameters are displayed in Table 33 in Appendix B – Groundwater Simulations. The results between the balance models varied only by minor decimals.

The 48-month simulations between the SPI and SGI were more beneficial in comparison to the 24-month simulations. Upon evaluating the results between the SGI and SPI, the Pearson correlation and the RMSE values did not have as much of a significance as initially thought, as most of the drought periods were indicated or decline in SGI was noted during historical drought events.

Table 31: Groundwater balance models correlation values

Geology	Borehole	Average Pearson correlation coefficient	Average RMSE
Teekloof FM	3222BC00151	0.561	0.524
Loam and sandy loam	033568	0.671	0.523
Malmani SBGRP	2627BC00051	0.831	0.018
ECCA GRP	2627BD00056	0.543	0.404
Hekpoort FM	036017	0.614	0.301
Strubenkop FM	2528CA00015	0.571	0.486
Diabase	11452	0.626	0.117
Kolobeng Norite	023502	0.839	0.232
Silverton FM	2528CD00065	0.849	0.137
Vryburg FM: Andesitic lava	2624DC00019	0.548	0.808
Dwyka Group	2624DC00026	0.678	0.488
Vryburg FM: Quartzitic sandstone	32611	0.12	3.45
Tierberg FM	2925CD00009	0.601	0.781

The GDSI and SGI had similar trend results. Most of the groundwater droughts were notable during identified drought periods for both the GDSI and SGI. However, the duration on groundwater droughts were different in comparison to the drought periods listed in 2.6 . The drought periods identified by drought indices, such as the SPEI-12, SPEI-24, and the SPI, are primarily based on meteorological factors whereas the SGI and GDSI are also based on meteorological factors (mainly precipitation), but with a strong reliance on the recharge percentage. The GDSI often displayed groundwater droughts before the start of the historically identified periods and also lasted longer. Whereas the SGI was reliant on the cross-correlation results with SPI to determine groundwater drought periods.

The lag time (values indicated in Table 18 to Table 30) between a precipitation event and the groundwater level recharge was determined by way of cross correlating the SPI and SGI results. All the study areas displayed the highest cross-correlation value in the 48-month simulation, except for the Teekloof Formation, which displayed the highest correlation in the 36-month simulation. Some study areas, such as Kolobeng Norite and the Tierberg Formation, displayed inconsistent lag times between the 24-, 36-and-48-month simulations, which can be caused by intricate geologies as the recharge rate and sub-surface water movement may be unpredictable. The lag time served as a good indication as to when groundwater table stress will start to recover, which can aid in determining the duration of a groundwater drought.

The GDSI correlated well with the drought periods mentioned in chapter 2.6 . The start of groundwater table stress was observed before these historical drought periods at most of the study areas. This only emphasises the importance of groundwater drought determination as it can often indicate groundwater drought warning periods. It should be noted that the GDSI simulated groundwater drought periods without the added correlation with the SPI.

In terms of the comparison to the SGI the GDSI can define the groundwater table stress periods more accurately. GDSI results defined the start of a groundwater drought, the variations and fluctuations during the drought period, as well as the point of recovery.

Historical drought periods were not always easily identifiable by the GDSI as found in the loam and sandy loam geology between 1989 and 1996. Whereas, in the Malmani Subgroup, the 1987 drought period displayed a GDSI value between 45% and 70%. But by calculating the drought percentage for these periods a stress period on the groundwater table is specified.

In addition to the above mentioned, the SGI results for the ECCA Group does not indicate groundwater table stress period as the SPI does between 2000 and 2005. The Average SGI is approximately 0.7 for this period indicating above normal groundwater table conditions. Whereas the GDSI indicates an average of 50.1%, and subsequently a drought percentage of 49.9%, which is considered a moderate drought. Therefore, the GDSI can better define groundwater droughts than the SGI and SPI simulations, as visualised in Figure 15: ECCA Group SPI and SGI results, and Figure 28: ECCA Group GDSI results.

Chapter 6 CONCLUSIONS

An analysis of groundwater droughts in South Africa is challenging due to the lack of available data. Precipitation-based indices, such as the SPI, can be calculated as adequate data sets are available on a public platform. As for groundwater level-based indices, such as the SGI, there are very rarely adequate groundwater level data sets available on a public platform.

By making use of recharge groundwater balance models to simulate complete groundwater level data sets without monitoring gaps, the SGI can be calculated. Similar trends between the available observed and simulated water levels proved to be helpful in simulating groundwater levels. Groundwater levels were, therefore, evaluated according to their Pearson correlation value, the RMSE as well as their trend in comparison to the available observed periods.

The Teekloof Formation, Vryburg Formation (andesitic lava) and the ECCA Group all had poor Pearson correlation values. However, the SGI values for these study areas indicated decreases in value during known historical drought periods. The SGI did not necessarily display drought periods but indicated that the groundwater resources were under strain.

Study areas, such as the loam and sandy loam areas found in quaternary catchment G30E, displayed poor correlation values. This is due to the groundwater level record barely having 20 years of data. Drought periods are visible on the 48-month timescale diagram and periods of groundwater level decline can be identified in comparison to the SPI values and known drought periods. However, the duration, start and end periods of the groundwater droughts are unclear for this study area. On the other hand, the Tierberg Formation had a weak Pearson correlation value but a high cross-correlation value of 0.9 despite having less than 20 years of consecutive groundwater level data. Therefore, sparse data records can also be misleading in terms of the correlation values, as a decrease in SGI value during historical drought periods are still identifiable.

Study areas, such as the Silverton Formation and the Vryburg Formation (Andesitic lava), both had relatively good correlations, but not all of the known drought periods were indicated in their respective diagrams.

Most of the study areas that had less than 30 years of data had weak correlation values with the SPI. Study areas, such as the Malmani Subgroup (Karst environment), also

displayed weak correlation values, despite having a strong Pearson correlation with regard to the groundwater level simulations. This only emphasises the complexity of the geology. Areas with geologies, such as the Karst environment, have to be analysed more thoroughly to incorporate anthropogenic and subsurface influences. Therefore, more complex lithologies such as karst environments was challenging to analyse using the GDSI. Geological environments that has been exposed to anthropogenic activities, severe weathering, pressure etc. are difficult to analyse, unless all possible influences is modelled during the groundwater level simulations.

Groundwater level data, as previously mentioned, is the most important variable to this study, especially the length of the groundwater level record. It was found that 20 to 30 years of data was enough to conduct simulations, but for the most accurate results more than 30 years of data would be beneficial.

In addition, cross-correlation values between the SGI and SPI gave an indication of the lag times between meteorological droughts and groundwater droughts. Each study area indicated declines in SGI values compared to the SPI. Based on the results, the 24 to 48-month simulation timescales proved to be the most useful for analysing and identifying groundwater level droughts.

The SGI results obtained, based on the simulated groundwater levels, indicated groundwater level droughts for most of the study areas in accordance with other drought indices applied in South Africa. The degree of groundwater table stress was however not defined.

The developed groundwater drought indicator, the GDSI, quantifies groundwater table drought/stress by measuring a groundwater drought period between 70% and 30%. The GDSI also defines the degree of the groundwater drought period given in drought percentage, which indicates the state of the groundwater table for a certain period (Table 4). This assists in identifying the severity of stress periods.

In contrast to the SGI the GDSI can define groundwater table stress periods by degree (severity of groundwater table stress) and duration of groundwater drought period. Whereas the SGI cannot define the degree of the groundwater table stress period and requires additional cross correlation calculation with the SPI to give an indication on the groundwater drought duration. The duration is also subject to the accuracy of the cross-correlation result between the two indices, which seldomly indicates a high correlation value (see Table 18 to Table 30).

The GDSI can, therefore, be defined as an indication tool and a guide as to a definite groundwater drought analysing model, as various parameter values are determined by simulations. Factors, such as simulated groundwater levels, nearby accurate precipitation data sets, as well as the groundwater balance model parameters are calculated and simulated, but the results are dependent on the accuracy of the data and parameters used. Therefore, small discrepancies in the simulation or lack in data can result in less accurate GDSI results. The developed groundwater drought indicator indicated groundwater level stress periods relatively well in comparison to reliable drought indices and known drought periods, considering the amount of unavailable data and numerous simulations models used. The GDSI is, therefore, a good indicative resource in quantifying groundwater tables on regional scale as minimal data on groundwater levels is required.

Chapter 7 Recommendations

The aim of the study was to develop a groundwater drought indicator to identify groundwater droughts to sustainably manage groundwater resources. Based on the results obtained, the indicator has the capability of identifying groundwater droughts and quantifying the severity.

To improve the accuracy of the results, more reliable and longer data records are required. Precipitation data can be considered the basis of the groundwater level simulation, which ultimately determines the accuracy of the SGI values. By using more reliable precipitation data that is area-relevant, the accuracy of the simulated groundwater levels will result in a more reliable representation of groundwater level fluctuations.

The groundwater level data acquired from governmental departments and open-source sites are not as accurate and reliable. To acquire more reliable data, privately owned monitoring sites should be considered.

Borehole log data was not acquired, as this data was not captured in the National Groundwater Archive (NGA) or CHART. Log data can be beneficial when simulating groundwater levels, as the geological effects can be better understood and simulated accordingly.

By identifying an area of concern and focusing on acquiring all applicable data that can affect the groundwater level simulations, the accuracy of the results will surely increase. Factors such as the geology, surface-groundwater interactions and anthropogenic influences are all important factors to incorporate.

It should also be noted that poor correlations between observed and simulated groundwater level periods do not necessarily obtain inaccurate SGI results. Decline in groundwater table levels can still be identified and, as such, the models should be evaluated also according to known stress or drought periods.

Lag time as calculated between the SGI and SPI can be a beneficial simulation to determine the approximate dates of groundwater table stress periods in comparison to meteorological drought periods. However, the GDSI determines start and end dates of groundwater table stress periods as a decline in GDSI percentage defined as percentage drought. It may in some cases be beneficial to alter the outer GDSI

percentage values for different areas, as the degree of groundwater table stress can be varying for each area.

Moreover, forecasting groundwater droughts using the groundwater drought indicator or GDSI is heavily dependent on forecasted rainfall. For forecasting long-term rainfall, linear and non-linear modelling approaches can be implemented. The subsequent data can then be used to simulate groundwater levels, which, in turn, can be incorporated in the groundwater level drought indicator process, ultimately calculating GDSI and percentage drought values for future periods. This can lead to the sustainable management of groundwater resources and other dependant water resources.

As Donnenfeld *et al.,* (2018) stated, drought was not the cause of water scarcity during the 2014–2017 drought in South Africa, the drought merely highlighted the existing vulnerabilities in the countries water systems. In most cases the study areas indicated a decline in GDSI before the meteorological and historical drought periods. By analysing the GDSI data, one can identify water resource stress periods and then manage resources more sustainably.

References

Adams, S., Titus, R. & Xu, Y. 2004. *Groundwater recharge assessment of the basement aquifers of Central Namaqualand.* Western Cape, South Africa: WRC (Water Research Commission).

Aplin, A., Fleet, A. & Macquaker, J. 1999. Muds and mudstones: physical and fluid-flow properties. *Geological Society,* London, Special Publications. 158(1):1-8.

Baudoin, M., Vogel, C., Nortje, K. & Naik, M. 2017. Living with drought in South Africa: lessons learnt from the recent El Niño drought period*. International Journal of Disaster Risk Reduction*, 23:128-137.

Beguería, S., Vicente-Serrano, S., Reig, F. & Latorre, B. 2013. Standardized precipitation evapotranspiration index (SPEI) revisited: parameter fitting, evapotranspiration models, tools, data sets and drought monitoring. *International Journal of Climatology*, 34(10):3001-3023.

Bezdan, J., Bezdan, A., Blagojević, B., Mesaroš, M., Pejić, B., Vranešević, M., Pavić, D. & Nikolić-Đorić, E. 2019. SPEI-based approach to agricultural drought monitoring in Vojvodina region. *Water,* 11(7):1481.

Bhuiyan, C., Singh, R. & Kogan, F. 2006. Monitoring drought dynamics in the Aravalli region (India) using different indices based on ground and remote sensing data. *International Journal of Applied Earth Observation and Geoinformation,* 8(4):289-302.

Bloomfield, J. & Marchant, B. 2013. Analysis of groundwater drought building on the standardised precipitation index approach. *Hydrology and Earth System Sciences*, 17(12):4769-4787.

Bloomfield, J., Marchant, B., Bricker, S. & Morgan, R. 2015. Regional analysis of groundwater droughts using hydrograph classification. *Hydrology and Earth System Sciences,* 19(10),4327-4344.

Bordy, E. 2018. Lithostratigraphy of the Tshidzi Formation (Dwyka Group, Karoo Supergroup), South Africa. *South African Journal of Geology,* 121(1):109-118.

Bordy, E., Spelman, S., Cole, D. & Mthembi, P. 2017. Lithostratigraphy of the Pietermaritzburg Formation (ECCA Group, Karoo Supergroup), South Africa. *South African Journal of Geology*, 120(2):293-302

Botai, C., Botai, J., de Wit, J., Ncongwane, K. & Adeola, A. 2017. Drought characteristics over the Western Cape province, South Africa. *Water*, 9(11):876-892.

Botai, C., Botai, J., Dlamini, L., Zwane, N. & Phaduli, E. 2016. Characteristics of droughts in South Africa: A case study of Free State and North West provinces. *Water*, 8(10):439-462.

Botha, J., Woodford, A. & Chevallier, L. 2003. *Hydrogeology of the main Karoo Basin. Gezina,* South Africa: Water Research Commission.

Bothe, O. 2018. What even is 'Climate'? *International Journal of Geosciences*, 1-18.

Bredenkamp, D., Botha, L., van Tonder, G. & van Rensburg, H. 1995. *Manual on quantitative estimation of groundwater recharge and aquifer storativity.* WRC (Water Research Commission).

Burgoyne, P. 2013. *Phytosociology of the North-Eastern Transvaal high mountain grasslands.* (Dissertation – MSc). University of Pretoria.

Chang, T. & Cleopa, X. 1991. A proposed method for drought monitoring. *Journal of the American Water Resources Association*, 27(2):275-281.

CHART | Home [WWW Document]. 2021. [WWW Document]. Dwa.gov.za. http://www.dwa.gov.za/chart/home/default.aspx.

Chevallier, L., Goedhart, M. & Woodford, A. 2001. *Influence of dolerite sill and ring complexes on the occurrence of groundwater in Karoo fractured aquifers.* Pretoria: WRC.

Clay, A. 1981. *The geology of the Malmani Dolomites Subgroup in the Carltonville area, Transvaal.* University of the Witwatersrand. (Dissertation – MSc).

de Wit, M. 2004. The diamondiferous sediments on the farm Nooitgedacht (66), Kimberley South Africa. *South African Journal of Geology,* 107(4):477-488.Donnenfeld, Z., Crookes, C. & Hedden, S. 2018. *A delicate balance: Water scarcity in South Africa.* Institute for Security Studies.

Delin, G., Healy, R., Lorenz, D. & Nimmo, J. 2007. Comparison of local- to regional-scale estimates of ground-water recharge in Minnesota, USA. *Journal of Hydrology,* 334(1-2):231-249.

DWAF, 2005. *Groundwater Resource Assessment II – Task 3aE Recharge*. Pretoria, South Africa: Department of Water Affairs and Forestry, 1-85.

DWAF, 2019. Hydrological Services - https://www.dws.gov.za/Hydrology/Default.aspx. Date of access: 13 July. 2019.

Edossa, D., Woyessa, Y. and Welderufael, W., 2014. Analysis of droughts in the central region of South Africa and their association with SST anomalies. *International Journal of Atmospheric Sciences*, 2014:1-8.

El Chami, D. & Moujabber, M. 2016. Drought, climate change and sustainability of water in agriculture: A roadmap towards the NWRS2. *South African Journal of Science,* 112(910).

Eriksson, P., Hattingh, P. & Altermann, W. 1995. An overview of the geology of the Transvaal Sequence and Bushveld Complex, South Africa. *Mineralium Deposita,.* 30(2).

Eriksson, P., Twist, D., Snyman, C. & Burger, L. 1990. The geochemistry of the Silverton Shale Formation, Transvaal Sequence. *South African Journal of Geology,* 93(3):454-462.

Guttman, N. 1998. COMPARING THE PALMER DROUGHT INDEX AND THE STANDARDIZED PRECIPITATION INDEX. Journal of the American Water Resources Association. 34(1):113-121.

Haas, J. & Birk, S. 2016. Characterizing the spatiotemporal variability of groundwater levels of alluvial aquifers in different settings using drought indices. *Hydrology and Earth System Sciences Discussions,* 21(5): 1-30.

Hayes, M., Svoboda, M., Wilhite, D. & Vanyarkho, O. 1999. Monitoring the 1996 drought using the Standardized Precipitation Index. *Bulletin of the American Meteorological Society,* 80(3):429-438.

Healy, R. 2010. *Estimating groundwater recharge.* Cambridge, England: Cambridge University Press.

Healy, R. & Cook, P. 2002. Using groundwater levels to estimate recharge. *Hydrogeology Journal,* 10(1):91-109.

Heim, R. 2002. A review of twentieth-century drought indices used in the United States. *Bulletin of the American Meteorological Society,* 83(8):1149-1166.

Hendrickx J, Walker G (1997) Recharge from precipitation. In: Simmers I (ed) Recharge of phreatic aquifers in (semi-)arid areas. AA Balkema, Rotterdam pp 19 – 98.

Humbert, F., Elburg, M., Ossa, F., de Kock, M. & Robion, P. 2018. Variolites of the Paleoproterozoic Hekpoort Formation (Transvaal Sub-basin, Kaapvaal Craton): Multistage undercooling textures? *Lithos,* 316-317:48-65.

Huttenlocker, A. & Smith, R. 2017. New whaitsioids (Therapsida: Therocephalia) from the Teekloof Formation of South Africa and therocephalian diversity during the end-Guadalupian extinction. *PeerJ.* 5:3868.

Jönson, R. 2017. Groundwater drought explained by climate, hydrogeological and environmental controls in southern Sweden (Master of Science). Göteborg University.

Keyantash, J & National Center for Atmospheric Research Staff (Eds). 2018. The Climate Data Guide: Standardized Precipitation Index (SPI). URL https://climatedataguide.ucar.edu/climate-data/standardized-precipitation-index-spi. Date of access: 10 Feb. 2020.

Kumar, R., Musuuza, J., Van Loon, A., Teuling, A., Barthel, R., Ten Broek, J., Mai, J., Samaniego, L. & Attinger, S. 2016. Multiscale evaluation of the Standardized Precipitation Index as a groundwater drought indicator. *Hydrology and Earth System Sciences,* 20(3):1117-1131.

Lerner, D., Issar, A. & Simmers, I. 1990. *Groundwater recharge*. Heise, Hannover, Germany: International Contributions to Hydrogeology 8.

Li, B. & Rodell, M. 2015. Evaluation of a model-based groundwater drought indicator in the conterminous U.S. *Journal of Hydrology,* 526:78-88.

Liu, S., Yan, D., Wang, H., Li, C., Weng, B. & Qin, T. 2016. Standardized water budget index and validation in drought estimation of Haihe River Basin, North China. *Advances in Meteorology,* 2016:1-10.

Liu, X., Zhuang, Y., Liang, L. & Xiong, J. 2019. Investigation on the influence of water-shale interaction on stress sensitivity of organic-rich shale. *Geofluids,* 2019: 1-14.

McKee, T., Doesken, N. & Kleist, J. 1993. The relationship of drought frequency and duration of time scales., in: Eighth Conference On Applied Climatology. Colorado: Department of Atmospheric Science Colorado State University pp. 1 - 6.

Mishra, A. & Singh, V. 2010. A review of drought concepts. Journal of Hydrology. 391(1-2):202-216.

Mohammad, A., Jung, H., Odeh, T., Bhuiyan, C. & Hussein, H. 2018. Understanding the impact of droughts in the Yarmouk Basin, Jordan: monitoring droughts through meteorological and hydrological drought indices. Arabian Journal of Geosciences. 11(5).

Monacelli, G., Gallucio, M. & Abbafati, M. 2005. Drought within the context of the region VI. World Meteorological Organization.

Naresh Kumar, M., Murthy, C., Sesha Sai, M. & Roy, P. 2009. On the use of Standardized Precipitation Index (SPI) for drought intensity assessment. Meteorological Applications. 16(3):381-389.

Nijhout, F., 1997. An introduction to genetic algorithms. *Complexity,* 2(5):39-40.

Palmer, W. 1965. Meteorological drought. Office of Climatology: U.S Weather Bureau. 45:1 - 65.

Panagoulia, D. & Dimou, G. 1998. *Definition and effects of droughts* in: Conference on Mediterranean Water Policy: Building on existing experience. Valencia, Spain: Mediterranean Water Network, 1-11.

Quiero, F., Quintana, F. & Bennun, L. 2015. *A novel method based on cross-correlation maximization, for pattern matching by means of a single parameter*. Concepcion, Chile: Physics Department, Concepcion University.

Richard, Y., Fauchereau, N., Poccard, I., Rouault, M. & Trzaska, S. 2001. 20th century droughts in Southern Africa: spatial and temporal variability, teleconnections with oceanic and atmospheric conditions. *International Journal of Climatology,* 21(7):873-885.

Risser, D., Gburek, W. and Folmar, G., 2008. Comparison of recharge estimates at a small watershed in east-central Pennsylvania, USA. *Hydrogeology Journal,* 17(2), 287-298.

Rouault, M., Monyela, B., Kounge, R., Njouodo, A., Dieppois, B., Illig, S. and Keenlyside, N., 2019. *Ocean impact on Southern African climate variability and water resources.* Water Research Commission, 1-134.

Rouse, J., Haas, R., Deering, D. & Sehell, J. 1974. *Monitoring the vernal advancement and retrogradation (green wave effect) of natural vegetation.* Remote Sensing Center, Texas A&M University, College Station.

Sami, K. & Druzynski, A. 2003. *Predicted spatial distribution of naturally occurring arsenic, selenium and uranium in groundwater in South Africa – reconnaissance survey, mapping of naturally occurring hazardous trace constituents in groundwater*. Pretoria, South Africa: Water Research Commission.

Scanlon, B., Healy, R. & Cook, P. 2002. Choosing appropriate techniques for quantifying groundwater recharge. *Hydrogeology Journal,* 10(2):347-347.

Tessema, A., Nzotta, U. & Chirenje, E. 2020. *Assessment of groundwater potential in fractured hard rocks around Vryburg, North West Province, South Africa*. Water Research Commission:1-142.

Thamm, A. 1993. *Lithostratigraphy of the Piekenierskloof Formation (Table Mountain Group).* Council for Geoscience.

The Directorate: Climate Change and Disaster Management. 2014. *Determination of drought indicators.* Pretoria: Department: Agriculture, Forestry and Fisheries.

Tóth, J. 1999. Groundwater as a geologic agent: An overview of the causes, processes, and manifestations. *Hydrogeology Journal,* 7(1):1-14.

Soulé, P. 1992. Spatial patterns of drought frequency and duration in the contiguous USA based on multiple drought event definitions. *International Journal of Climatology,* 12(1):11-24.

Sruthi, S. & Aslam, M. 2015. Agricultural drought analysis using the NDVI and land surface temperature data; a case study of Raichur District. *Aquatic Procedia*, 4:1258-1264.

Svoboda, M., Hayes, M. & Wood, D. n.d. *Standardized precipitation index user guide.* World Meteorological Organization (WMO).

Tóth, J. 1999. Groundwater as a geologic agent: An overview of the causes, processes, and manifestations. *Hydrogeology Journal*, 7(1):1-14.

Trenberth, & Jones, P. & Ambenje, & Bojariu, Roxana & Easterling, David & Tank, Klein & Parker, David & Rahimzadeh, Fatemeh & Renwick, James & Rusticucci, Matilde & Soden, & Zhai, Panmao & Folland, Chris. (2007). *Observations: Surface and atmospheric climate change. Cambridge, UK: Cambridge University Press.*

Van der Lee, J. and Gehrels, J.C., 1990. *Modelling Aquifer Recharge: Introduction to the Lumped Parameter Model EARTH*. Free University of Amsterdam.

van Dijk, D., Channing, A. & van den Heever, J. 2002. Permian trace fossils attributed to tetrapods (Tierberg Formation, Karoo Basin, South Africa) by *Palaeontologia Africana,* 38:49-56.

Van Loon, A. 2015. Hydrological drought explained. *Wiley Interdisciplinary Reviews: Water,* 2(4):359-392.

Van Loon, A. & Laaha, G. 2015. Hydrological drought severity explained by climate and catchment characteristics. *Journal of Hydrology,* 526:3-14.

Varni, M., Comas, R., Weinzettel, P. & Dietrich, S. 2013. Application of the water table fluctuation method to characterize groundwater recharge in the Pampa plain, Argentina. *Hydrological Sciences Journal,* 58(7):1445-1455.

Vegter, J. 2001. *Groundwater development in South Africa and an introduction to the hydrogeology of groundwater regions. WRC Report TT 134/00.* Pretoria: Water Research Commission.

Vicente-Serrano, S., Beguería, S. & López-Moreno, J. 2010. A multiscalar drought index sensitive to global warming: The Standardized Precipitation Evapotranspiration Index. *Journal of Climate,* 23(7):1696-1718.

Vittecoq, B., Reninger, P., Lacquement, F., Martelet, G. & Violette, S. 2019. Hydrogeological conceptual model of andesitic watersheds revealed by high-resolution heliborne geophysics. *Hydrology and Earth System Sciences,* 23(5):2321-2338.

Vogel, C. & Drummond, J. 1993. Dimensions of drought: South African case studies. *GeoJournal,* 30(1):93-98.

Wang, B., Jin, M. & Liang, X. 2014. Using EARTH model to estimate groundwater recharge at five representative zones in the Hebei Plain, China. *Journal of Earth Science,* 26(3):425-434.

Wang, L., Ó Dochartaigh, B. & Macdonald, D. 2010. A literature review of recharge estimation and groundwater resource assessment in Africa. *British Geological Survey Internal Report*, 1-31.

Weinert, H. 1968. Engineering petrology for roads in South Africa. *Engineering Geology,* 2(6):363-395.

Werndl, C. 2014. On defining climate and climate change. *The British Journal for the Philosophy of Science,* 67: 337-364.

Wilhite, D. 2000. Drought as a natural hazard: concepts and definitions. *Drought: A Global Assessment,* 1(1): 3-18.

Wilhite, D. & Glantz, M. 1985. Understanding the drought phenomenon: The role of definitions. *Water International,* 10(3):111-120.

Wossenyeleh, B., Worku, K., Verbeiren, B. & Huysmans, M. 2020. Drought propagation and its impact on groundwater hydrology of wetlands. *Natural and earth system sciences*,1-27.

Xu, Y. & Van Tonder, G. 2001. Estimation of recharge using a revised CRD method*. Water SA,* 27(3):341-343.

Zargar, A., Sadiq, R., Naser, B. & Khan, F. 2011. *A review of drought indices*. Kelowna, Canada: NRC Research Press.

Zin, W., Jemain, A. & Ibrahim, K. 2012. Analysis of drought condition and risk in Peninsular Malaysia using Standardised Precipitation Index. *Theoretical and Applied Climatology*, 111(3-4):559-568.

Zoljoodi, M. & Didevarasl, A. 2013. Evaluation of Spatial-Temporal Variability of Drought Events in Iran Using Palmer Drought Severity Index and Its Principal Factors (through 1951-2005). Atmospheric and Climate Sciences. 03(02):193-207.

Appendix A – Description of study areas

7.1 Rainfall description

7.1.1.1 Rainfall

South Africa's climatic condition varies from region to region. It ranges from a more Mediterranean climate in the south-western corner of the country to a temperate climate on the interior plateau. The rainfall across South Africa also differs from region to region. Rainfall generally occurs during the summertime across the country, except near Cape Town in the Western Cape where there is winter rainfall.

The regions of higher precipitation are situated in the eastern part of the country and lower precipitation occurs in the north western region of the country, mainly in the Northern Cape province. The average rainfall across South Africa is in the region of 460 mm per annum.

The climate in terms of rainfall found for each study area differs dependent on the quaternary catchment, as the WR2012 rainfall is based on a quaternary catchment level.

Figure 38 below illustrates the variation in rainfall across South Africa as the mean annual precipitation.

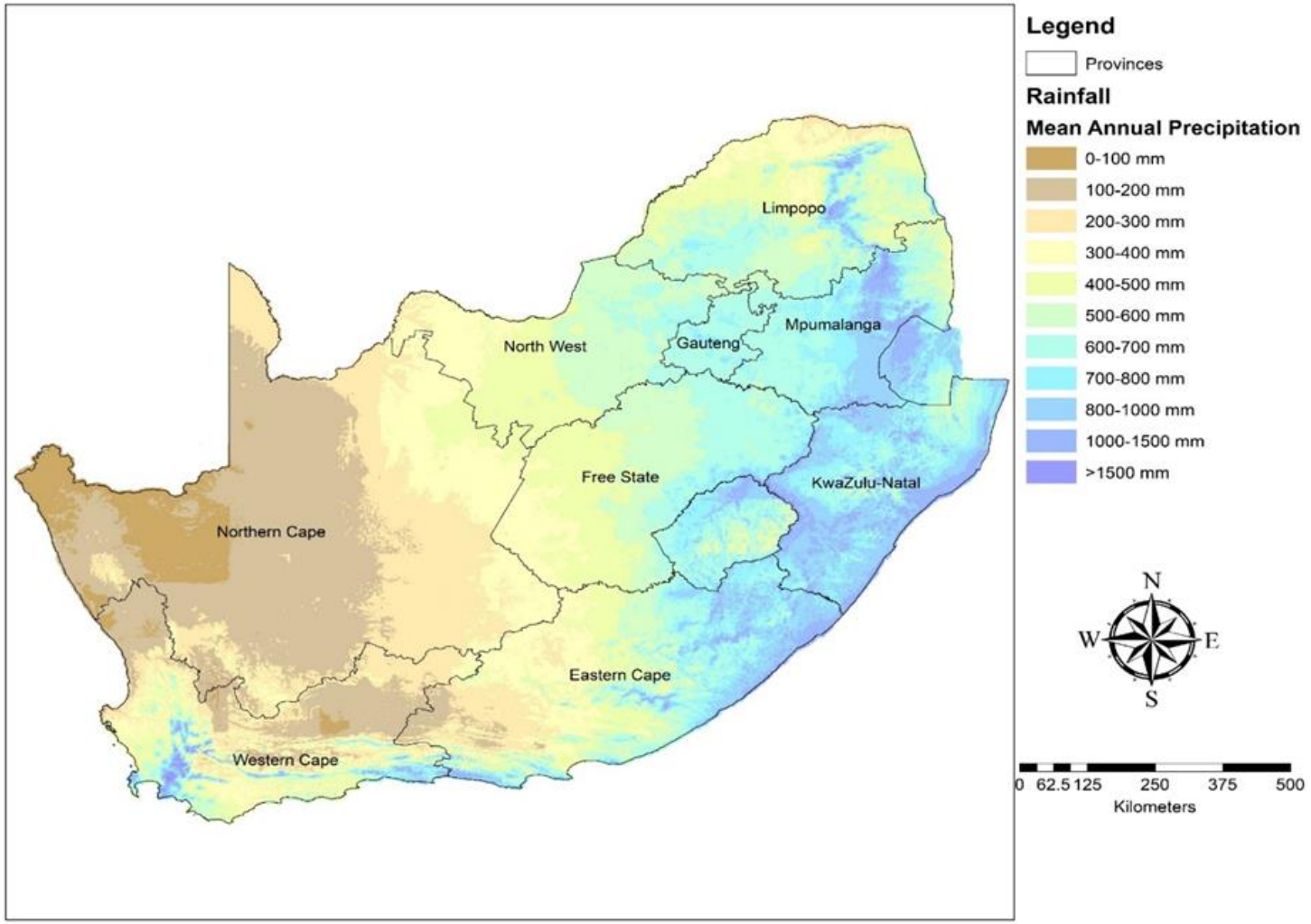

Figure 38: Mean annual rainfall map of South Africa

7.2 Borehole description

Borehole water levels are measured from the top of the aquifer, known as the water table, to the surface of the earth or ground level. Borehole water levels are expressed in metres above mean sea level (mamsl) or meters below ground level (mbgl). The average water levels for each study area are shown in Table 32.

Table 32: Summary of boreholes information

Geology	Quaternary catchment	Borehole	Average groundwater level (mamsl)	Average depth (mbgl)	Coordinates	
					Latitude	Longitude
Teekloof FM	J21A	3222BC00151	827.7	12.3	-26.29380	27.66575
Loam and sandy loam	G30E	033568	15.7	24.3	-26.32660	27.78386
Malmani SBGRP	C23D	2627BC00051	1533.9	34.1	-25.80470	28.32411
ECCA GRP	C22A	2627BD00056	1585.1	24.9	-25.72930	28.23018
Hekpoort FM	A23A	036017	1468.3	24.7	-25.72630	28.23282
Strubenkop FM	A23E	2528CA00015	1340.5	19.5	-29.75030	25.31622
Diabase	A23E	11452	1301.1	18.9	-32.35078	22.58274
Kolobeng Norite	A22H	023502	1361.9	18.0	-32.30638	18.42062
Silverton FM	A22G	2528CD00065	1223.4	16.6	-25.74060	27.23241
Vryburg FM: Andesitic lava	C32B	2624DC00019	1193.8	16.2	-25.78310	27.25180
Dwyka Group	C32B	2624DC00026	1203.1	19.9	-26.92069	24.69131
Vryburg FM: Quartzitic sandstone	C32B	32611	1023.9	16.2	-26.93719	24.69164
Tierberg FM	C51J	2925CD00009	1345.7	14.3	-26.95725	24.71797

7.3 GRAII groundwater level

Figure 39 displays the average groundwater level across South Africa based on GRA II (DWAF, 2005) project data. Figure 40 displays the GRAII recharge map of South Africa and Figure 41 the Vegter Groundwater registration of South Africa. Each study area is indicated on the Figure 39.

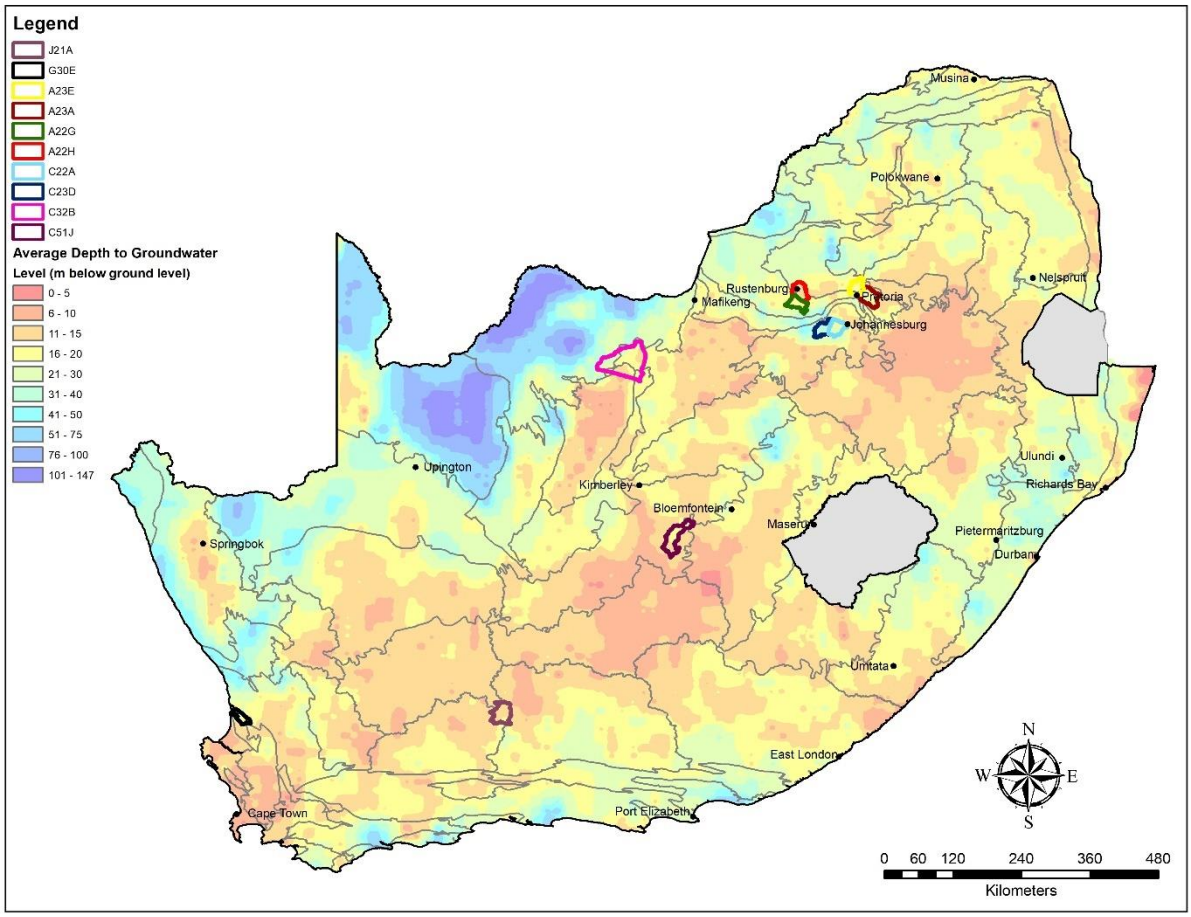

Figure 39: GRAII average groundwater level depth

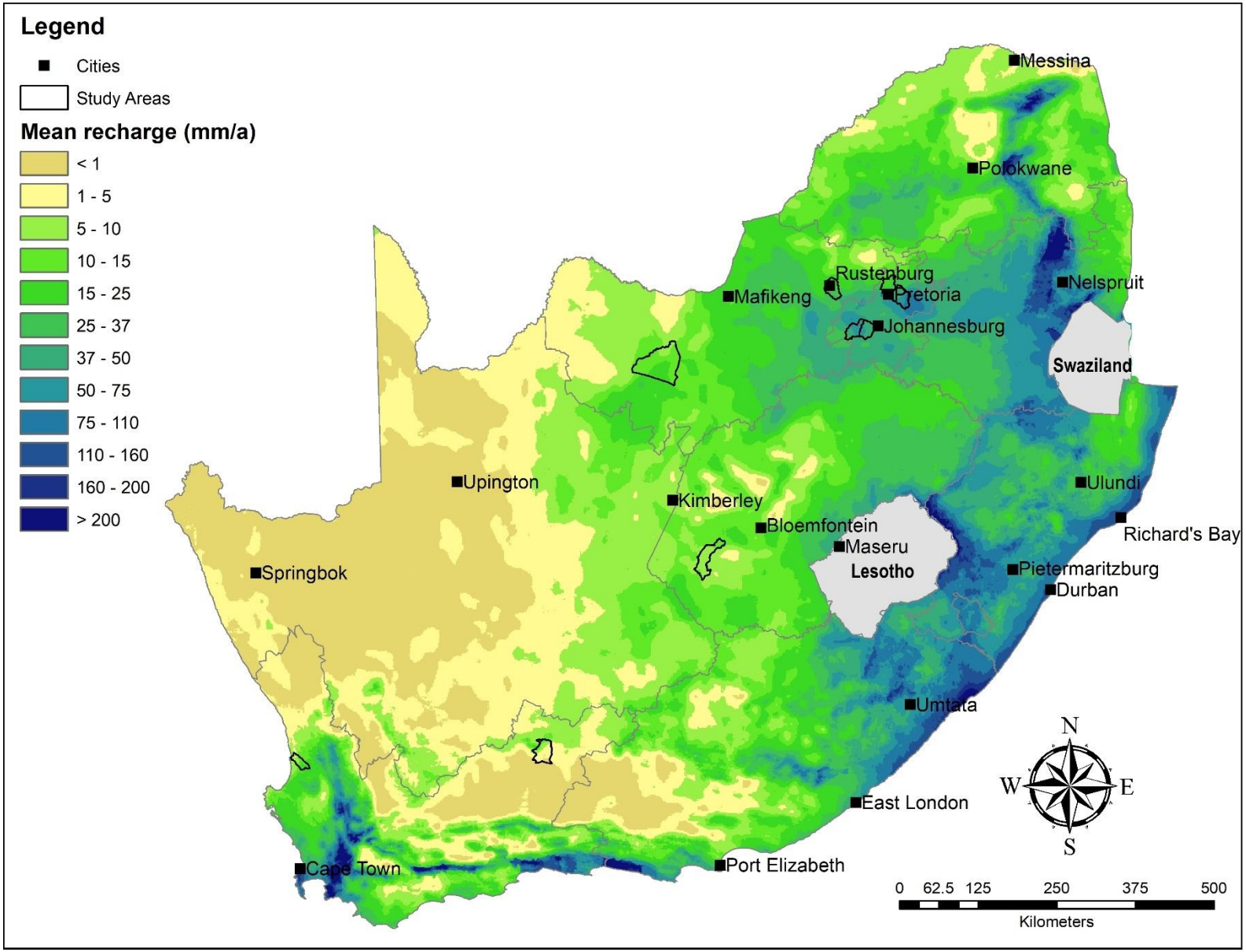

Figure 40: GRAII recharge map of South Africa

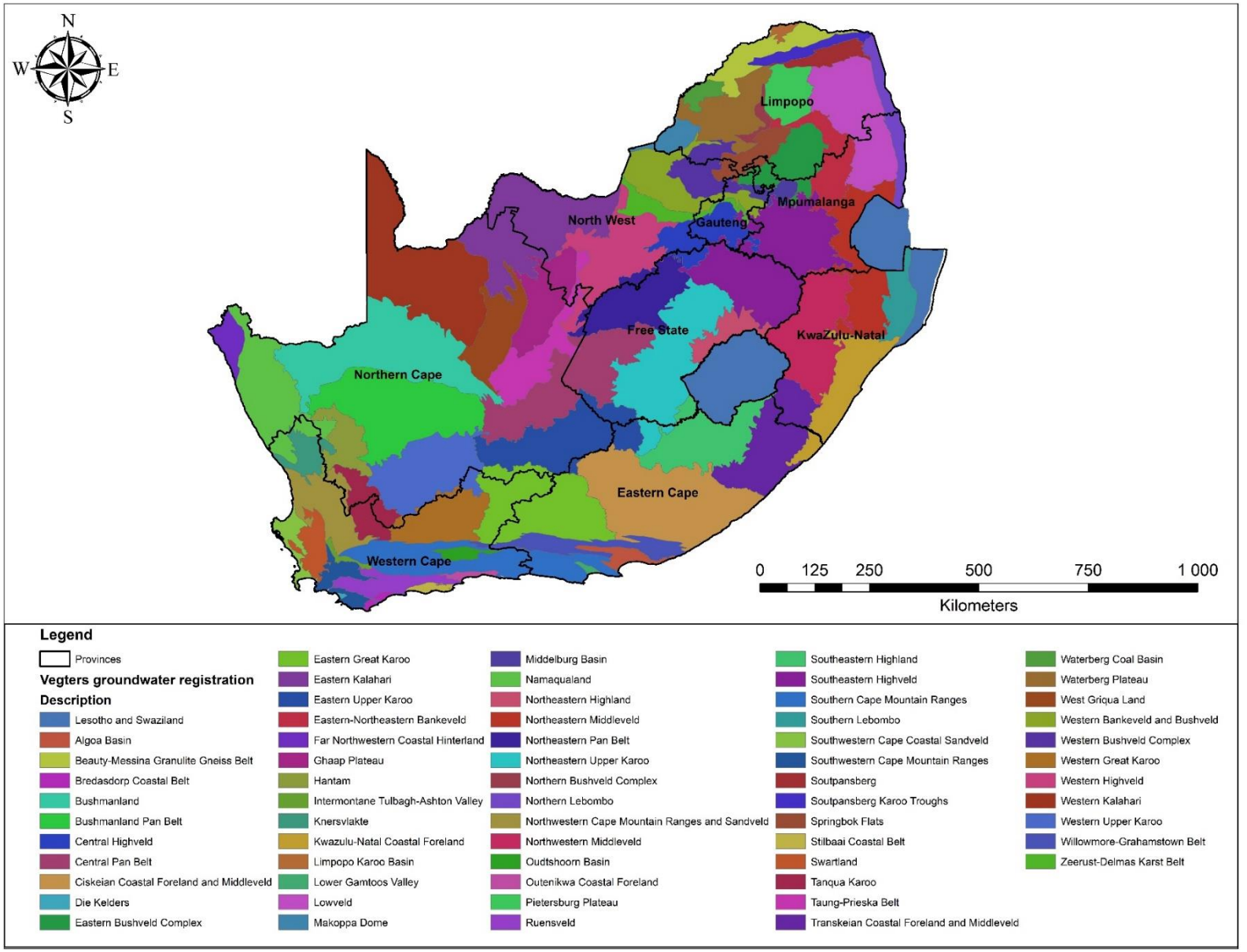

Figure 41: Vegter groundwater registration classification of South Africa

7.4 Study area description

Each study area is described in terms of their locality, geology, recharge and observed and simulated groundwater levels below. The rainfall and groundwater level diagrams indicate the rainfall, available groundwater level data and groundwater balance model simulated groundwater levels. The observed groundwater levels in each study area display the gaps in the monitored groundwater level data for each time series. Therefore, the lack in groundwater level data available on public platforms is evident. Not one of the study areas had more than 20 years of consecutive groundwater level data. The simulated groundwater levels (Fit) indicated the simulated groundwater levels as simulated through groundwater balance models.

7.4.1 Teekloof Formation

7.4.1.1 Locality and geology

We find the Teekloof Formation in quaternary catchment J21A (Western Province). Borehole 3222BC00151 (refer to Figure 42) is within a Teekloof Formation. The groundwater yield of the Teekloof Formation in this area in over 5.5 L/s.

The Teekloof Formation (Karoo Basin, South Africa) forms part of the Beaufort Group (Huttenlocker & Smith, 2017). Source area tectonism, which deposited a 2 700 m thick succession of fluvial channel overbank mudstone and sandstones, known as the Teekloof and Abrahamskraal Formations, caused the Beaufort group sedimentation (Huttenlocker & Smith, 2017).

The Teekloof Formation consists of mudstone (75-80%) and sandstone (20-25%). Mudstones, according to Aplin *et al.,* (1999), are not only the world's most common sedimentary types but also one of the prime controlling agents for sedimentary basins and near-surface environments, which leads to a high groundwater yield. Mudstones can act as aquitards, influencing overpressure and restricting water flow (Aplin et al., 1999).

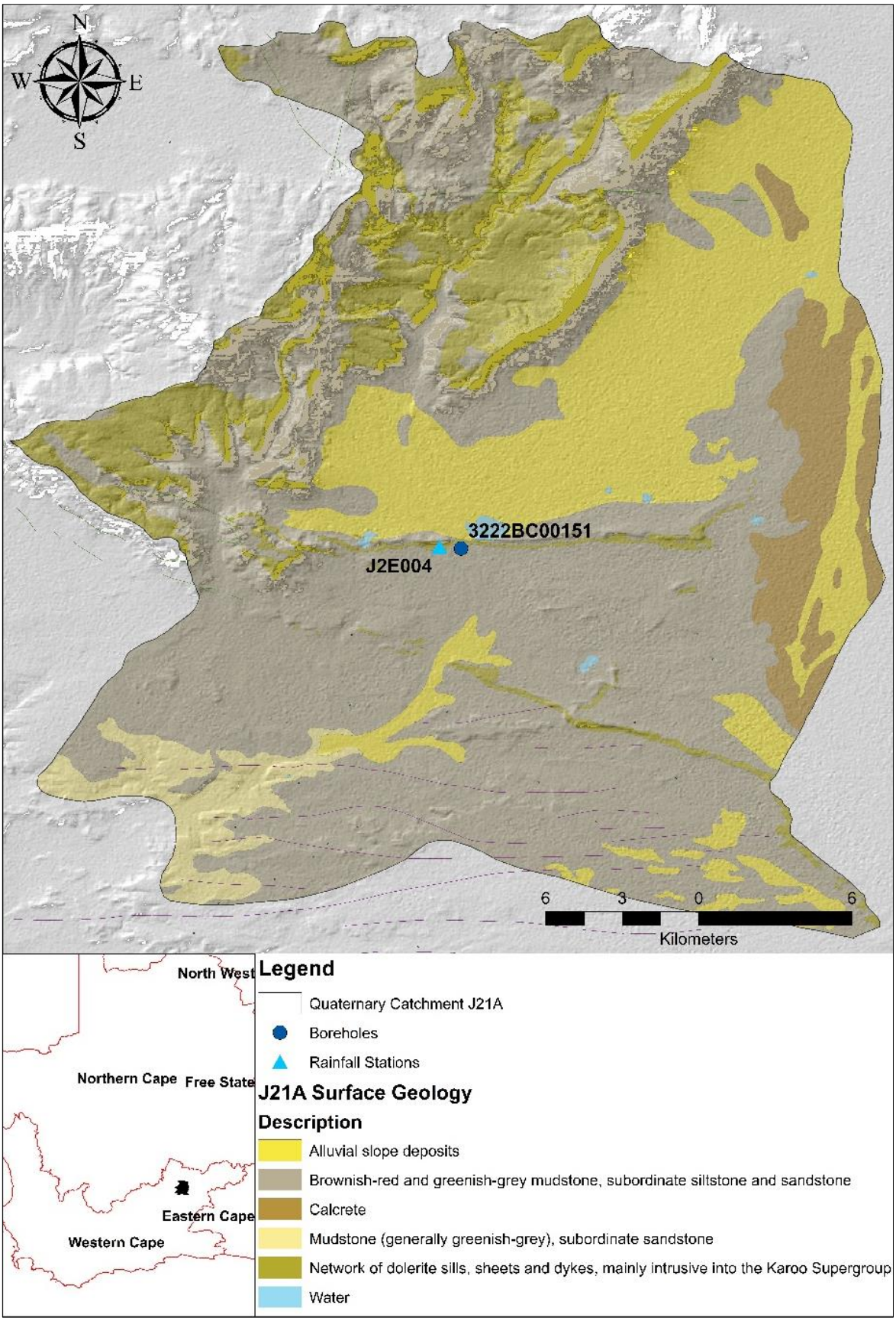

Figure 42: Geology map of quaternary catchment J21A

7.4.1.2 Recharge

The mean annual recharge for borehole 3222BC00151 is approximately 3 mm/a. Quaternary catchment J21A is classified as an arid region, which is the reason for the low recharge rate as it is situated in the Western Great Karoo groundwater registration region.

7.4.1.3 Rainfall and groundwater levels

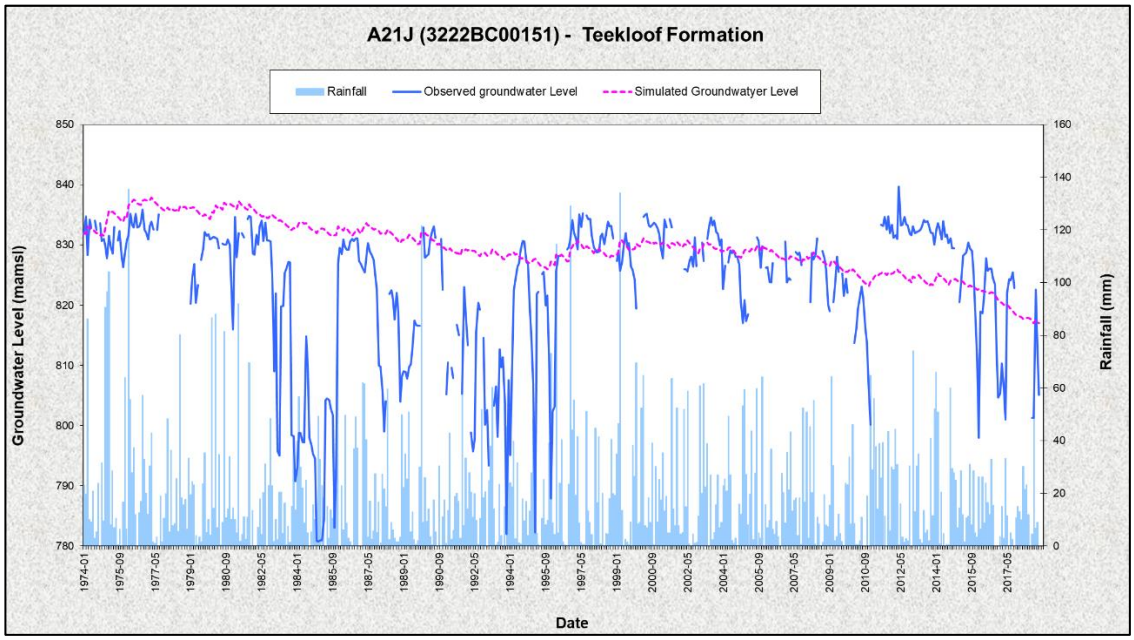

Figure 43: Teekloof Formation rainfall and groundwater levels

7.4.2 Loam and sandy loam

7.4.2.1 Locality and geology

Borehole 33568 is in quaternary catchment G30E. There is no distinct geological group defining the geology of the area. Loam and sandy loam are considered to be pedological geological material. Pedological refers to the surficial materials, therefore the loam and sandy loam are weathered geological material. Borehole is situated near the outcrops of the Piekenierskloof Formation and the Peninsula Formation. Both these formations are part of the Table Mountain Group (refer to Figure 44). The Peninsula Formation dominates the cliff areas in the region (Thamm, 1993), whereas the Piekenierskloof Formation is one of the lowermost formations of the Table Mountain Group (Thamm, 1993), consisting of sandstone with conglomerates and mudrock. Mudrock may comprise of siltstone, claystone, mudstone, slate, or shale (Thamm, 1993). The underlying geology of the area may well be that of the Piekenierskloof Formation (Thamm, 1993).

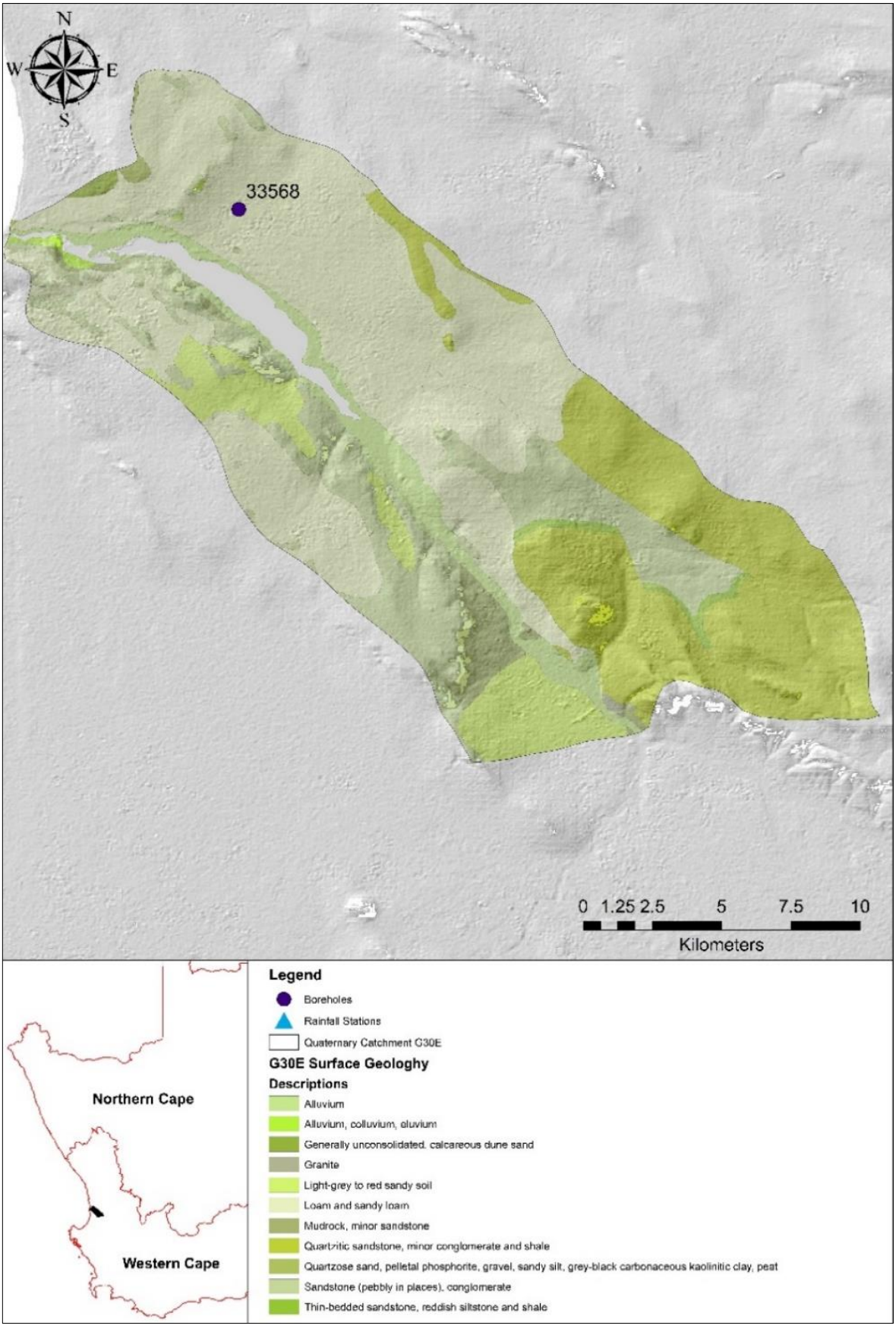

Figure 44: Geology map of quaternary catchment G30E

7.4.2.2 Recharge

The mean annual recharge for borehole 33568 is between 4 and 5 mm/a. Quaternary catchment G30E is situated in the North Western Cape Mountain Ranges and Sandveld groundwater registration region. The area surrounding borehole 33568 has higher recharge values; this can be due to the geology. The geology borehole 33568 is situated in a weathered geology (loam and sandy loam), which is the result of deposition from the outcrops of the Piekenierskloof and Peninsula Formations.

7.4.2.3 Rainfall and groundwater levels

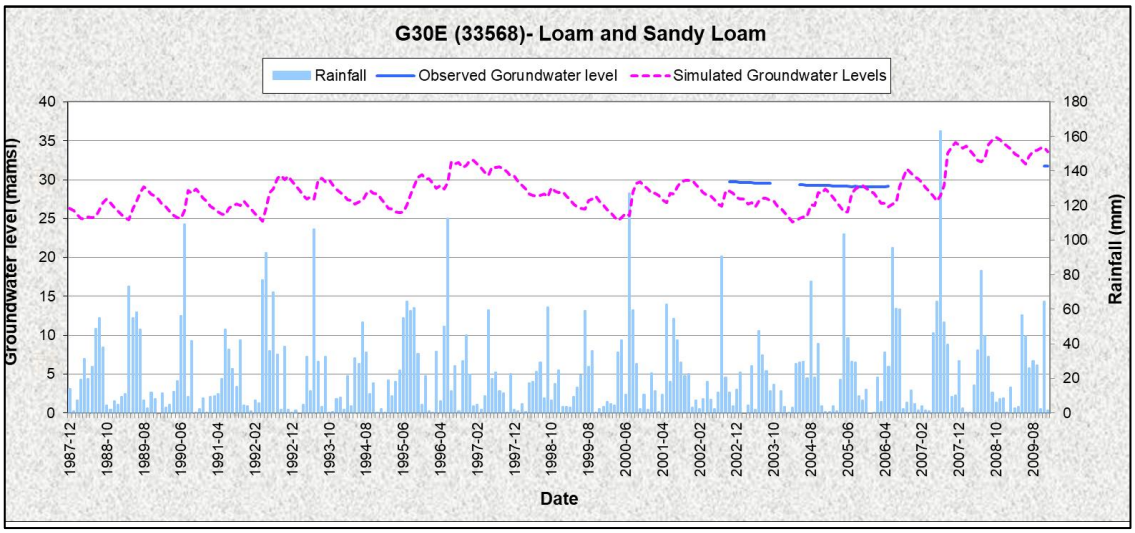

Figure 45: Loam and sandy loam rainfall and groundwater levels

7.4.3 Malmani Subgroup

7.4.3.1 Locality and geology

We find the Malmani Subgroup in quaternary catchment C23D. Borehole 2627BC00051 (refer to Figure 46) is within the Malmani Subgroup in the eastern part of Gauteng.

The Malmani Subgroup forms part of one of the earliest sedimentary carbonate sequences and was the subject of a dolomitisation silicification. The Malmani Subgroup is part of the larger Transvaal Supergroup and consists of dolomite rocks, limestone, and calcareous sedimentary rocks (Tessema et al., 2020; Clay, 1981). The Malmani Subgroup in this region consists of dolomite, subordinate chert, minor carbonaceous shale, limestone and quartzite.

The Malmani Subgroup of the Transvaal basin, according to Tessema *et al.,* (2020), forms a karst aquifer, which leads to a high groundwater yield of over 5.0 L/s. Karst aquifers and areas of carbonate rocks (dolomite, limestone) have boreholes with high yields (Tessema et al., 2020) and the area is in a region with high groundwater yield and recharge value (Figure 40) compared to other areas in South Africa. Therefore, groundwater retention and movement in the subsurface is of such class that the water from rainfall events can infiltrate and diffuse well (Tessema et al., 2020).

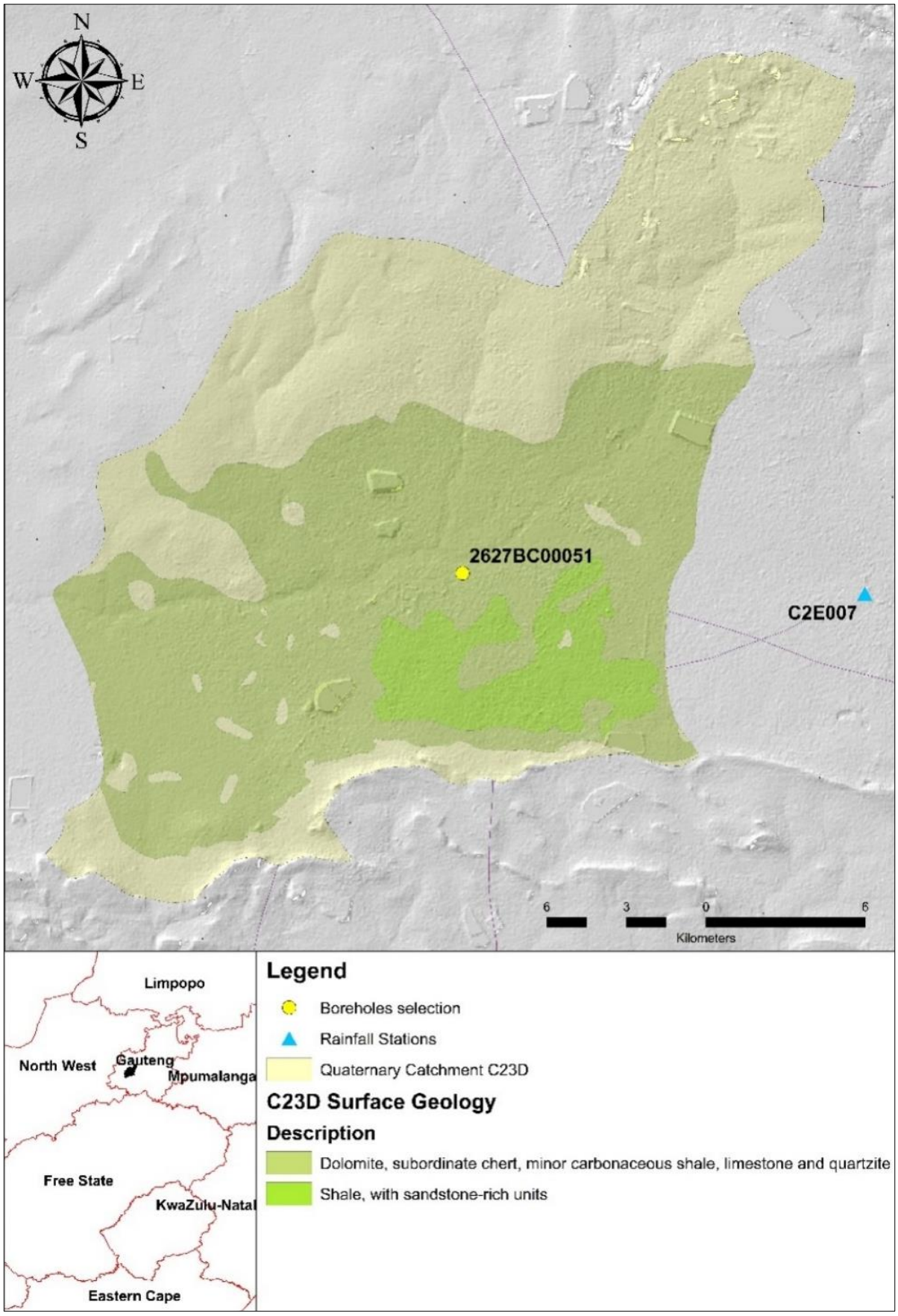

Figure 46: Geology map of quaternary catchment C23D

7.4.3.2 Recharge

The mean annual recharge for borehole 3222BC00051 is approximately 60 mm/a. Quaternary catchment C23D is situated in the Central Highveld groundwater registration region. The Central Highveld is characterised by Vegter (2001) as a region with high groundwater recharge.

7.4.3.3 Rainfall and groundwater levels

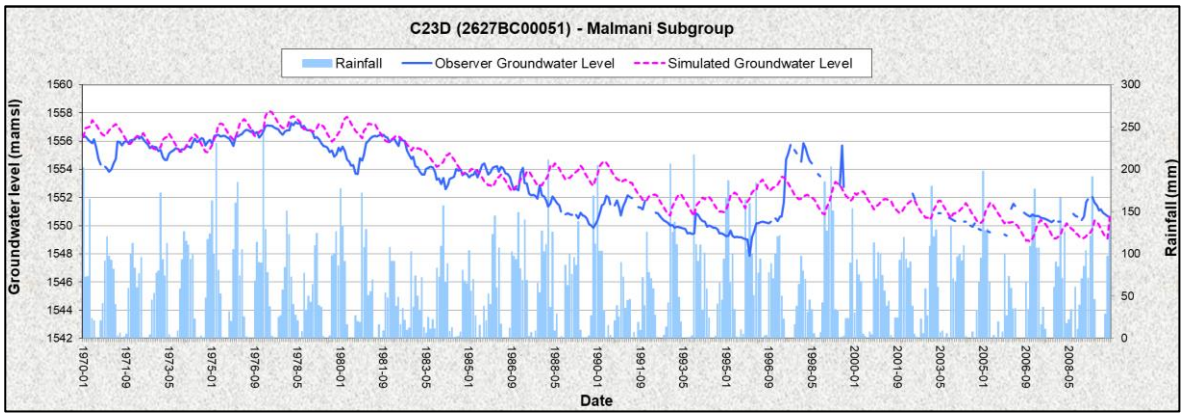

Figure 47: Malmani Subgroup rainfall and groundwater levels

7.4.4 ECCA Group

7.4.4.1 Locality and geology

Borehole 2627BD00056, also situated in quaternary catchment C22A, forms part of the ECCA Group (refer to Figure 48). The ECCA Group forms part of the Karoo Basin. Drilling activities have shown that the Karoo Basin is between the overlying Vryheid Formation, part of the ECCA Group, and the underlying Dwyka Group (Bordy et al., 2017). The ECCA Group consists of shale, with sandstone-rich units present towards the basin margins in the south, west and northeast and coal seams in the northeast.

Shale has low permeability and natural fractures (Liu et al., 2019). In time, permeability will increase because of water-shale interaction, causing fractures to increase in amount and size (Liu et al., 2019). Therefore, the amount of groundwater flow within the fractures and the amount of infiltration depends on the state of the shale.

Boreholes in the ECCA Group have medium to high groundwater potential with yields between of 1.4 L/s to 2.8 L/s. The degree of fracturing in the shale will influence the groundwater yield (permeability, porosity, infiltration rate etc.). Fractured shale will lead to higher yields.

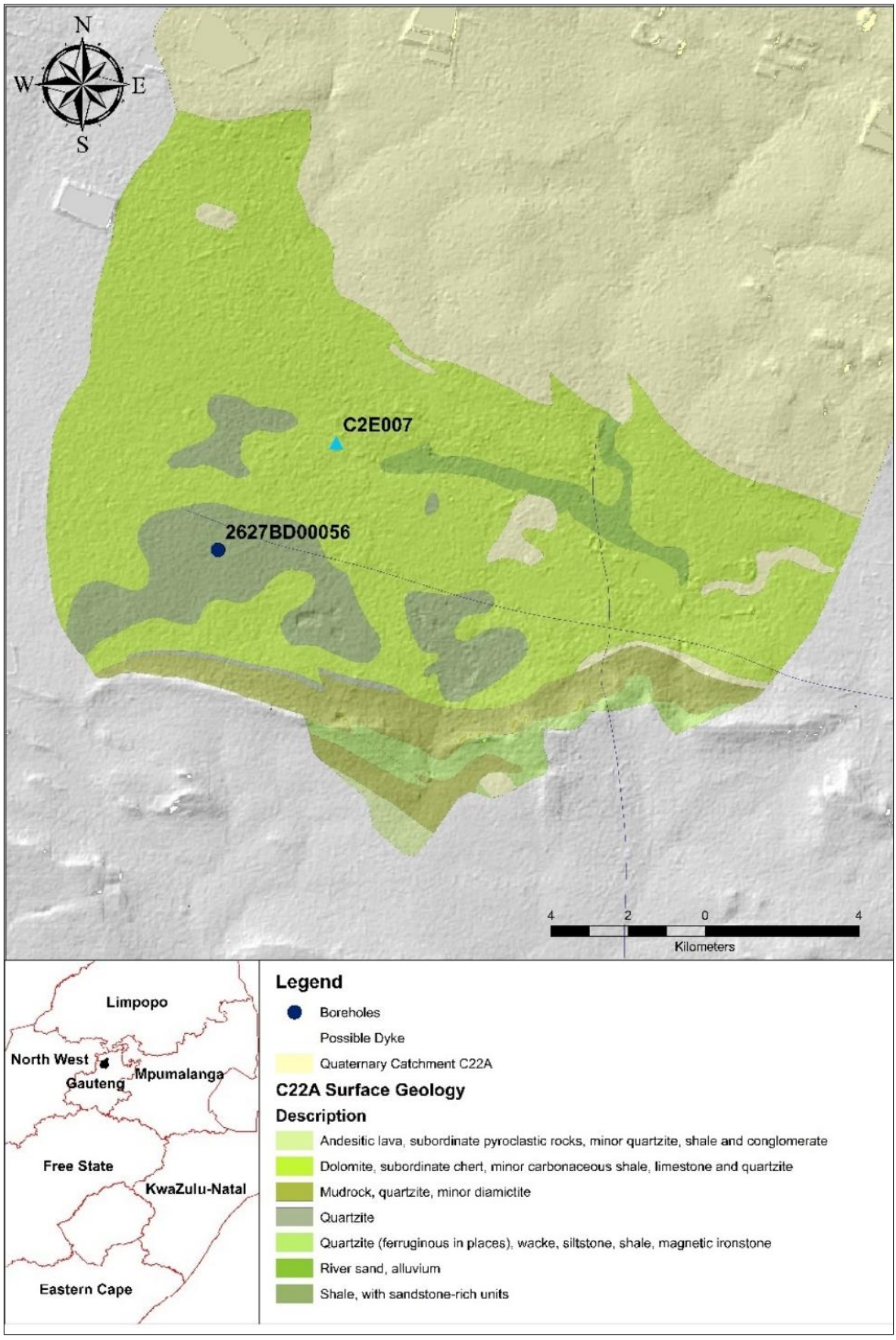

Figure 48: Geology map of quaternary catchment C22A

7.4.4.2 Recharge

The mean annual recharge for borehole 2627BD00056 is similar to borehole 3222BC00051 as both are situated in the Central Highveld groundwater registration region.

7.4.4.3 Rainfall and groundwater levels

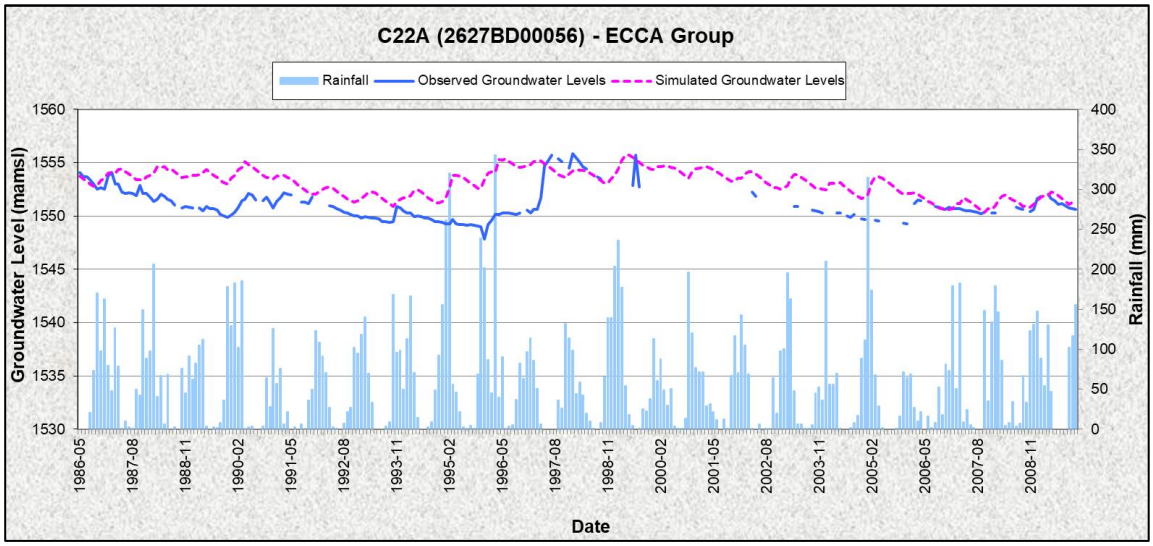

Figure 49: ECCA Group rainfall and groundwater levels

7.4.5 Hekpoort Formation

7.4.5.1 Locality and geology

The Hekpoort Formation is part of the Pretoria Group, the Pretoria Group forms the upper part of the sedimentary Transvaal Supergroup (Humbert et al., 2018). Borehole 36017 in quaternary catchment A23A is part of the Hekpoort Formation (refer to Figure 50).

The Hekpoort Formation overlies the Timeball Hill Formation mudrocks or in some areas the alluvially and fluvially deposited sandstones and conglomerates (Humbert et al., 2018). The formation consists of andesitic lava, subordinate pyroclastic rocks, minor quartzite, shale and conglomerate.

Vittecoq *et al.,* (2019) conducted a study on andesitic watersheds with the aid of high-resolution heliborne geophysics. They found that the hydrogeological functions in andesitic aquifers are influenced by geological structures in terms of the interactions between surface water resources (such as rivers) and aquifers and the groundwater flow within the aquifers (Vittecoq et al., 2019). The resistivity values obtained from the heliborne geophysics analysis determined that andesitic domes or structures have high resistivity values, therefore the andesitic aquifers or geologies are fractured and fissured, conferring to high hydraulic conductivity (Vittecoq et al., 2019). High hydraulic conductivity values pertain to permeable material. The effect droughts can have on geologies, such as the Hekpoort Formation, is dependent on the geological structures within the formation’s capabilities to store water from precipitation, as it has a high groundwater yield.

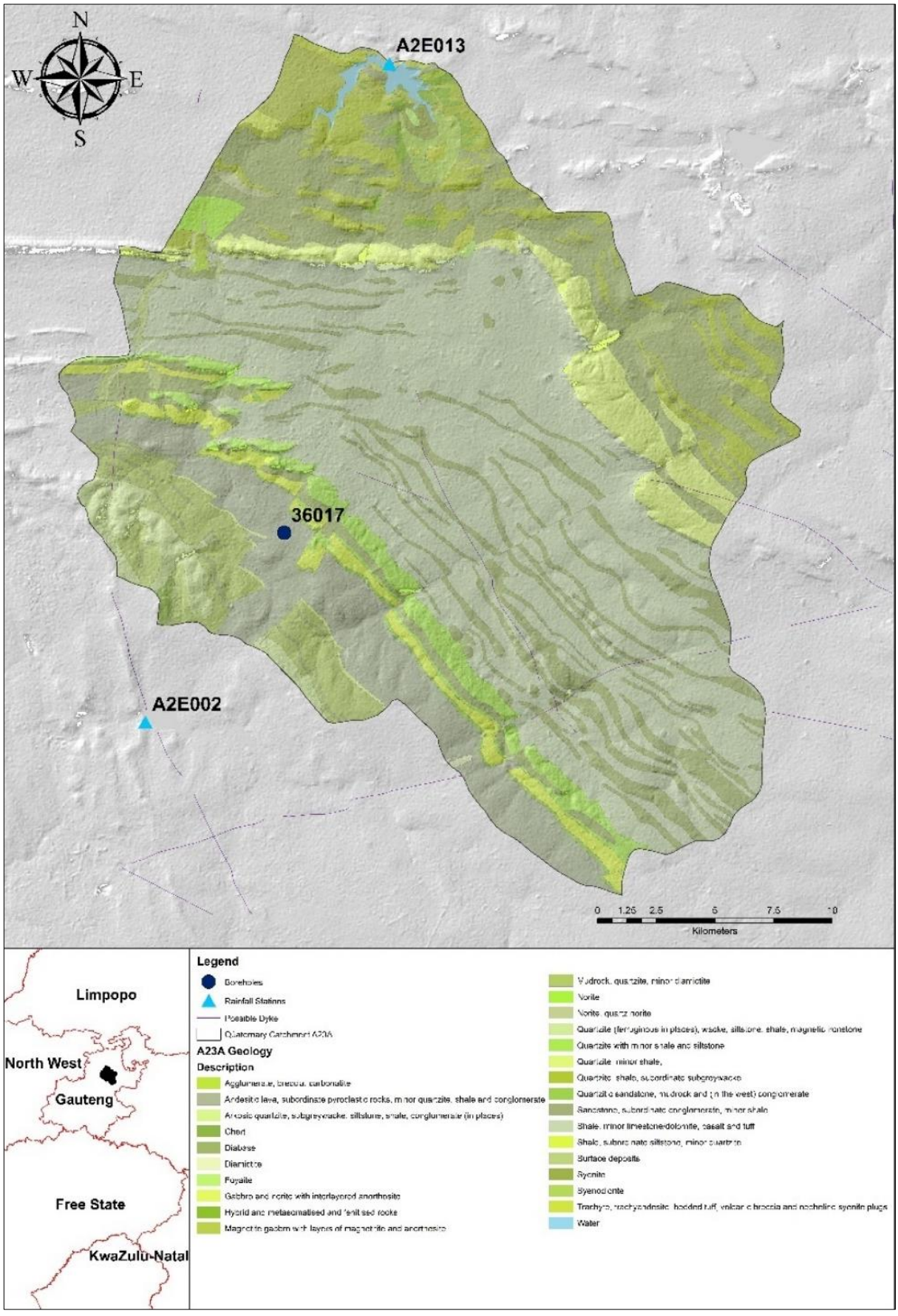

Figure 50: Geology map of quaternary catchment A23A

7.4.5.2 Recharge

The mean annual recharge for borehole 036017 is approximately 50 mm/a. Quaternary catchment A23A is situated in the Western Bankeveld and Bushveld groundwater registration region.

7.4.5.3 Rainfall and groundwater levels

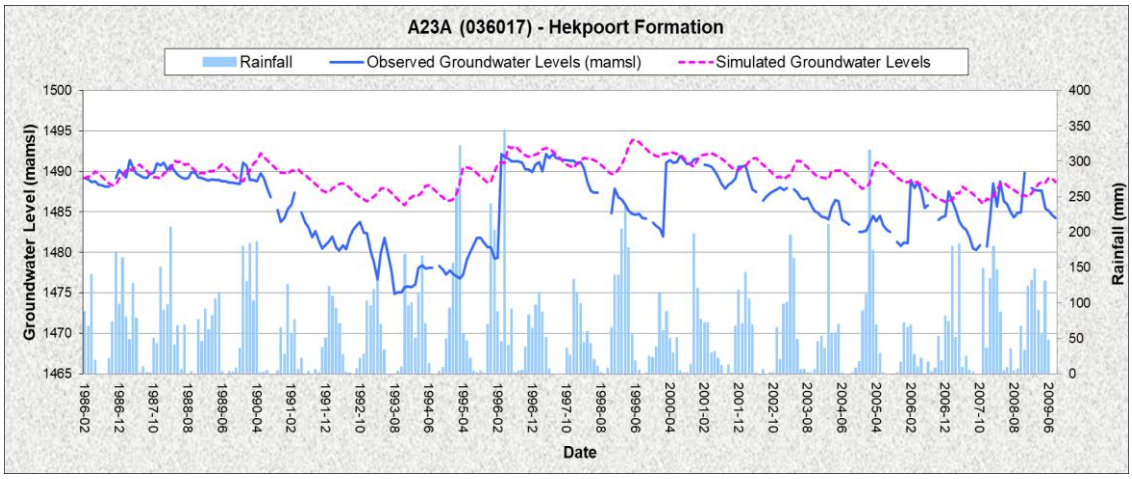

Figure 51: Hekpoort Formation rainfall and groundwater levels

7.4.6 Strubenkop Formation

7.4.6.1 Locality and geology

Borehole 2528CA00015 is in the Strubenkop Formation in quaternary catchment A23E in the northern parts of Gauteng (Refer to Figure 52).

The Strubenkop Formation forms part of the Pretoria Group and consists of fine-grained shale with inter-layered shale sandstone (Immature sandstone), subordinate siltstone, minor quartzite, mudstone and in some places we can also find hornfels (Burgoyne, 2013; Eriksson et al., 2006). Soils emanating from this formation are weaker and shallow in arid conditions and deeper and richer in wetter conditions (Burgoyne, 2013).

The area gets 25-37 mm/a recharge and a groundwater yield between 0.1-0.5 L/s. The groundwater yield for the Strubenkop Formation is low compared to the formations of the other groups in Gauteng. Droughts can affect the geology because of good recharge rates and low yields. This implies that the formation's water percolation period may be longer, because of the low groundwater yield.

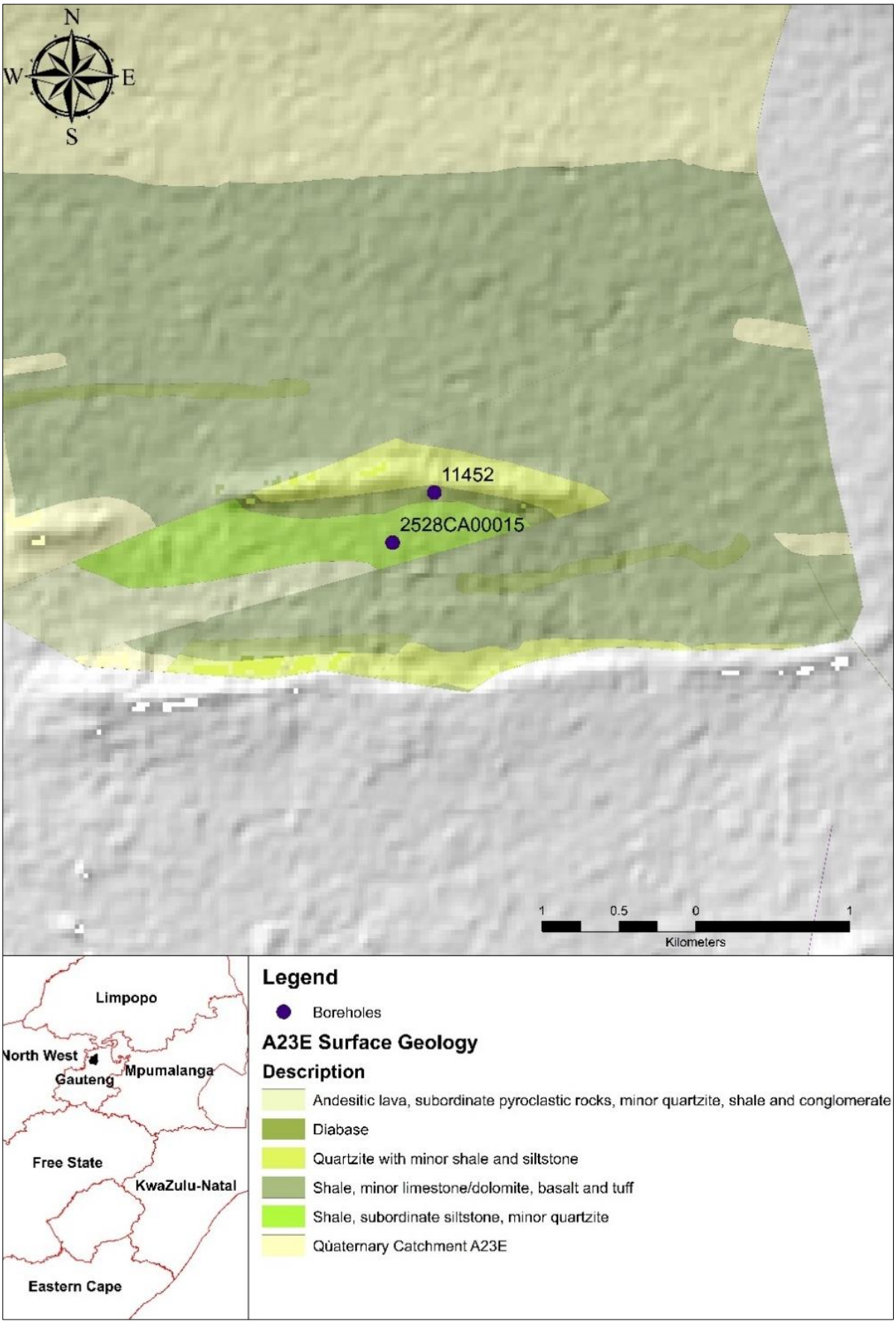

Figure 52: Geology map of quaternary catchment A23E

7.4.6.2 Recharge

The mean annual recharge for borehole 2528CA00015 is approximately 37 mm/a. Borehole 2528CA00015 is also situated in the Western Bankeveld and Bushveld groundwater registration region. The recharge rate is however less than that of borehole 036017.

7.4.6.3 Rainfall and groundwater levels

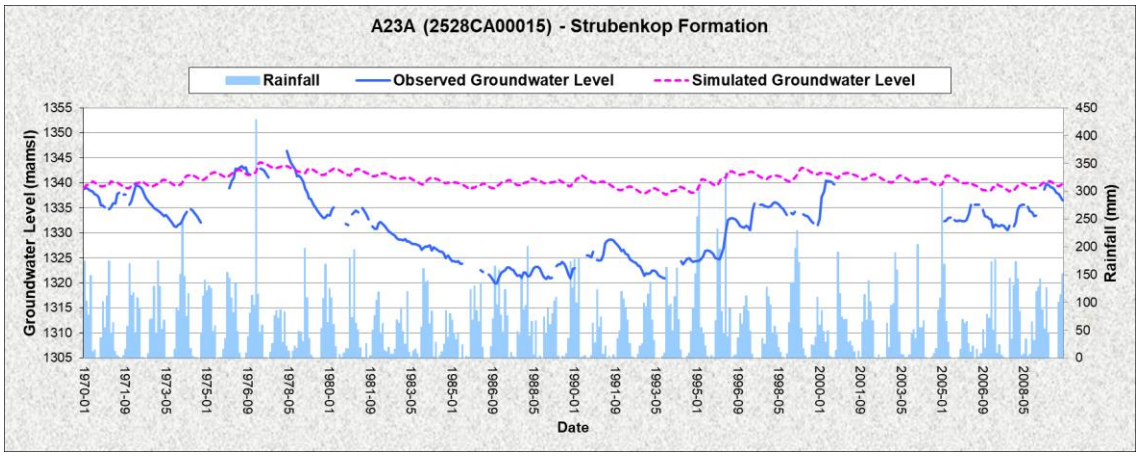

Figure 53: Strubenkop Formation rainfall and groundwater levels

7.4.7 Diabase

7.4.7.1 Locality and geology

Borehole 11452 is found in the northern parts of Gauteng in quaternary catchment A23E in a diabase type geology. Diabase residing in this area forms part of the Vaalian Era chronostratigraphy, the same era as the bushveld igneous complex and the Wolkberg Group (Refer to Figure 54).

Weinert (1968) stated that dolerite is more of an age denomination than a petrological term, and the associated igneous rocks with similar texture and composition found in South Africa are what we can refer to as diabase.

Diabase appears as shallow intrusions such as dykes and sills. The diabase intrusion is between the Strubenkop and Daspoort Formation (Refer to Figure 24), both formations having shale geologies. The Strubenkop Formation and Daspoort Formation have a groundwater yield or occurrence between 0.1 L/s and 0.5 L/s, which is low compared to formations such as the Malmani Subgroup. The diabase is an igneous intrusion between these two formations. These intrusions are characterised by thin linear zones and act as conduits for groundwater flow within aquifers permeability (Chevallier et al., 2001). The groundwater level varies more in borehole 011452 (diabase) than in borehole 2528CA00015 (Strubenkop Formation), which indicates a more permeable geology with a higher groundwater yield.

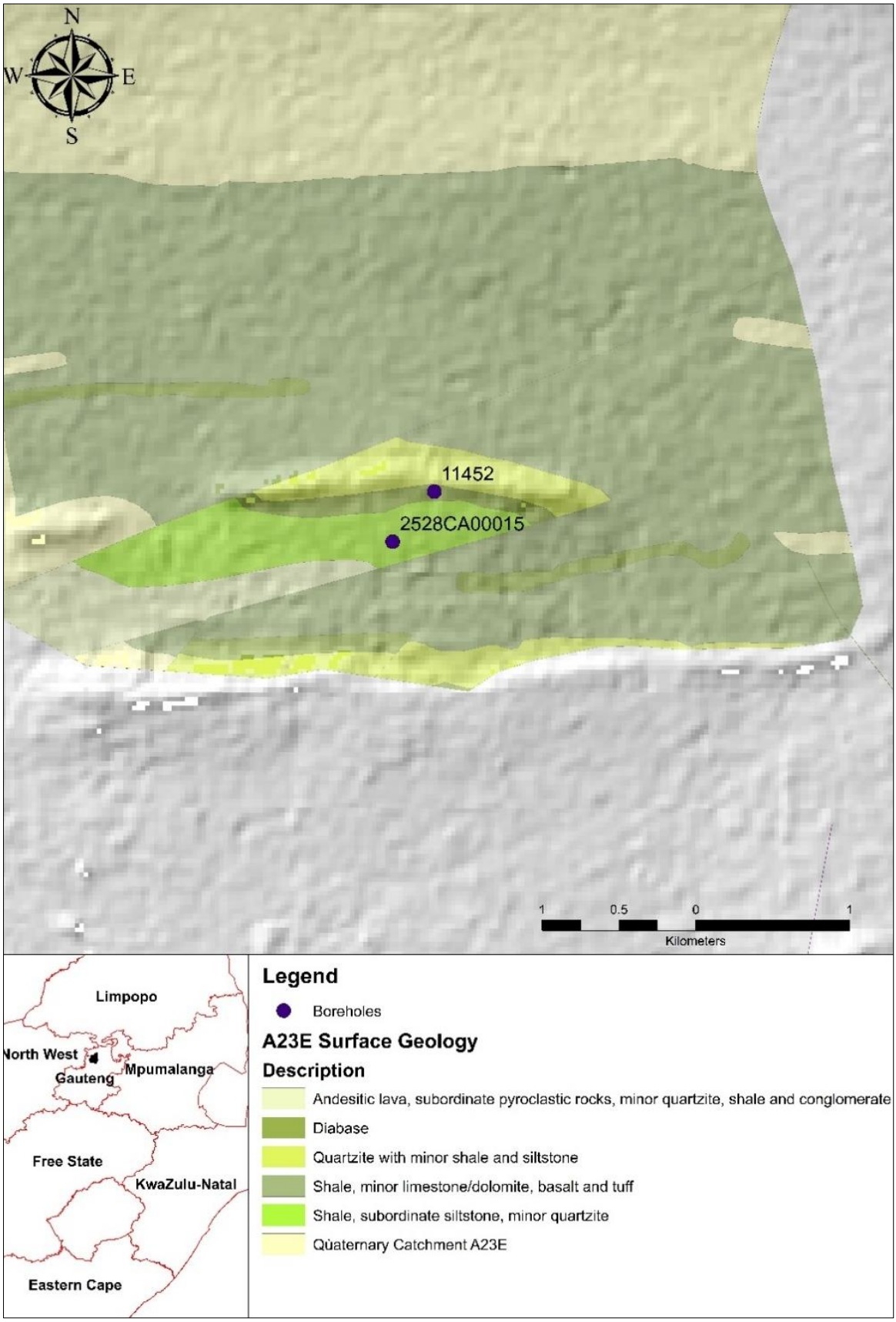

Figure 54: Geology map of quaternary catchment A23E

7.4.7.2 Recharge

The mean annual recharge for borehole 11452 is similar to borehole 2528CA00015. Borehole 11452 is also situated in the Western Bankeveld and Bushveld groundwater registration region.

7.4.7.3 Rainfall and groundwater levels

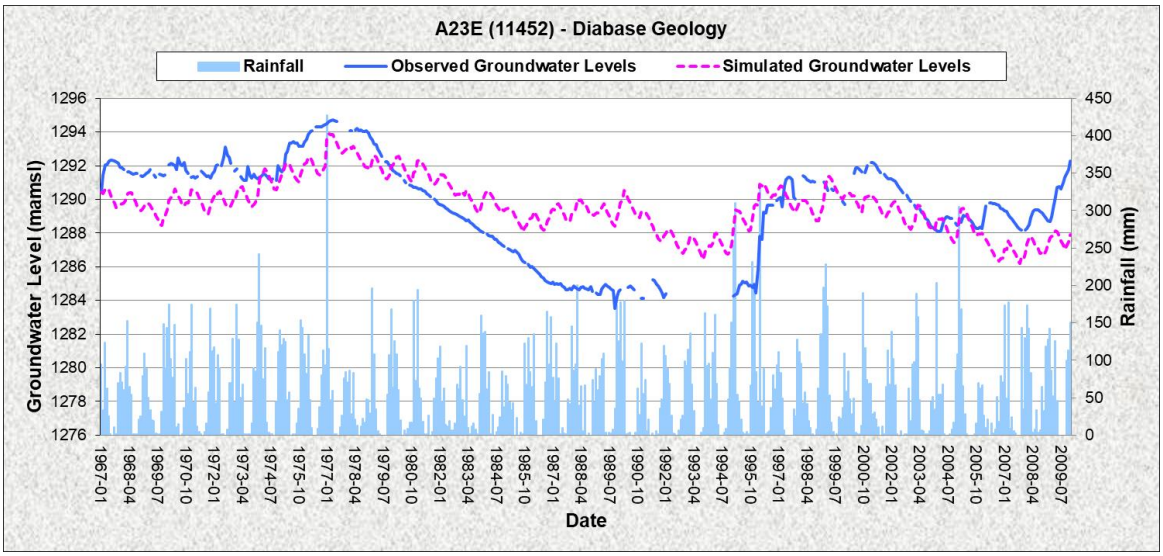

Figure 55: Diabase geology rainfall and groundwater levels

7.4.8 Kolobeng Norite Formation

7.4.8.1 Locality and geology

Borehole 23502 is found in the Kolobeng Norite Formation in quaternary catchment A22H in the North West (Refer to Figure 56). The Kolobeng Norite Formation forms part of the Rustenburg Layered Suite of the Bushveld igneous complex (Sami & Druzynski, 2003).

The recharge is 29 mm/annum and the A22H is between 6 and 14 mm/annum. Aquifers in the area can be described as fractured, having a yield of between 0.5 - 2.0 L/s. The yields of the formation are similar to the values reported by Barnard (2000) for the Rustenburg Layered Suite, with an average of 2.0 ℓ/s for gabbro, norite, chromitite and magnetite rocks pertaining to the Suite. The formations of the bushveld igneous such as the Kolobeng Norite have intricate hydraulic properties in the unweathered layers; this is because of the heterogeneity related to the fractures in the rocks. Storativity values also vary within these formations, affecting transmissivity and groundwater yield.

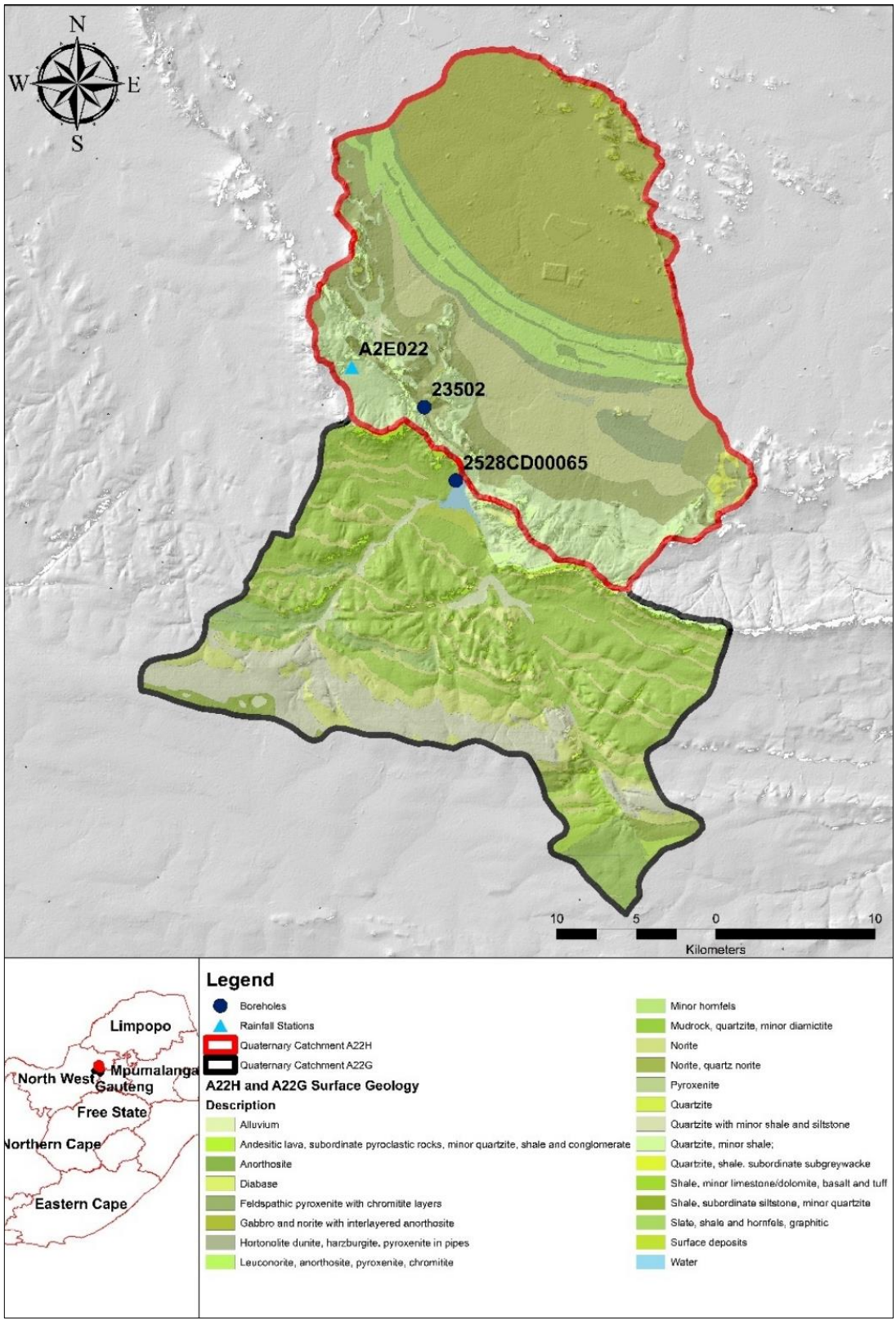

Figure 56: Geology map of quaternary catchment A22H and A22G

7.4.8.2 Recharge

The mean annual recharge for borehole 023502 in the Kolobeng Norite Formation is approximately 32 mm/a. Borehole 023502 is situated in the Western Bankeveld and the Bushveld groundwater registration region.

The mean annual recharge for borehole 2528CD00065 in the Silverton Formation is similar to borehole 2528CA00015. Borehole 2528CD00065 has a slightly higher (34 mm/a) recharge than 2528CA00015 although they are situated in the same groundwater registration region.

7.4.8.3 Rainfall and groundwater levels

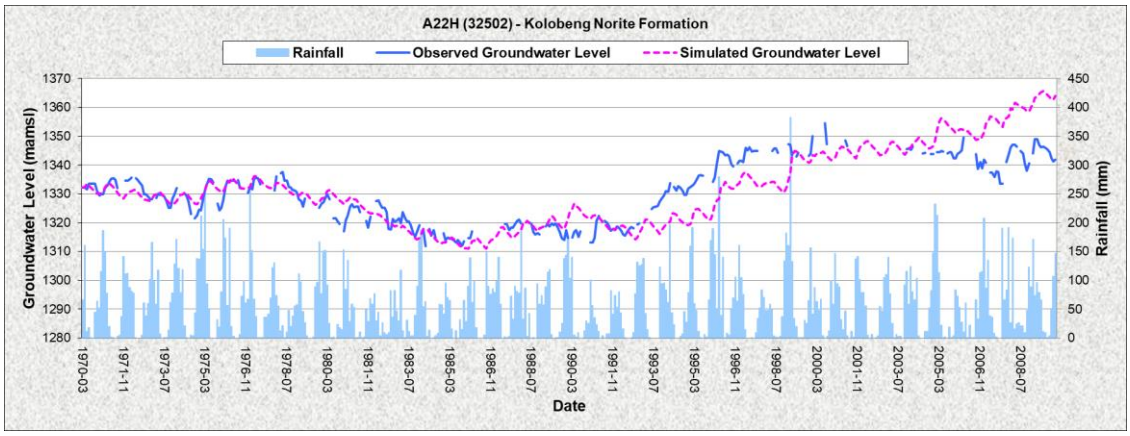

Figure 57: Kolobeng Norite rainfall and groundwater levels

7.4.9 Silverton Formation

7.4.9.1 Locality and geology

Borehole 2528CD00065 in the Silverton Formation is found in quaternary catchment A22G (refer to Figure 56). Recharge is about 31 mm/annum in the area. The area has an intergranular and fractured geology, having a groundwater yield of between 0.5 - 2.0 L/s.

Borehole 2528CD00065 is in the Silverton Formation, which forms part of the Pretoria Group. The Silverton Formation consists of shales, thick sequence of mudrocks with subordinate interbedded carbonate rocks, quarzitic sandstones, and andesitic lavas, agglomerates and tuffs (Eriksson et al., 1990; Mothoa & Lombaard, 2009). Intrusive diabase sills are also found in the Silverton Formation (Eriksson et al., 1990).

Groundwater occurrence in the Silverton Formation favours the weathered shale layers, jointed zones and the contact zone between the intrusive diabase sheets. Mothoa and

Lombaard (2009) conducted a groundwater study of the Silverton Formation. They classed the groundwater yield potential as good, based on 40% of the boreholes on record that produce over 2 L/s and 22% of the boreholes that produce over 5 L/s. The groundwater rest level lies between 10 and 30 mbgl (Mothoa & Lombaard, 2009).

7.4.9.2 Recharge

The mean annual recharge for borehole 2528CD00065 in the Silverton Formation is similar to borehole 2528CA00015. Borehole 2528CD00065 has a slightly higher (34 mm/a) recharge than 2528CA00015 although it is situated in the same groundwater registration region.

7.4.9.3 Rainfall and groundwater levels

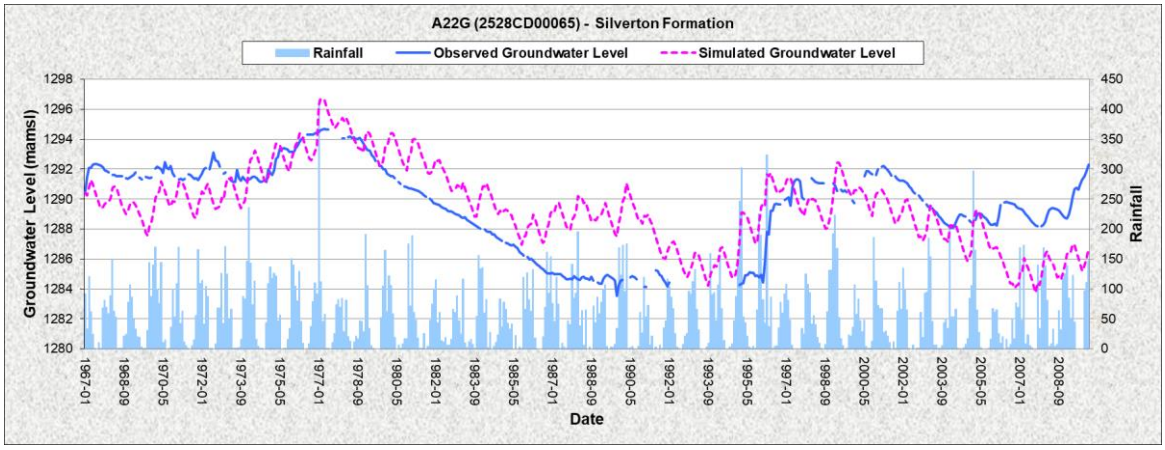

Figure 58: Silverton Formation rainfall and groundwater levels

7.4.10 Vryburg Formation

7.4.10.1 Locality and geology

The Vryburg Formation forms part of the Transvaal Supergroup. Boreholes 2528DC00019, 2528DC00026, and 32611 are situated in the Vryburg Formation in quaternary catchment C32B (refer to Figure 59). The Vryburg Formation is composed primarily of siltstone with subordinate shale, quartzite and andesitic lava (Eriksson et al., 1995).

Borehole 2528DC00019 is found in the andesitic lava geology of the Vryburg Formation, whereas Borehole 32611 is found in the siltstone, quarzitic sandstone and dolomite/limestone geology of the formation.

The boreholes in the andesitic lava geology have a groundwater yield of 2–5 L/s in a (fractured aquifer). 32611 in the siltstone geology has a groundwater yield between 0.5 L/s and 2 L/s. The recharge across the quaternary catchments is approximately 15 mm/a.

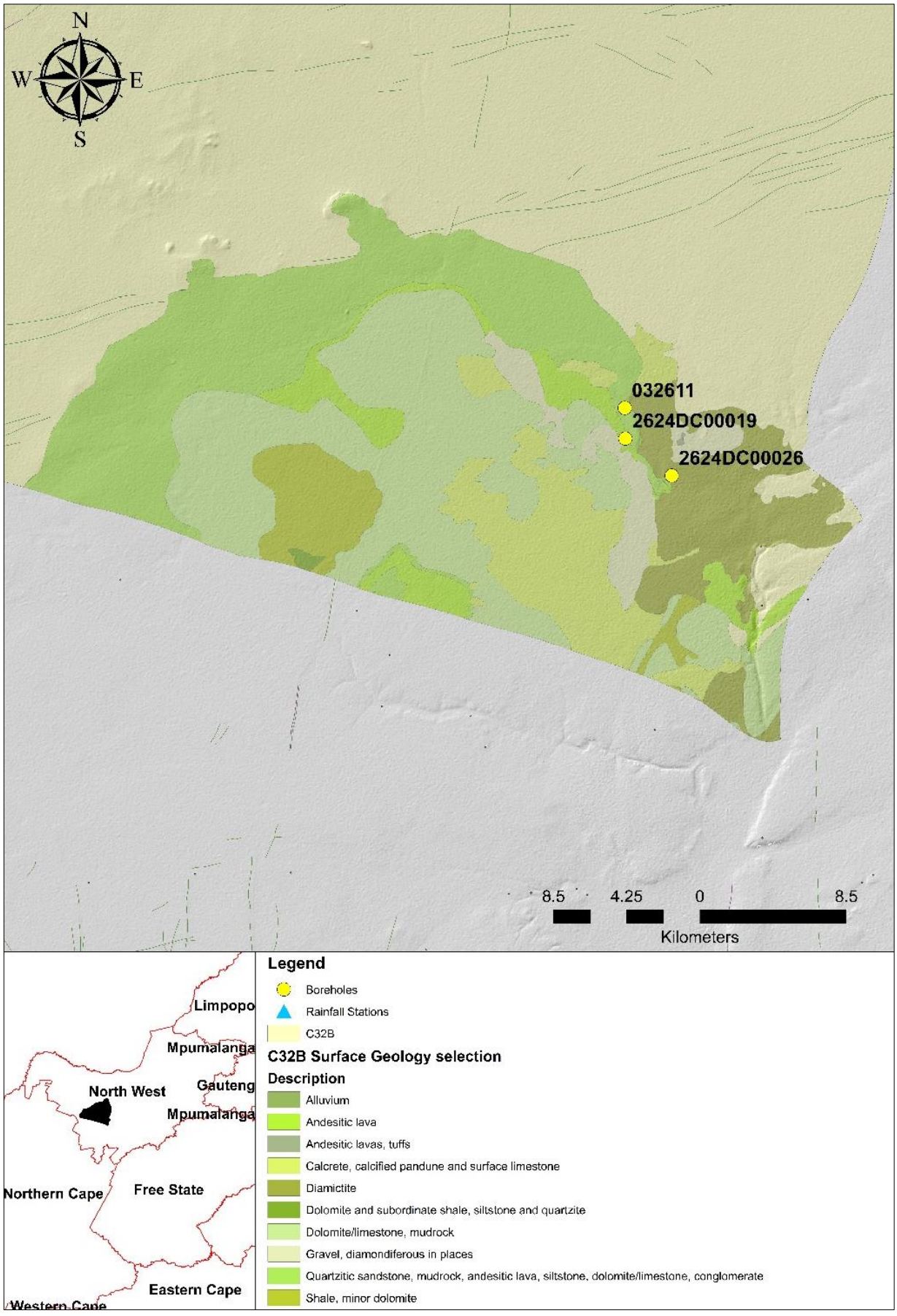

Figure 59: Geology map of quaternary catchment C32B

7.4.10.2 Recharge

The mean annual recharge for borehole 2624DC00019 is between 14 and 15 mm/a. Borehole 2624DC00019 is situated in the Chaap Plateau groundwater registration region. The lithology of the Chaap Plateau is known to have dolomite, chert and subordinate limestone.

Although in the same quaternary catchment as 2624DC00019, the mean annual recharge for borehole 2624DC00026 is approximately 14 mm/a. Borehole 2624DC00026 is situated in a different groundwater registration region from 2624DC00019, namely the Taung-Prieska Belt groundwater registration region.

7.4.10.3 Rainfall and groundwater levels (Vryburg Formation: Andesitic lava*)*

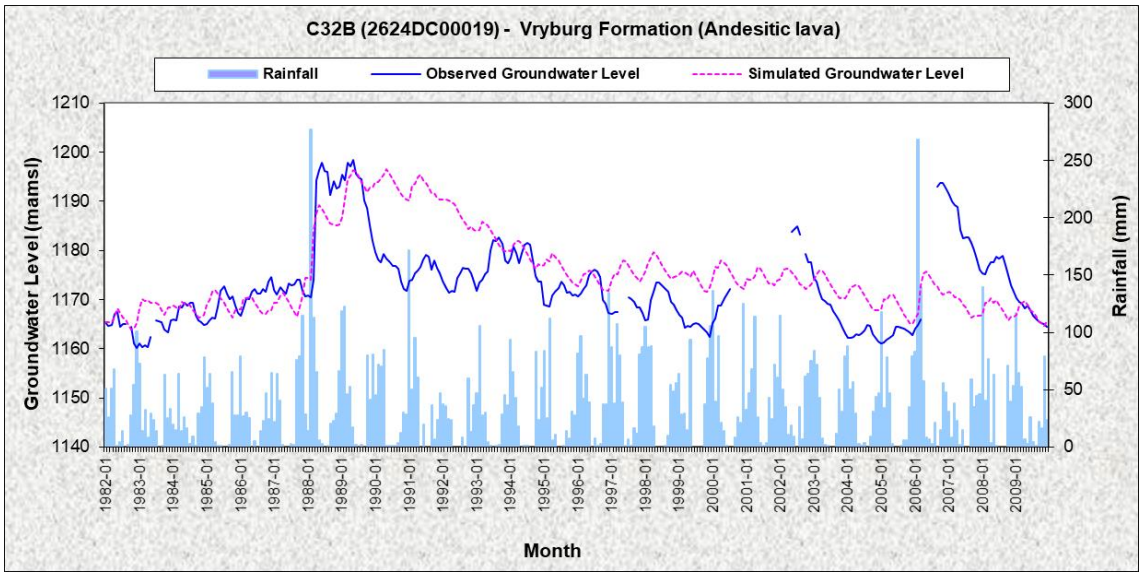

Figure 60: Vryburg Formation (Andesitic lava) rainfall and groundwater levels

7.4.10.4 Rainfall and groundwater levels (Vryburg Formation: Quartzitic sandstone)

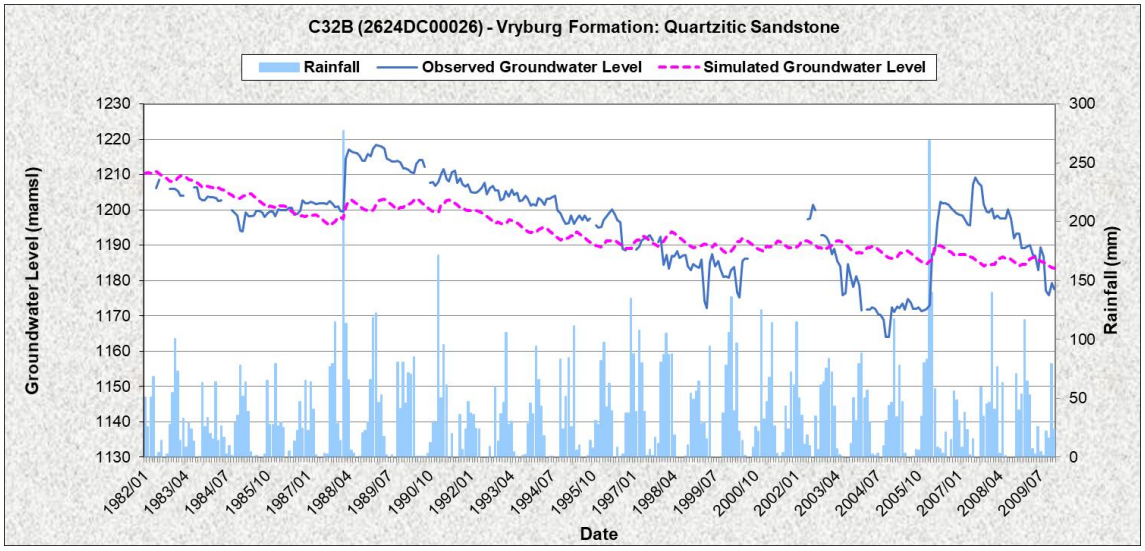

Figure 61: Vryburg Formation (quartzitic sandstone) rainfall and groundwater levels

7.4.11 Dwyka Group

Locality and geology

The Dwyka Group is one of the four geological groups that form the Karoo Supergroup (Bordy, 2018). Borehole 2624DC00026 is situated in the Dwyka Group in quaternary catchment C32B (refer to Figure 59).

The Dwyka Group in this region comprises mainly diamictite with shale, mudstone with dropstones and fluvio-glacial gravel (Herbert & Compton, 2007).

The Dwyka Group in this area has similar recharge values as the Vryburg Formation, also situated in quaternary catchment C32B. The groundwater yield however differs from the andesitic lava geology of the Vryburg Formation, but is similar to the siltstone geology as it also ranges between 0.5 and 2 L/s.

Borehole 032611 is situated in a diamondiferous type geology. The diamondiferous geology originated from the weathering of the Ventersdorp bedrock, resulting in remnants of diamondiferous sediments consisting of subangular and locally derived gravel (de Wit, 2004). The diamondiferous geology originated from the weathering of lithostratigraphic groups in the surrounding area, geology groups/formations, such as the Dwyka Group, Venterdorp Supergroup, and the Vryburg Formation.

7.4.11.1 Recharge

Borehole 032611 also differs from boreholes 2624DC00019 and 2624DC00026 in terms of its groundwater registration region. Borehole 032611 is situated in the Western Highveld with a recharge value between 14 and 15 mm/a.

7.4.11.2 Rainfall and groundwater levels

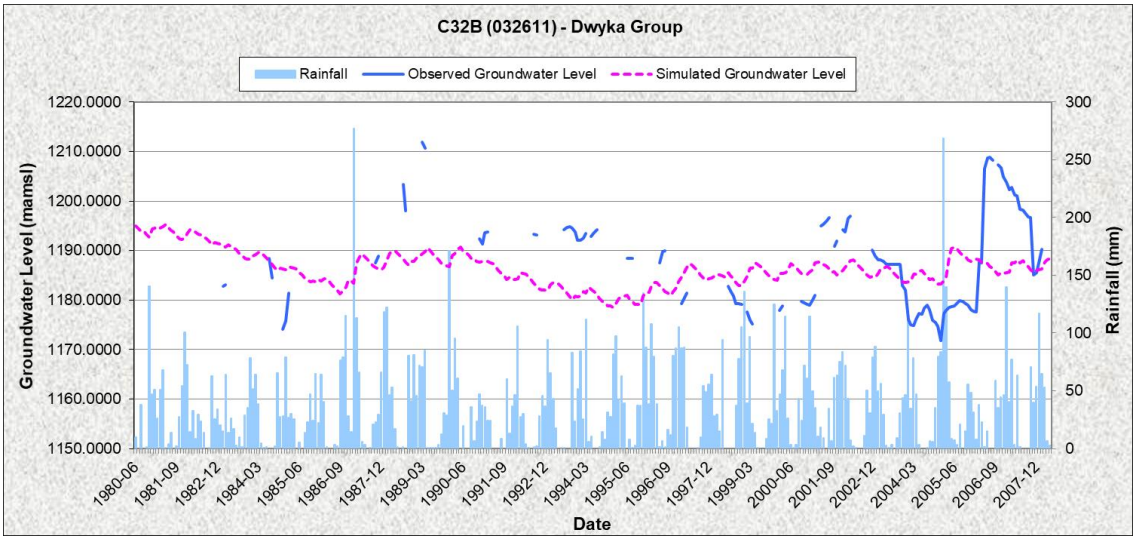

Figure 62: Dwyka Group rainfall and groundwater levels

7.4.12 Tierberg Formation

7.4.12.1 Locality and geology

Borehole 2925CD00009 is situated within the Tierberg Formation in quaternary catchment C51J (refer to Figure 63). The area is defined by a recharge of between 8–9 mm/a and as an intergranular and fractured geology with a groundwater yield between 0.5–2.0 L/s.

The Tierberg Shale Formation forms part of the Permian ECCA Group of the Karoo Supergroup (van Dijk et al., 2002). The formation consists mostly of grey to black shale with interbedded siltstones in the upper part (van Dijk et al., 2002; Botha et al., 2003). Most of the formation consists of well- laminated grey-to-black-coloured shale and in the lower part of the succession along the western and northern margins, yellowish tuffaceous beds of up to 10 cm thick occur (Botha et al., 2003).

The stratigraphy of the Tierberg Formation is similar to the Fort Brown Formation situated in the Southern Karoo. Both formations portray predominantly suspension deposition which, according to van Dijk *et al.,* (2002), hosts deep water fan complexes.

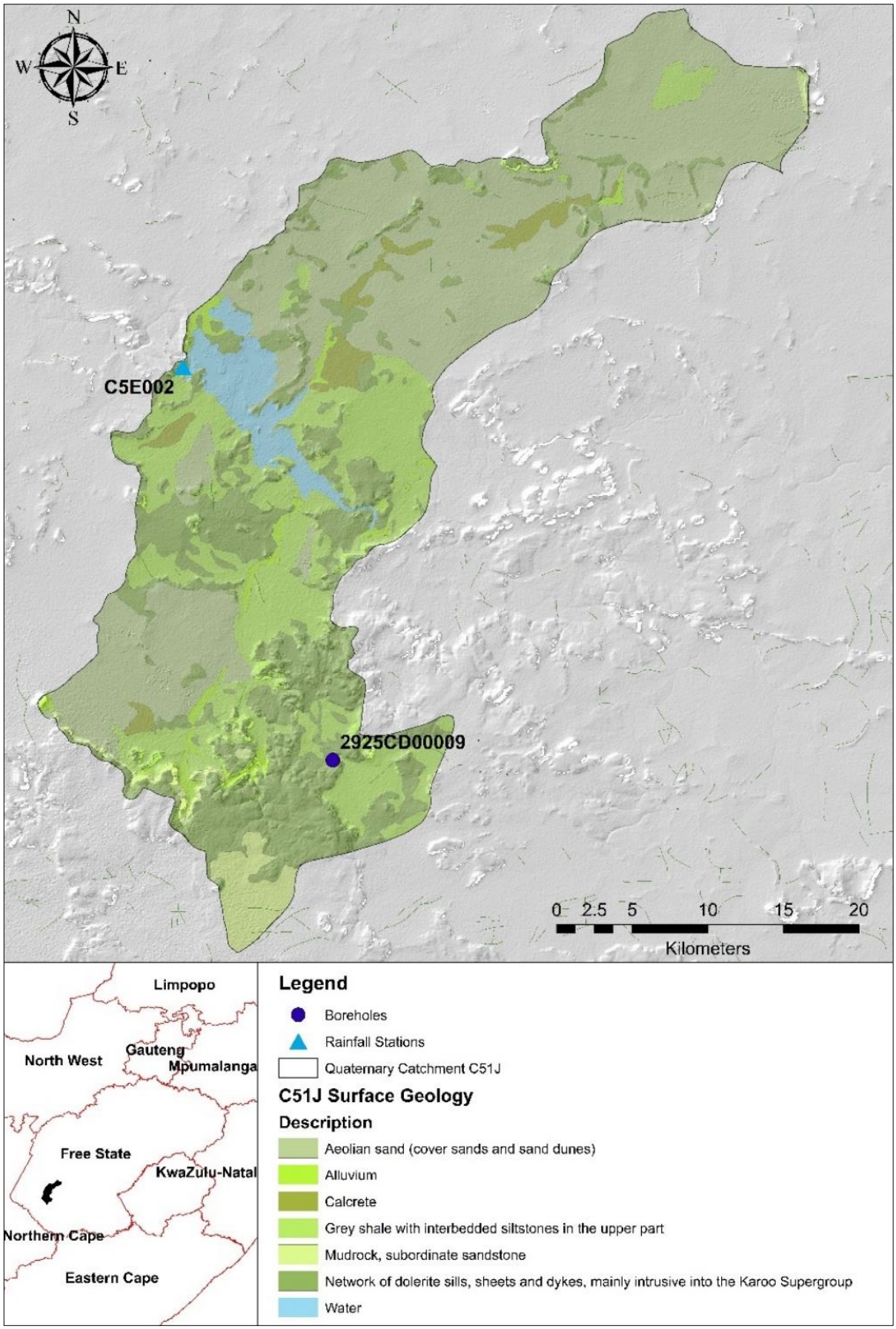

Figure 63: Geology map of quaternary catchment C51J

7.4.12.2 Recharge

The mean annual recharge for borehole 2925CD00009 is approximately 9 mm/a. Borehole 2925CD00009 is situated in the Central Pan Belt groundwater registration region.

7.4.12.3 Rainfall and groundwater levels

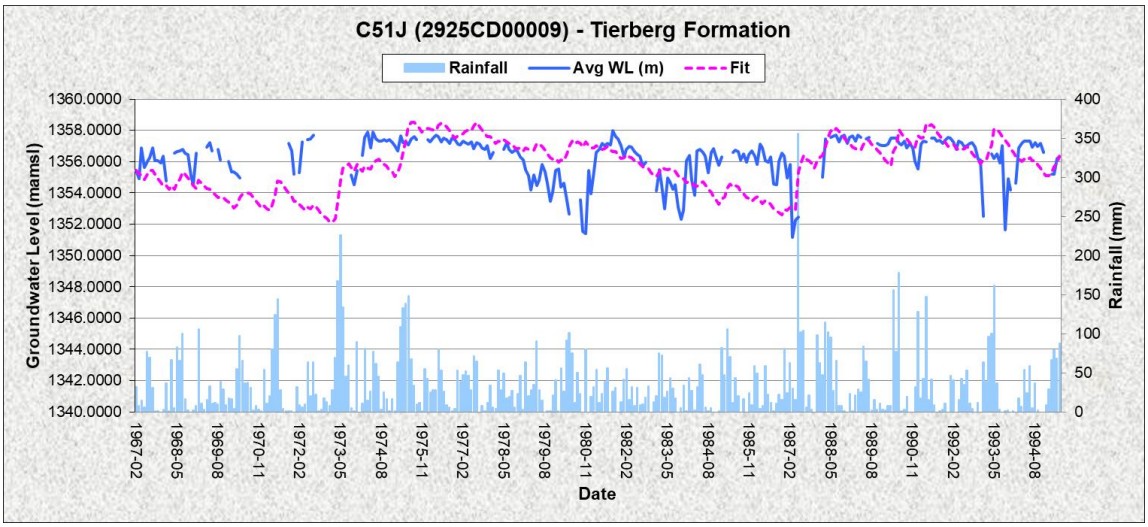

Figure 64: Tierberg Formation rainfall and groundwater levels

Appendix B – Groundwater Simulations

Table 33: Simulated groundwater level parameters

Geology	Borehole	Groundwater balance method	Recharge (%)	Specific yield	Inflows (m^3/day)	Outflows (m^3/day)	Resistance
Teekloof FM	3222BC00151	EARTH	4.890	0.0001	0	0	35.951
Loam and sandy loam	033568	SVF	2.925	0.001	50.000	500.000	0
Malmani SBGRP	2627BC00051	SVF	1.070	0.002	50.000	500.000	0
ECCA GRP	2627BD00056	SVF	1.165	0.002	49.996	500.004	0
Hekpoort FM	036017	SVF	1.736	0.002	49.996	505.613	0
Strubenkop FM	2528CA00015	SVF	1.154	0.002	49.996	505.613	0
Diabase	11452	EARTH	1.600	0.002	0.000	0.000	2805.270
Kolobeng Norite	023502	SVF	1.346	0.001	504.000	7000.000	0
Silverton FM	2528CD00065	SVF	1.116	0.001	49.996	505.613	0
Vryburg FM: Andesitic lava	2624DC00019	EARTH	3.997	0.001	0.000	0.000	1149.769
Dwyka Group	2624DC00026	SVF	1.613	0.001	49.999	500.001	0
Vryburg FM: Quartzitic sandstone	32611	SVF	1.705	0.001	50.000	500.000	0
Tierberg FM	2925CD00009	SVF	1.878	0.002	49.996	400.613	0

Appendix C – Groundwater Drought Index Calculation

The SGI was determined using an Excel model that converts the simulated groundwater levels to a value range similar to that of the SPI. The model makes use of PERCENTRANK.EXC and the NORMSINV functions to calculate the SGI in the same value range as the SPI. The PERCENTRANK.EXC returns the rank of a value of a data set to a percentage of that data set, whereas the NORMSINV function returns the inverse of the standard normal cumulative distribution. By applying these functions to the simulated groundwater level, the SGI is determined in the same value range as the SPI and can, therefore, be compared to one another.